THE DEVELOPMENT AND APPLICATION OF A FRAMEWORK FOR EXPLORING THE ENERGETICS OF GAIT STRATEGY ADAPTATIONS

by

Anahid Ebrahimi

A dissertation submitted to the Faculty of the University of Delaware in partial fulfillment of the requirements for the degree of Doctor of Philosophy in Mechanical Engineering

Spring 2018

THE DEVELOPMENT AND APPLICATION OF A FRAMEWORK FOR EXPLORING THE ENERGETICS OF GAIT STRATEGY ADAPTATIONS

by

Anahid Ebrahimi

Approved: ______________________________________

Ajay K. Prasad, Ph.D.
Chair of the Department of Mechanical Engineering

Approved: ______________________________________

Babatunde A. Ogunnaike, Ph.D.
Dean of the College of Engineering

Approved: ______________________________________

Ann L. Ardis, Ph.D.
Senior Vice Provost for Graduate and Professional Education

I certify that I have read this dissertation and that in my opinion it meets the academic and professional standard required by the University as a dissertation for the degree of Doctor of Philosophy.

Signed: ____
Jill S. Higginson, Ph.D.
Professor in charge of dissertation

I certify that I have read this dissertation and that in my opinion it meets the academic and professional standard required by the University as a dissertation for the degree of Doctor of Philosophy.

Signed: ____
Steven J. Stanhope, Ph.D.
Member of dissertation committee

I certify that I have read this dissertation and that in my opinion it meets the academic and professional standard required by the University as a dissertation for the degree of Doctor of Philosophy.

Signed: ____
Dustyn P. Roberts, Ph.D.
Member of dissertation committee

I certify that I have read this dissertation and that in my opinion it meets the academic and professional standard required by the University as a dissertation for the degree of Doctor of Philosophy.

Signed: ____
Saryn R. Goldberg, Ph.D.
Member of dissertation committee

ACKNOWLEDGMENTS

First, I am tremendously grateful for my advisers, Dr. Steven Stanhope and Dr. Jill Higginson. I thank Dr. Stanhope for training me in the fundamental principles of biomechanics. I thank him for inspiring and encouraging me to use this training to run after problems and to look for generalizable solutions. I thank Dr. Higginson for her infinite guidance in helping me develop skills and goals for my career. I thank her for providing opportunities for me to gain a breadth of knowledge not only in research, but also in teaching and in service. I also wish to thank my committee members Dr. Saryn Goldberg and Dr. Dustyn Roberts. Their input on this dissertation has elevated its scientific accuracy and quality.

I received generous advisement over the years in not only the scientific development of this dissertation, but also in my professional development as a researcher. I especially thank Dr. Jenni Buckley, Dr. Elisa Arch, and Dr. Kota Takahashi for their mentorship in this regard.

I am thankful to all my colleagues in the BADER and Neuromuscular Biomechanics labs, and the Mechanical Engineering and BIOMS programs. I particularly wish to thank Travis Pollen, Amy Bucha, Lisa Katzmire, John Collins, Michael Christensen, and Eryn Gerber for their constant encouragement and help.

I wish to express my gratitude to all my family and friends near and far who have supported and encouraged me over the years. I thank my father and brother for inspiring me to become an engineer. Finally, I am indebted to my mother for her unconditional support and for being with me every single step of the way.

Chapters 3, 4, and 5 of this document were previously published by Elsevier and reprinted with permission (Appendix A). As first author, I made primary contributions to the conception of ideas, analysis of data, and final written form of these articles. Complete information on these articles is listed:

Chapter 3. A. Ebrahimi, S.R. Goldberg, S.J. Stanhope, Changes in relative work of the lower extremity joints and distal foot with walking speed, Journal of Biomechanics, 58 (2017), 212-216.

Chapter 4. A. Ebrahimi, S.R. Goldberg, J.M. Wilken, S.J. Stanhope, Constituent Lower Extremity Work (CLEW) approach: A novel tool to visualize joint and segment work, Gait & Posture, 56 (2017), 49-53.

Chapter 5. A. Ebrahimi, J.D. Collins, T.M. Kepple, K.Z. Takahashi, J.S. Higginson, S.J. Stanhope, A mathematical analysis to address the 6 degree-of-freedom segmental power imbalance, Journal of Biomechanics, 66 (2018), 186-193.

Support for dissertation research presented in this document was provided by the National Science Foundation (NSF) Graduate Research Fellowship under Grant No. 1247394, by the University of Delaware College of Health Sciences, and by the University of Delaware Mechanical Engineering Department David Helwig Fellowship. Any opinions, findings, and conclusions or recommendations expressed in this material are those of the author and do not necessarily reflect the views of the NSF. Additional funding and acknowledgments are listed at the conclusion of each chapter, when applicable.

TABLE OF CONTENTS

LIST OF TABLES

LIST OF FIGURES

ABSTRACT

How a person walks, or their gait strategy, has substantial ties to their ability to function in society. Gait strategies are formed by the contributions of each lower extremity constituent (i.e., hips, knees, ankles, and feet) to the walking pattern. The formation of a gait strategy is dependent on several factors (purpose, environment, and physical health), of which each has a spectrum of conditions (e.g., speed, terrain, muscle weakness, etc.). Understanding the rules by which individuals adapt gait strategies to accommodate a spectrum of conditions is useful for informing assistive device design and rehabilitation protocols that help individuals reach their highest levels of function. Recognizing the relationship between changes in mechanical energetics (work and energy) and movement, energetics variables are well suited to be quantitative summary metrics that characterize gait strategy adaptations.

The overall purpose of this dissertation was to develop and apply a general framework to explore the energetics of gait strategy adaptations. Two novel approaches using mechanical energetics were developed to create the Gait Energetics Adaptations Resource (GEAR) framework. The Constituent Lower Extremity Work (CLEW) approach represents the proportion of constituent lower extremity work contributing to the absolute work done over a time interval – such as a gait cycle. Then, the Work-Energy Profiles approach was developed using the work-energy relationship to examine the mechanical energetics of gait strategies within and between a set of conditions.

These two approaches were developed by quantifying the gait strategy adaptations that occur when typical, unimpaired individuals walk at slow, moderate, and typical speeds. The CLEW approach revealed that the relative ankle and foot work adapt by increasing from slow to typical walking speeds while the relative hip and knee work remain constant across speeds. The Work-Energy Profiles approach revealed that the gait strategy implemented at a slow speed uses more pendular mechanics to raise the center of mass compared to the other speeds, while the strategy at a typical speed is more effective at "propelling" the body into its next step compared to the other speeds.

An application of the GEAR framework was conducted by quantifying the gait strategy adaptations that occur when a cohort of unimpaired individuals walked with and without an artificial ankle impairment unilaterally and bilaterally. The CLEW approach revealed that the knee compensates during stance when the stance limb ankle is partially impaired unilaterally, but that the hip and knee both compensate when ankles are impaired bilaterally. The Work-Energy Profiles demonstrated that the compensatory strategies with both unilateral and bilateral ankle impairment are effective in propelling the body during double support phase compared with no ankle impairment, but the compensatory strategies are less effective during single support.

The CLEW and Work-Energy Profiles approaches under the GEAR framework are the first methodologies to use comprehensive energetics metrics for the quantification of gait strategy adaptations and their effectiveness. The GEAR framework will be used in the future to explore gait adaptations across the spectra of many different conditions that can be helpful in fully understanding the underlying rules and mechanisms by which humans adapt their gait strategies.

Chapter 1

INTRODUCTION

> "Before people with disabilities will be able to truly enter the social and economic mainstream of American society, they will need to maximize their ability to function physically and behaviorally."
>
> (*Research Plan for the National Center for Medical Rehabilitation Research*, 1993)

1.1 Background

Gait is one of the most common human movements. It has substantial ties to a person's ability to function in society, and thus has become a focus of rehabilitation research. A scientific approach to understanding the mechanisms by which humans ambulate is critically important for improving functional recovery post-injury (*Research Plan for the National Center for Medical Rehabilitation Research*, 1993). A gait strategy is defined here as the coordination of constituents of the body to walk, where constituents include the lower limb hips, knees, ankles, and feet, as well as the head-arms-trunk (HAT). Choice of gait strategy will not only change based on several factors but also the spectrum of conditions within each factor (Table 1.1). As an example of one such factor, gait strategies change depending on the purpose of getting from one place to another at the desired time (e.g., crossing the street, exercising, etc.). Changes in gait strategy by typical, able-bodied individuals along this spectrum of conditions is referred to as an "adaptation." *The understanding of the underlying mechanism by which individuals adapt their gait strategies to different conditions along a spectrum is incomplete.*

Table 1.1: Select factors and example spectra of conditions that influence the choice of gait strategy.

Factor	Example [spectrum of conditions]
Purpose	Speed [standstill to maximum velocity]
Environment	Slope [horizontal to vertical grade]
Physical health	Muscle weakness [none to complete loss of strength]

Historically, there have been two main methodologies for measuring gait strategy adaptations, which often occur in a setting that controls for several above-mentioned factors. The first is a visual examination of an individual's gait, which involves a descriptive analysis of the gait strategy. This method can be subjective even to the trained and experienced clinician. For example, some patients are able to compensate for quadriceps insufficiency such that observation of a disability is not apparent (Perry, 1992). The second is a dynamics method within biomechanics, which involves objective measures of limb forces and motions (via force-sensing platforms and motion-capture cameras, respectively). This dynamics method is not new to this era (Baker, 2007), but it has been refined in precision and accuracy with the development of modern computers. While various discrete temporal-spatial parameters (e.g., stride length) and kinematic and kinetic measures (e.g., peak joint angles and moments) are calculated in this method, several metrics are needed to identify the strategy used. These metrics often provide information only at an instant in time (e.g., maximum or minimum values).

Recognizing the causal relationship between the flow of energy and movement and the cyclic nature of gait, a second biomechanical method using energetics is well-suited to produce summary metrics to measure gait adaptations across conditions. For example, the net work of the center of mass (COM) is minimal over the gait cycle, independent of strategy (Bertram and Hasaneini, 2013; Cavagna et al., 2000; DeVita et al., 2007; Farris and Sawicki, 2012; Kuo, 2007; Miller and Verstraete, 1996; Zelik and Kuo, 2010). Like net work, there appear to be certain prerequisites that are met for gait strategies, despite myriad options. Using the dynamics method, David Winter explored this concept when he found the support moment (summed ankle, knee, and hip moment) was positive across walking speeds while individual joint moments varied (Winter, 2009). However, moment and work provide different information. Absolute limb work is a summary metric of all the positive and absolute negative work done by the hip, knee, ankle, and foot over the gait cycle. While absolute limb work may change with condition (e.g., increasing in magnitude with walking speed) (Zelik et al., 2015), it is unclear if the work done by each constituent relative to the absolute limb work maintains the same proportions across conditions. The relative constituent work provides an objective energetics metric of how the constituents coordinate to achieve a gait strategy. Thus, absolute limb work and relative constituent work are summary energetics metrics that can be used to quantify gait strategies, where the change in these metrics across a spectrum of conditions quantifies the gait strategy adaptations.

Furthermore, mechanical energy variables represent the results of motions and positions of the body, which can be used to better understand how a certain gait strategy is achieved. Mechanically, gait can be divided into sub-tasks: raising the COM then lowering the COM during single support phase, and propelling the body during double support phase. Changes in energy forms (e.g., gravitational potential, translational kinetic, and rotational kinetic energy) over these sub-tasks of a gait cycle are quantitative energetics metrics. Mathematically, the work-energy relationship refers to the property that net work done over an interval is equal to the summed changes in energy forms over that interval. Thus, the work-energy relationship and theoretical models of economic gait can be used to understand how and why certain gait energetics patterns occur under different conditions. Then, the gait energetics can be used to assess how aligned, or effective, a strategy is relative to another strategy. For example, the work-energy relationship can reveal the effectiveness of compensatory gait strategies due to impairment relative to a typical, unimpaired gait strategy.

While work and energy metrics provide valuable insight into characterizing gait strategies and assessing their effectiveness across a spectrum of conditions, an energetics method has yet to be presented in a clinically useful form. Patient data using the dynamics method are often presented in a clinical gait report, which includes normative curves or values from typical, healthy individuals for comparison (Perry, 1992). However, a standard report for energetics metrics has yet to be presented, and these metrics have thus far had limitations. For example, researchers have analyzed relative joint work as a percentage of absolute limb work but these metrics were only calculated in the sagittal plane (Teixeira-Salmela et al., 2008). There is now support for a more comprehensive six degree-of-freedom (6 DOF) analysis (Zelik et al., 2015). The work-energy relationship has long been utilized; however, experimental data show a "power imbalance" (difference between power and rate of energy change) (McGibbon and Krebs, 1998). It is necessary to address these limitations and develop general, easily interpreted reports for data using the energetics method so that the utility of this method is fully realized. Thus, development of a framework for the energetics method can fill the gap in understanding the mechanism for gait adaptations.

1.2 Overall Framework

This dissertation introduces a general framework for understanding the mechanism for gait adaptations using an energetics method (Fig. 1.1). Creating this framework required the development of two novel approaches: first, an approach to measure gait adaptations across a spectrum of conditions, and next, an approach to compare the effectiveness of these gait strategies. These approaches were developed by modulating purpose (walking speed) and controlling environment (walking on a level ground treadmill) and physical health (individuals without impairment).

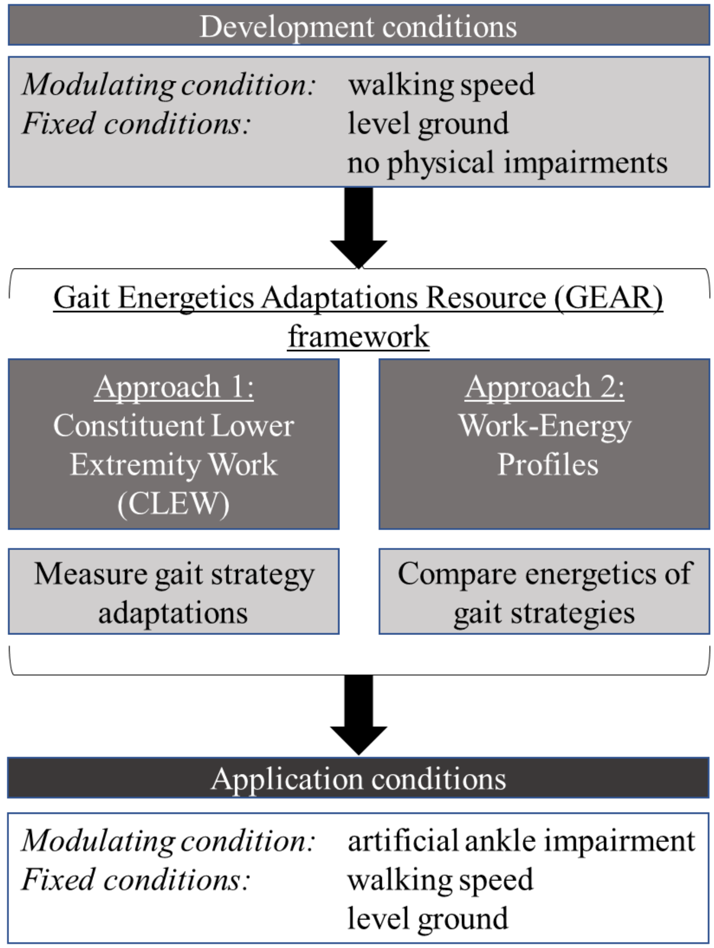

Figure 1.1: Schematic of the conditions used and approaches developed to create the Gait Energetics Adaptations Resource (GEAR) framework to understand the mechanism for gait adaptations using an energetics method.

The applicability of this general framework was then demonstrated for a new set of conditions by controlling environment and purpose and modulating physical health by inducing an artificial ankle impairment (Fig. 1.1). Using the energetics method, a constituent compensation is quantified by a significant change in relative constituent work while walking with an impairment as compared to typical, unimpaired walking. All the constituent compensations over a gait cycle resulting from one or more constituents impaired is a compensatory gait strategy. Individuals with unilateral ankle impairment exhibit reduced push-off power compared to individuals without impairment, which requires some other joints of the limbs to compensate (Bregman et al., 2012). Predicting the compensatory gait strategy when both ankles are impaired is challenging. It has yet to be explored if the combination (interaction) of two unilateral ankle impairment strategies is simply additive. The energetics method of the GEAR framework can be used to probe the form of this interaction, by holding all other factors constant and inducing unilateral and bilateral artificial ankle impairments in unimpaired individuals. Theoretically, for an additive interaction, the compensatory gait strategy due to bilateral impairment would be the sum of two compensatory gait strategies due to unilateral impairment. Thus, the GEAR framework can be used to explore the form of interaction that governs compensatory gait strategies when individuals have an impairment.

1.3 Specific Aims

A general framework to identify the mechanism by which gait strategies adapt under a spectrum of conditions will contribute to enhancing functional recovery post-injury. **Using an energetics method, the overall goal for this dissertation is to develop and apply a general framework to understand the mechanism for gait adaptations across a spectrum of conditions.**

The overall objective will be achieved through the following three aims:

1.3.1 Aim 1: Develop an approach to measure gait strategy adaptations across conditions using gait strategies from typical individuals walking at a range of walking speeds (Chapters 3 & 4).

The 6 degree-of-freedom work calculations of the four lower extremity constituents (hip, knee, ankle, and distal foot (Siegel et al., 1996)) were used to assess how the constituents coordinate to achieve a gait strategy and to measure the gait adaptation with slow, moderate, and typical walking speeds (Chapter 3). The absolute limb work indicates the level of limb effort over a stride, while the relative constituent work identifies the proportional amount each constituent's work contributes to absolute limb work during the stance and swing phases of gait. The Constituent Lower Extremity Work (CLEW) approach was developed to visualize and readily interpret gait strategies using these work metrics (Chapter 4).

1.3.2 Aim 2: Develop an approach to compare mechanical energetics across conditions using gait strategies from typical individuals walking at a range of walking speeds (Chapters 5 & 6).

Using the work-energy relationship, constituent work over distinct intervals of the stance phase of gait can be related to changes in mechanical energy forms of the whole body (e.g., potential gravitational, rotational kinetic, and translational kinetic energy). However, there existed a discrepancy in experimental work and change in energy, and their derivatives (power and rate of change in energy, respectively). First, this power imbalance was resolved using a mathematical proof (Chapter 5). The Work-Energy Profiles approach was then developed to analytically evaluate the mechanical energetics of gait strategies used by typical individuals walking at slow, moderate, and typical speeds (Chapter 6).

1.3.3 Aim 3: Identify the form of interaction that governs compensatory gait strategies due to artificially impaired ankle function using gait strategies from typical individuals walking with unilateral and bilateral ankle impairments (Chapters 7 & 8).

The CLEW and Work-Energy Profiles approaches developed under Aims 1 and 2 were used to assess the compensatory gait strategy that develops when one or more constituents are impaired. Custom ankle orthoses were used to provide a controlled amount of ankle restriction unilaterally and bilaterally to healthy individuals walking at a typical speed. Theoretically for an additive interaction, the compensatory gait strategy due to bilateral impairment would be the sum of two unilateral compensatory gait strategies (Chapter 7). The relative effectiveness of compensatory gait strategies due to unilateral and bilateral ankle impairment was then assessed via comparison to typical, unimpaired gait strategies using energetics metrics (Chapter 8).

Chapter 2

SIGNIFICANCE & INNOVATION

2.1 Significance

A primary goal for the nearly two million individuals living with lower limb amputations (Ziegler-Graham et al., 2008) is the ability to walk safely and comfortably in their community (Andrews et al., 2010). Improving functional recovery for individuals who have limb loss or other lower limb injuries requires an understanding of the mechanism guiding human ambulation under different conditions. This dissertation developed a Gait Energetics Adaptations Resource (GEAR) framework using energetics methods, which has potential for application in the field of orthotics and prosthetics. The GEAR framework was used to explore two conditions: walking speed and ankle impairment.

To begin, this dissertation used the GEAR framework to explore gait adaptations from slow to typical speeds. This parameter was chosen because the ability to effectively modulate walking speed is an important functional goal for individuals with gait impairments. While individuals without impairments increase peak joint moments (Goldberg and Stanhope, 2013; Holden et al., 1997; Kirtley et al., 1985; Lelas et al., 2003; Winter, 1984) and joint work (Cavagna and Kaneko, 1977; Umberger and Martin, 2007) to walk faster, passive prosthetic devices cannot adapt in the same manner (Herr and Grabowski, 2012; Silverman et al., 2008). Thus, information gained by using the GEAR framework to understand how typical individuals adapt their gait strategies to different walking speeds could help inform novel prosthetic device designs that could mimic this mechanism of adaptation.

Next, this dissertation used the GEAR framework to explore the form of interaction guiding compensatory gait strategies when individuals have one or more impairments. The ability to predict a compensatory gait strategy based on the constituents impaired could have broad impacts on the rehabilitation field, from diagnosing gait disorders to providing the most useful treatment options. Currently, predicting the form of interaction between constituent impairments and the resulting compensatory strategy is difficult. To begin probing if a possible interaction exists, data were collected on typical subjects walking with unilateral and bilateral artificial ankle impairment, serving as their own controls. Thus, information gained by using the GEAR framework to understand how typical individuals adapt their gait strategies to one or two ankle impairments could help inform rehabilitation protocols and a fundamental understanding of how humans compensate with impairments.

The GEAR framework is valuable for targeted rehabilitation protocols and subject-specific device design for individuals with impairments. For example, researchers have identified that the ankle has a peak power burst during pre-swing that increases in magnitude with faster walking speeds (e.g., Winter, 1983) and is vital to the forward progression of the body's COM (Neptune et al., 2008). Researchers have also found that peak joint moments increase linearly with increased walking speed (Goldberg and Stanhope, 2013; Lelas et al., 2003). Researchers have used findings related to natural ankle function to design prosthetic devices (Herr and Grabowski, 2012) and exoskeletons (Malcolm et al., 2015). However, these analyses tend to focus on the system at one joint (ankle) during one portion of the gait cycle (late stance).

An energetics analysis of all lower extremity limb constituents enables causal analysis of movement over the entire gait cycle. The GEAR framework measures gait strategy adaptations and compares the relative effectiveness of gait strategies using an energetics method. This framework can be used to attain information that will be significant for the (1) optimization of assistive device design, (2) assessment of the effectiveness of gait strategies, and (3) development of guidelines for rehabilitation.

2.1.1 Optimization of Assistive Device Design

The development of approaches using the energetics method to characterize how individuals adapt to walking speed can be used to elucidate the underlying principles by which gait strategies are formed and adapt at different speeds (Aim 1). With this information, a device can be designed to create the same functional outcome as a natural limb, without necessarily needing to be biomimetic (i.e., mimicking the anatomical form of a natural limb).

2.1.2 Assessment of the Effectiveness of Gait Strategies

Determining if a compensatory movement due to an impairment is “good” or “bad” is difficult. However, by looking at the energy forms of the whole body, which represent the result of motions and positions of the body over an interval, one may be able to say if the compensatory strategy is effective in achieving the sub-task of that interval. One sub-task, for example, is to propel the body (i.e., to change the velocity of the COM) during double support phase, which is effective if it results in positive translational kinetic energy. Typical individuals do more limb work as walking speed increases (Zelik et al., 2015). The work-change in energy relationship can be used as a tool to identify how much positive, negative, and net constituent work is done and how much net work goes into changing the energy forms of the body (Aim 2). This approach can then be used to observe how individuals walking with impairments alter their constituent work to walk at the same speed as individuals without impairments, and determine if that compensatory strategy is more, less, or equally effective for propelling the body in gait (Aim 3).

2.1.3 Development of Guidelines for Rehabilitation

This dissertation presents typical limb gait adaptations with walking speed using a novel energetics method, which can be a new energetics "gold standard" for gait analysis. Clinicians and biomechanists can use typical gait adaptations as guidelines to assess how an atypical limb may compare to typical, and whether an intervention to attain a profile similar to a typical limb is appropriate. For example, if an individual using a lower limb prosthesis exhibits similar adaptations to typical individuals walking at a range of slow speeds, the patient may be ready to progress to a higher mobility level of device. Furthermore, it is difficult to predict the compensatory gait strategy an individual will use when walking with an impairment. The GEAR framework can be used to explore the form of interaction for compensatory gait strategies (Aim 3).

Using an energetics method, this dissertation quantified how the coordination of constituent work (i.e., gait strategy) adapted to increase walking speed (Aim 1), as well as assessed the mechanical energetics during the sub-tasks of gait in order to increase walking speed (Aim 2). Developing a general framework for quantifying how the human body purposefully adapts to modulate gait demand can better guide decisions related to the design of devices and rehabilitation of individuals with impairments. Approaches from Aims 1 and 2 were used to assess the form of interaction between the compensatory gait strategies used in the presence of unilateral and bilateral impaired ankle function (Aim 3). The GEAR framework can be used in the future to explore the gait adaptations across the spectra of many different conditions, therefore creating a database of gait strategies and adaptations that can be helpful in fully understanding the mechanisms by which humans ambulate.

2.2 Innovation

Several studies have used experimental gait analysis, musculoskeletal modeling, and calculations of kinetics and kinematics using the dynamics method to determine the compensatory strategies used by individuals with impairments. While each study provides new evidence, there has yet to be a clear and cohesive understanding of how this information fits together. Thus, there is an incomplete understanding of the mechanisms by which lower extremity limbs adapt with modulating gait speed. This dissertation describes the development of a novel Gait Energetics Adaptations Resource (GEAR) framework using an energetics method to analyze lower extremity limb adaptations for the ultimate purpose of understanding the guiding principles by which the body adapts to different gait conditions.

Previously, researchers have studied temporal-spatial, kinematic, and kinetic variables to quantify gait adaptations occurring across walking speeds in typical individuals. Increased walking speed corresponds to increased step length and cadence (Bejek et al., 2006; Murray et al., 1984). Slower walking speeds result in less hip flexion-extension total excursion and vertical head motion over the gait cycle (Murray et al., 1984). Interestingly, the relative contributions from peak lower extremity joint moments differ with speed, and the ankle is most sensitive to gait changes (Goldberg and Stanhope, 2013). While these variables describe walking patterns and forces at different speeds, they are limited in providing a complete understanding of the mechanisms by which lower limbs adapt with speed. In other words, temporal-spatial, kinematic, and kinetic variables under the dynamics method do not elucidate the cause of movement adaptations.

The innovation in using an energetics method to develop the GEAR framework is the inherent causality between energetics and movement. Giovanni Cavagna was one of the first researchers to calculate the amount of external work produced by the body COM during walking using ground reaction forces (Cavagna, 1974). As work is equal to the change in energy, the researchers were able to identify how potential and kinetic energy of the COM were transferred over a gait cycle (Cavagna et al., 1976; Cavagna and Kaneko, 1977). Later, researchers theorized the work produced by the limb on the COM could be parsed into the work of the three lower extremity joints (ankle, knee, and hip) (Zelik and Kuo, 2010). While this approach was beneficial in determining the amount of work produced at each joint, it resulted in unaccounted residual positive work. The analysis was limited by 3 degree-of-freedom (DOF) rotational work calculations of the joints (ankle, knee, and hip), which do not account for the translational movement at the joints or the motion at the distal end of the foot. Furthermore, these calculations only quantify the work performed at each joint and not how the work contributes to the movement of the entire limb. (For a brief history of mechanical work calculations, the reader is referred to Appendix B.)

The GEAR framework is the first to use comprehensive energetics calculations to understand gait adaptations across a spectrum of conditions. Approaches within the framework use comprehensive energetics metrics including 6 DOF calculations, distal foot energetics, and the work-change in energy relationship. Recent literature has supported the use of 6 DOF inverse dynamics calculations and the inclusion of a distal foot work term for assessing lower extremity work of the limb and its constituents (ankle, knee, hip, and distal foot) (Zelik et al., 2015). Siegel and colleagues validated the inclusion of the distal foot work term by equating the segmental power of the foot (including the distal foot) to the rate of change in energy of the foot (Siegel et al., 1996). While several other research studies have used the segmental power-rate of change in energy relationship (e.g., Robertson and Winter, 1980), the measures of segmental power and rate of change in energy were not reported to be exactly equivalent, resulting in a power imbalance.

This dissertation dedicates a chapter to resolving this historical power imbalance and ensuring the equivalence of power and rate of change in energy. The segmental power-rate of change in energy relationship was used to relate the 6 DOF constituent work to the overall change in energy form of the body during distinct intervals of stance phase. A general approach was developed for quantifying and visualizing the gait strategy used to do constituent work, which created a change in the whole body energy in its different mechanical forms. The relative effectiveness of the strategy was assessed based on how the energy forms related to the sub-tasks during different intervals of gait.

Furthermore, the GEAR framework was then used to investigate the compensatory strategy used by the limbs when the ankle, a key contributor to forward progression of the body, was impaired unilaterally and bilaterally. This novel framework can be used to probe the mechanism for compensatory strategies based on the level and number of impairments. In the future, a database for exploring compensatory strategies may be developed using the GEAR framework.

Chapter 3

CHANGES IN RELATIVE WORK OF THE LOWER EXTREMITY JOINTS AND DISTAL FOOT WITH WALKING SPEED (PUB: 2017)

(Ebrahimi, Goldberg, and Stanhope, 2017)

3.1 Abstract

The modulation of walking speed results in adaptations to the lower limbs which can be quantified using mechanical work. A six degree-of-freedom (DOF) power analysis, which includes additional translations as compared to the 3 DOF (all rotational) approach, is a comprehensive approach for quantifying lower limb work during gait. The purpose of this study was to quantify the speed-related 6 DOF joint and distal foot work adaptations of all the lower extremity limb constituents (hip, knee, ankle, and distal foot) in healthy individuals. Relative constituent 6 DOF work, the amount of constituent work relative to absolute limb work, was calculated during the stance and swing phases of gait. Eight unimpaired adults walked on an instrumented split-belt treadmill at slow, moderate, and typical walking speeds (0.4, 0.6, and 0.8 statures/s, respectively). Using motion capture and force data, 6 DOF powers were calculated for each constituent. Contrary to previously published results, 6 DOF positive relative ankle work and negative relative distal foot work increased significantly with increased speed during stance phase ($p < 0.05$). Similar to previous rotational DOF results in the sagittal plane, negative relative ankle work decreased significantly with increased speed during stance phase ($p < 0.05$). Scientifically, these findings provide new insight into how healthy individuals adapt to increased walking

speed and suggest limitations of the rotational DOF approach for quantifying limb work. Clinically, the data presented here for unimpaired limbs can be used to compare with speed-matched data from limbs with impairments.

3.2 Introduction

The effective modulation of walking speed results in adaptations by the lower limbs which can be quantified using various gait parameters. Recognizing that the flow of energy gives rise to movement, analyses to quantify lower limb adaptations with speed are ideally suited to use the principles of energy, work, and power.

Biomechanical joint work has historically been calculated using a sagittal (1 degree-of-freedom (DOF) rotational) or 3 DOF (all rotational) approach. Teixeira-Salmela, et al. calculated positive and negative joint work as a percentage of absolute sagittal limb work (summed positive and absolute negative work of the hip, knee, and ankle) over the entire gait cycle (Teixeira-Salmela et al., 2008). The researchers found the relative percent contribution of both positive and negative ankle work decreased with increased walking speed, while the hip and knee contributions increased, suggesting the hip flexor muscles assist with limb forward progression. These findings were consistent with relative joint work calculations over stance phase only (Chen et al., 1997). Farris and Sawicki used 3 DOF data to calculate the percent average positive joint power relative to the total average positive power of the limb over a stride (Farris and Sawicki, 2012) and found that positive relative joint average power did not differ across speeds.

Recently, Zelik et al. utilized a 6 DOF approach to determine changes in lower limb work with speed (Zelik et al., 2015). The analysis used 6 DOF power calculations for the hip, knee, and ankle joints (Buczek et al., 1994) and the inclusion of a distal foot segmental power term (Siegel et al., 1996). (The term “constituent” will be used throughout this manuscript to refer to the hip, knee, and ankle joints and the distal foot segment.) A 6 DOF approach, which includes joint translations unlike the 3 DOF approach, is currently the most comprehensive means for analyzing the energy changes of the system. Summing the constituent work to generate a measure of 6 DOF limb work, Zelik et al. found that both positive and negative 6 DOF limb work increased with speed (Zelik et al., 2015). However, it remains unclear if the relative constituent contributions to the absolute 6 DOF limb work adapt by increasing proportionally with walking speed.

6 DOF work calculations of the four lower limb constituents were used to quantify the relative constituent work, or the percentage of positive or negative work each constituent contributed to absolute 6 DOF limb work, across a stride, revealing the primary constituent “drivers” and “brakers,” respectively. Work at the joint and segmental levels is defined here as a measure of energy generation (positive) and dissipation (negative) (e.g., by muscles). However, it is noted that inverse dynamics calculations of work do not account for co-contraction, work done by two-joint muscles, partition of energy stored in elastic structures versus muscle, or heat dissipation (Purkiss and Robertson, 2003; Umberger and Martin, 2007). Relative constituent work can be meaningful for characterizing how constituent contributions to gait change throughout the gait cycle and how these contributions are affected by speed. The objective of this study was to quantify the speed-related 6 DOF work adaptations of all the lower extremity limb constituents in healthy individuals.

3.3 Methods

A subset of previously reported data (Goldberg and Stanhope, 2013) was used for data analysis. Briefly, eight healthy adult subjects (height 1.77 ± 0.08 m, mass 71.8 ± 15.5 kg) walked on an instrumented treadmill (Model TM-06-B, Bertec Corp., Columbus, OH) while kinematic and force platform data were collected. All subjects provided informed consent under IRB (Institutional Review Board) protocol. Reflective markers were placed on subjects using a modification to a previously reported marker configuration (Holden et al., 1997) and a six-camera motion capture system was used to collect kinematic data (Vicon, Los Angeles, CA).

Subjects walked at three stature-scaled speeds (0.4, 0.6, and 0.8 statures/s, ranging from approximately 0.7 to 1.4 m/s), which will be denoted as slow, moderate, and typical walking speeds, respectively. All conditions were randomized, and subjects were given sufficient time to acclimate to each condition (approximately 1.5 – 2 minutes) (Donelan and Kram, 1997). Motion capture data were sampled at 120 Hz and low-pass filtered at 6 Hz, and treadmill force data were sampled and low-pass filtered at 1040 Hz and 10 Hz, respectively.

Using Visual3D software (C-Motion, Inc. Germantown, MD), 6 DOF constituent powers were calculated using published methods (Buczek et al., 1994; Takahashi and Stanhope, 2013). The stance phase of gait was defined as the period over which the vertical ground reaction force exceeded a threshold of 20 N. Power data were scaled by body mass and averaged across strides for each condition within subjects, with a minimum of five strides per condition. Left leg stance (heel-strike to toe-off) and swing (toe-off to heel-strike) data for clean strides are presented.

Positive and negative constituent work values were calculated for each subject by integrating the respective portions of the constituent power curves over stance and swing phases. Absolute 6 DOF limb work ($^{abs}W_{limb}$) was the sum of the positive and absolute value of the negative 6 DOF limb work over both stance and swing (Eq. 1). Relative work (RW) was the absolute value of each constituent's work divided by the absolute 6 DOF limb work as a percent (e.g., negative relative ankle work in Eq. 2). Absolute relative work was the sum of the positive and negative relative work contributions for that constituent. Each work value was scaled by body mass and averaged over all subjects at each speed.

$$^{abs}W_{limb} = ({}^{+}W_{hip}+{}^{+}W_{knee}+{}^{+}W_{ankle}+{}^{+}W_{distal\ foot})_{stance} + |({}^{-}W_{hip}+{}^{-}W_{knee}+{}^{-}W_{ankle}+{}^{-}W_{distal\ foot})_{stance}| + ({}^{+}W_{hip}+{}^{+}W_{knee}+{}^{+}W_{ankle})_{swing} + |({}^{-}W_{hip}+{}^{-}W_{knee}+{}^{-}W_{ankle})_{swing}| \quad (1)$$

$$^{-}RW_{ankle} = (|{}^{-}W_{ankle}| \,/\, {}^{abs}W_{limb}) * 100\% \quad (2)$$

Differences in relative constituent work were compared separately across the three walking speeds using several three-way and two-by-three way repeated measures ANOVAs with an overall *p* value of 0.05. All post-hoc comparisons reported have been adjusted using the Bonferroni correction using SPSS software (IBM Corp., Armonk, NY). Due to violating sphericity a number of times, a more conservative Greenhouse-Geisser adjustment was used. For the ankle, knee, and hip, the repeated measures ANOVAs took into account two phases (stance and swing) and three speeds (slow, moderate, and typical). A significant phase-by-speed interaction indicates that the way in which relative work changed with speed depends on the phase (stance or swing). If a phase-by-speed interaction was significant, then pairwise comparisons at each phase for the three speeds were examined. For the distal foot, the repeated measures ANOVA compared the major effect of only speed (slow, moderate, and typical) and not phase; distal foot calculations are not applicable in swing since the foot does not contact the ground.

3.4 Results

Power curves for each constituent are shown in Fig. 3.1. Absolute 6 DOF limb work over a gait cycle significantly increased with walking speed ($p < 0.001$): 0.93 ± 0.20 J/kg, 1.28 ± 0.25 J/kg, and 1.66 ± 0.31 J/kg for slow, moderate, and typical speeds, respectively (all $p < 0.001$). Average relative constituent work values with standard deviations are represented in bar charts in Fig. 3.2. Table 3.1 lists the means and standard deviations for relative constituent work values (J/kg) during stance and swing.

There were no noteworthy trends in the few significant pairwise comparisons for the hip and knee across speeds in the two phases. For ${}^{+}RW_{ankle}$ and ${}^{-}RW_{ankle}$, there were significant phase-by-speed interactions (p = 0.005 and 0.001, respectively). In stance, ${}^{+}RW_{ankle}$ significantly increased with speed ($p = 0.022$, slow-moderate; $p = 0.014$, slow-typical; $p = 0.011$, moderate-typical). The ${}^{-}RW_{ankle}$ significantly decreased with speed in stance ($p = 0.023$, slow-moderate; $p = 0.005$, slow-typical; $p = 0.005$, moderate-typical). The ${}^{-}RW_{distal\ foot}$, significantly increased with speed in stance, ($p = 0.018$, slow-moderate, $p < 0.001$, slow-typical; $p = 0.013$, moderate-typical).

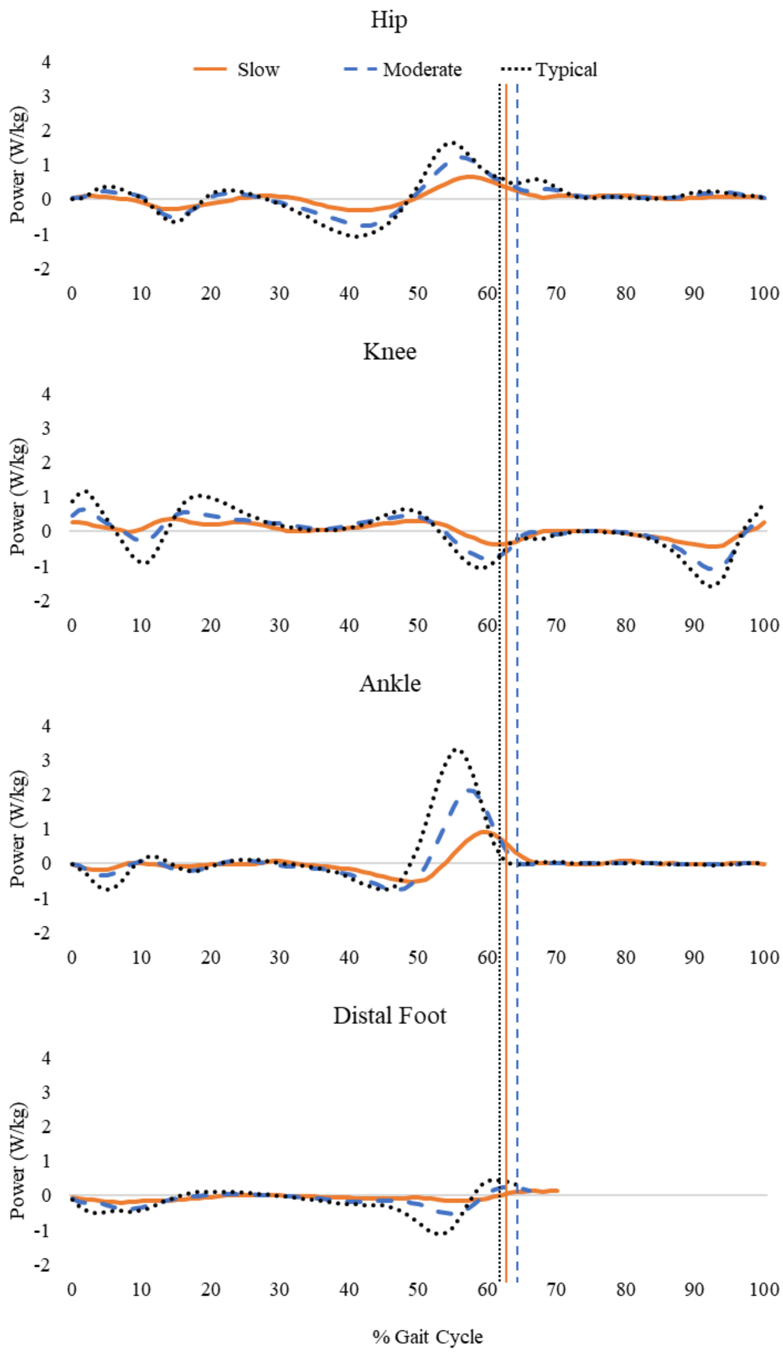

Figure 3.1. Average constituent power curves scaled by body mass from all subjects over entire gait cycle for three walking speeds (slow, moderate, and typical). Left toe-off defined the beginning of swing phase and began at 62.7%, 63.3%, and 61.9% of the gait cycle for slow, moderate, and typical walking speeds, respectively.

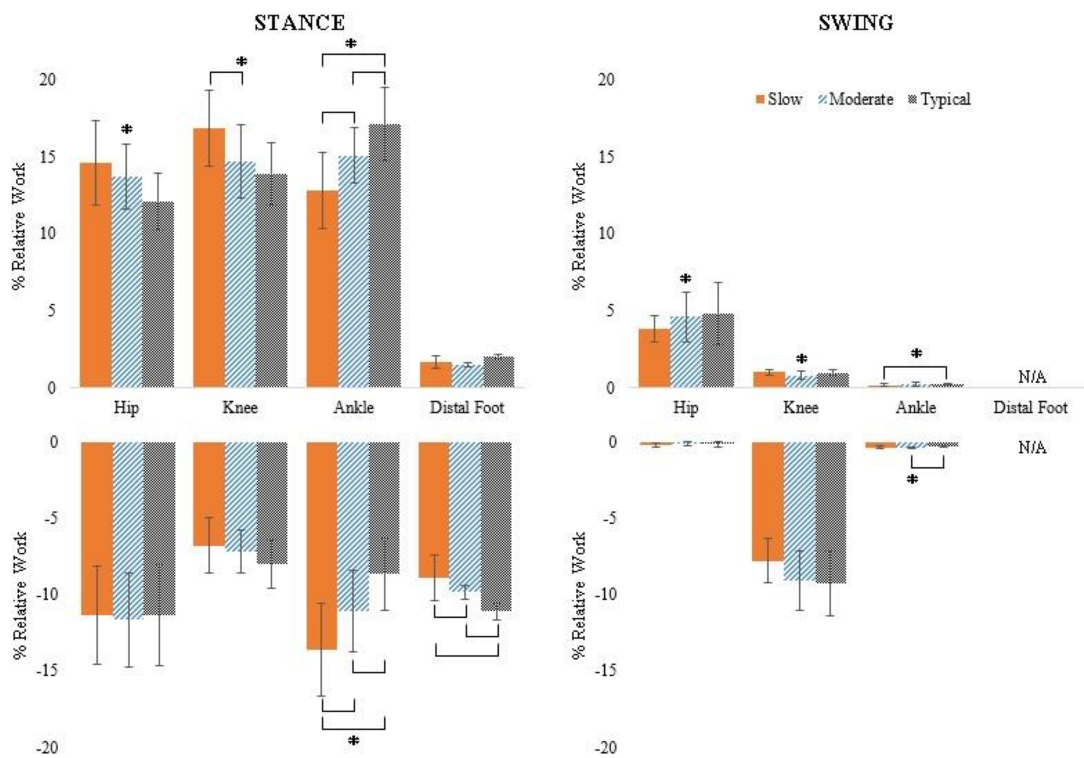

Figure 3.2: Positive and negative relative constituent work as a percentage of absolute limb work across speeds (mean with standard deviation error bars). Note, distal foot calculations are not applicable in swing phase as the foot is not in contact with the ground. A phase-by-speed interaction is denoted by an asterisk ($p < 0.05$) which indicates that the effect of speed is dependent on the phase (stance or swing). A bracketed bar indicates significant pairwise differences.

Table 3.1: Positive, negative, and absolute constituent work ($^{+}W_{constituent}$, $^{-}W_{constituent}$, and $^{abs}W_{constituent}$, respectively) and limb work ($^{+}W_{limb}$, $^{-}W_{limb}$, $^{abs}W_{limb}$, respectively) (mean ± standard deviation). Note, distal foot calculations are not applicable in swing phase as the foot is not in contact with the ground.

		Slow		*Moderate*		*Typical*	
		Stance	Swing	Stance	Swing	Stance	Swing
Hip	$^{+}W_{hip}$ (J/kg)	0.13 ± 0.03	0.03 ± 0.01	0.18 ± 0.05	0.06 ± 0.02	0.20 ± 0.06	0.08 ± 0.03
	$^{-}W_{hip}$ (J/kg)	0.11 ± 0.05	0.00 ± 0.00	0.15 ± 0.06	0.00 ± 0.00	0.19 ± 0.09	0.00 ± 0.00
	$^{abs}W_{hip}$ (J/kg)	0.24 ± 0.08	0.04 ± 0.01	0.33 ± 0.10	0.06 ± 0.02	0.40 ± 0.15	0.08 ± 0.03
Knee	$^{+}W_{knee}$ (J/kg)	0.16 ± 0.04	0.01 ± 0.00	0.19 ± 0.06	0.01 ± 0.00	0.23 ± 0.07	0.02 ± 0.00
	$^{-}W_{knee}$ (J/kg)	0.06 ± 0.02	0.07 ± 0.01	0.09 ± 0.03	0.11 ± 0.02	0.13 ± 0.04	0.15 ± 0.03
	$^{abs}W_{knee}$ (J/kg)	0.22 ± 0.05	0.08 ± 0.01	0.28 ± 0.07	0.12 ± 0.02	0.37 ± 0.10	0.17 ± 0.03
Ankle	$^{+}W_{ankle}$ (J/kg)	0.12 ± 0.05	0.00 ± 0.00	0.20 ± 0.06	0.00 ± 0.00	0.29 ± 0.08	0.00 ± 0.00
	$^{-}W_{ankle}$ (J/kg)	0.12 ± 0.03	0.00 ± 0.00	0.14 ± 0.04	0.00 ± 0.00	0.14 ± 0.04	0.01 ± 0.00
	$^{abs}W_{ankle}$ (J/kg)	0.25 ± 0.07	0.01 ± 0.00	0.34 ± 0.08	0.01 ± 0.00	0.43 ± 0.10	0.01 ± 0.00
Distal Foot	$^{+}W_{distal\ foot}$ (J/kg)	0.02 ± 0.01	N/A	0.02 ± 0.00	N/A	0.03 ± 0.01	N/A
	$^{-}W_{distal\ foot}$ (J/kg)	0.08 ± 0.01	N/A	0.12 ± 0.01	N/A	0.18 ± 0.02	N/A
	$^{abs}W_{distal\ foot}$ (J/kg)	0.10 ± 0.02	N/A	0.14 ± 0.02	N/A	0.22 ± 0.03	N/A
Limb	$^{+}W_{limb}$ (J/kg)	0.43 ± 0.11	0.05 ± 0.01	0.58 ± 0.14	0.07 ± 0.02	0.76 ± 0.18	0.10 ± 0.03
	$^{-}W_{limb}$ (J/kg)	0.38 ± 0.08	0.08 ± 0.01	0.51 ± 0.10	0.12 ± 0.02	0.65 ± 0.13	0.16 ± 0.03
	$^{abs}W_{limb}$ (J/kg)	0.80 ± 0.19	0.12 ± 0.02	1.09 ± 0.24	0.19 ± 0.04	1.41 ± 0.32	0.26 ± 0.06

3.5 Discussion

The purpose of this study was to use 6 DOF calculations of work to identify lower limb constituent adaptations that occur with increased walking speed. In healthy individuals without lower limb impairments, constituent work relative to absolute limb work calculations identified that primarily the relative work contributions of the ankle and distal foot in stance change with increases in walking speed (Fig. 3.2).

Relative constituent work characterizes how constituent contributions to gait change throughout the gait cycle, as well as how these contributions are affected by speed. In stance, the positive relative ankle work and negative relative distal foot work increased while the negative relative ankle work decreased with speed (Fig. 3.2). Interestingly, the absolute relative ankle work did not significantly differ with speed while the absolute relative distal foot work did significantly increase during stance (Table C.1 in Appendix C). The ratio of positive to negative relative work of the combined ankle-foot across speeds never exceeded 1, which supports previous findings that the combined ankle-foot acts similarly to a spring in terms of net energy storage and return (Takahashi and Stanhope, 2013).

A post hoc analysis found that the ratio of positive ankle work to negative distal foot work was similar across speeds (1.51, 1.58, and 1.57 for slow, moderate, and typical). This may suggest some coupling of the ankle-foot system. Similar coupling was found in a recent study where researchers used a footplate to artificially restrict metatarsal joint extension and decrease negative distal foot work which resulted in decreased positive ankle work (Arch and Fylstra, 2016). The compensation of work by either the ankle or foot when the other is restricted may be a result of a motor coordination strategy by the brain to maintain smooth and steady walking. However, others are investigating this coupling from a biomechanical approach to determine how the activity of the long toe flexors relates to ankle plantar flexor power during late stance (Honert and Zelik, 2016; Zelik et al., 2014). An understanding of whether a portion of the negative distal foot work is dissipated or transferred as positive work to the ankle joint by long toe flexors will affect the magnitude of muscle-tendon work generated or absorbed by the body, which is not accounted for in our model. Future studies will be necessary to conclude if the suggested ankle-foot coupling is due to motor coordination factors, biomechanical factors, or a combination of both.

Our results partially contradict findings from previous studies that used a sagittal approach (Chen et al., 1997; Teixeira-Salmela et al., 2008), where both positive and negative relative ankle work decreased with speed in the sagittal plane. Interestingly, our 6 DOF results agree with previous 3 DOF average power results for knee and hip work (Farris and Sawicki, 2012), indicating that the positive relative knee and hip work did not significantly differ with increased walking speeds. Using 6 DOF work calculations and including a distal foot constituent, Zelik and colleagues accounted for most of the residual positive net (summed positive and negative) 6 DOF limb work which was not previously accounted for using 3 DOF calculations (Zelik et al., 2015). Our finding in this study that the ankle-foot system shows significantly different contributions across walking speeds compared to previous studies using sagittal work calculations may provide further justification for the importance of 6 DOF work calculations and the inclusion of a distal foot term in limb energetics analyses, especially with regard to the ankle-foot complex.

The conclusions drawn from this study should be limited to healthy individuals walking at slow to typical walking speeds on a treadmill. Future studies could use relative constituent work calculations to quantify how constituent contributions may vary for atypical gait patterns. Determining how relative work may change bilaterally with use of a prosthetic device would improve our understanding of the primary constituents that drive compensatory gait strategies with increasing gait speed. Further investigations are needed to identify how relative constituent work adapts across faster walking speeds and for other tasks, like running (Riddick and Kuo, 2016).

This study provides novel information about the relative work contributions of the constituents of the lower limb using a 6 DOF analysis. For a population without impairments, the ankle-foot complex adapts to increasing walking speed. The relative constituent work profiles of a healthy limb presented here can be used as a guideline for comparison to speed-matched data from a limb with an impairment.

3.6 Acknowledgments

This material is based upon work supported by the National Science Foundation (NSF) Graduate Research Fellowship under Grant No. 1247394 and by the University of Delaware College of Health Sciences and the Mechanical Engineering department. The authors would like to thank Tom Kepple for assistance with data analysis, and Dr. Ryan Pohlig for assistance with statistical analysis. Any opinions, findings, and conclusions or recommendations expressed in this material are those of the authors and do not necessarily reflect the views of the NSF.

3.7 Glossary

Definition of terms

Adaptations	Changes or adjustments made by the lower limb and/or its constituents due to a change in gait intensity which in this case is increasing walking speed. Quantified by relative work.
Constituent work	The work done by a constituent (a joint or distal foot segment of the lower limb, i.e., hip, knee, ankle, distal foot). Modified by positive/negative/net/absolute; specified during a phase of gait (stance/swing). Notation: ${}^{Modifier}W_{constituent}$
Limb work	The work done by a limb; calculated as the summed work of the constituents. Modified by positive/negative/net/absolute; specified during a phase of gait (stance/swing) or over the gait cycle. Notation: ${}^{Modifier}W_{limb}$
Relative work	The percentage of absolute limb work done by a particular constituent; calculated as work of a particular constituent divided by absolute limb work over the gait cycle as a percentage. Modified by positive/negative/absolute and constituent name; specified during a phase of gait (stance/swing). Notation: ${}^{Modifier}RW_{constituent}$

List of Modifiers

Positive work	Quantifies energy “generation”; results from integrating the position portion of the constituent or limb power.

Negative work	Quantifies energy "absorption"; results from integrating the negative portion of the constituent or limb power.
Net work	Calculated as positive plus negative work.
Absolute work	Calculated as positive plus absolute value of negative work.

Chapter 4

CONSTITUENT LOWER EXTREMITY WORK (CLEW) APPROACH: A NOVEL TOOL TO VISUALIZE JOINT AND SEGMENT WORK (PUB: 2017)

(Ebrahimi, Goldberg, Wilken, and Stanhope, 2017)

4.1 Abstract

Work can reveal the mechanism by which movements occur. However, work is less physically intuitive than more common clinical variables such as joint angles, and are scalar quantities which do not have a direction. Therefore, there is a need for a clearly reported and comprehensively calculated approach to easily visualize and facilitate the interpretation of work variables in a clinical setting. We propose the Constituent Lower Extremity Work (CLEW) approach, a general methodology to visualize and interpret cyclic tasks performed by the lower limbs. Using six degree-of-freedom power calculations, we calculated the relative work of the four lower limb constituents (hip, knee, ankle, and distal foot). In a single pie chart, the CLEW approach details the mechanical cost-of-transport, the percentage of positive and negative work performed in stance phase and swing phase, and the individual contributions of positive and negative work from each constituent. This approach can be used to compare the constituent-level adaptations occurring between limbs of individuals with impairments, or within a limb at different gait intensities. In this article, we outline how to generate and interpret the CLEW pie charts in a clinical report. As an example of the utility of the approach, we created a CLEW report using average reference data from eight unimpaired adult subjects walking on a treadmill at

0.8 statures/s (1.4 m/s) compared with data from the intact and prosthetic limbs of an individual with a unilateral amputation walking with an above-knee passive prosthesis.

4.2 Introduction

Several researchers have used the principles of energetics to explain the compensatory strategies used by individuals with impairments (e.g., Cofré et al., 2011; Sawicki et al., 2009; Teixeira-Salmela et al., 2008). Relative joint work, or the comparative amount each joint's work contributed to absolute limb work, can reveal the primary limb "drivers" (positive) and "brakers" (negative) during a movement task like walking. However, work is less physically intuitive than more common clinical variables such as joint angles, partly because it is a scalar quantity which does not have a direction.

Previously, researchers have reported the work generated (positive) and absorbed (negative) by each of the joints using line (Chen et al., 1997; Teixeira-Salmela et al., 2008) and bar charts (Silverman et al., 2008). While these graphs can be used to compare joint work across gait intensity and between limbs of the same joint at one intensity, the overlapping lines and error bars can be confusing to interpret. There is a need for a clearly reported approach to visualize and facilitate the interpretation of work variables in a clinical setting.

The objective of this article is to introduce the Constituent Lower Extremity Work (CLEW) approach, a general methodology to visualize and interpret cyclic tasks performed by the lower limbs. The term "constituents" will be used to refer to the hip, knee, ankle, and distal foot of the limb. The utility of this tool is demonstrated by presenting a report with the relative work of the four lower limb constituents in both limbs of a sample of healthy, unimpaired individuals and in the prosthetic and intact limbs of an individual with a unilateral amputation walking on a treadmill.

4.3 Methods

As a representative case study, data were collected from an adult individual (height 1.68 m, mass 79.15 kg) walking on an instrumented treadmill (Bertec Corp., Columbus, OH) who required use of an above-knee prosthesis due to a congenital proximal femoral focal deficiency. Reflective markers were positioned using a modification of a six degree-of-freedom (6 DOF) marker set (Holden et al., 1997). A seven-camera motion capture system was used to collect kinematic data (Motion Analysis, Santa Rosa, CA). Motion capture and force data were sampled at 240 Hz and 1200 Hz and low-pass filtered at 6 Hz and 25 Hz, respectively. These data were compared to data from unimpaired subjects collected as part of a previous study (Goldberg and Stanhope, 2013) in which eight healthy adult subjects (height 1.77 ± 0.08 m, mass 71.8 ± 15.5 kg) walked on an instrumented treadmill (Bertec Corp., Columbus, OH) while a six-camera motion capture system was used to collect kinematic data (Vicon, Los Angeles, CA) using the same marker set. All subjects walked at a height-scaled speed of 0.8 statures/s (~1.4 m/s) and provided informed consent under an IRB approved protocol.

Methods previously described in the literature (Buczek et al., 1994; Takahashi and Stanhope, 2013) were used to calculate 6 DOF constituent powers in Visual3D software (C-Motion, Inc. Germantown, MD). A unified deformable segment model was used to characterize the power from the below-knee structures (i.e., combined ankle-foot) of the prosthetic limb during stance phase of the amputee subject (Takahashi et al., 2012).

Integrating the positive and negative portions of the constituent power curves over stance and swing phases resulted in the respective constituent work values. The absolute 6 DOF limb work ($^{abs}W_{limb}$) was defined as positive limb work summed with the absolute value of negative limb work over the gait cycle (where limb work is defined as summed hip, knee, ankle, and distal foot work). The cost-of-transport is $^{abs}W_{limb}$ scaled by stride length. Relative work (RW) was the absolute value of each constituent's work divided by the absolute 6 DOF limb work. Net limb work was the sum of the positive and negative 6 DOF limb work over both phases. Work values were scaled by body mass and averaged for all unimpaired subjects. Distal foot calculations were not relevant during swing phase. The CLEW approach pie charts were created using the steps depicted in Fig. 4.1.

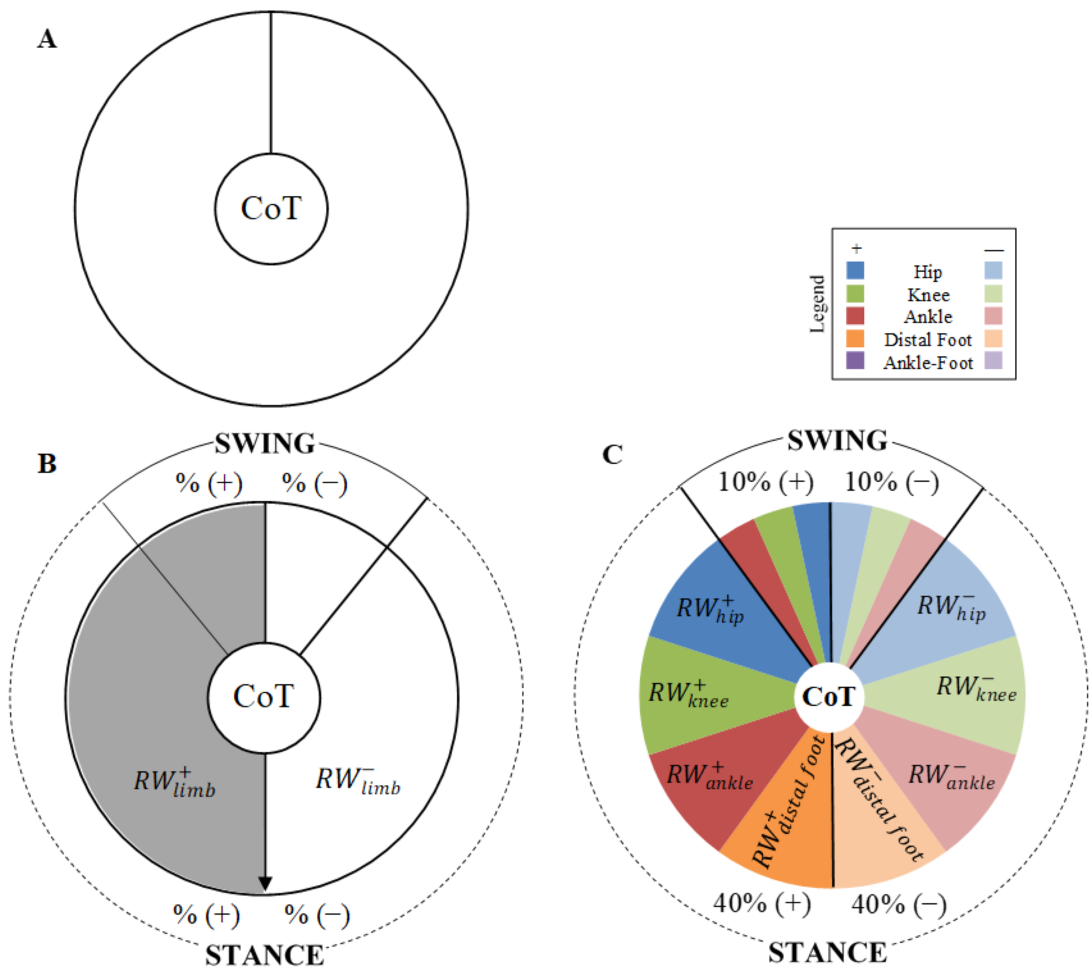

Figure 4.1: Steps for creating the CLEW approach pie charts for gait. (A) First, the area of the pie chart is scaled to the cost-of-transport (COT). Here 1 J/kg/m is a circle with area of 25.0 cm^2. The central reference line is defined from the center of the circle to the top. The COT is displayed in the center of the pie chart in a white circle. (B) Second, the relative constituent work contributions to absolute 6 DOF limb work during swing phase are grouped together and designated visually by a partial pie slice. From the central reference line, positive work will be to the left side of the circle (dark), while negative work is to the right (light). (C) Third, each relative constituent work is designated its portion of the pie, in the order of hip, knee, ankle, and distal foot (or ankle-foot) for swing, then stance, beginning from the central reference line. The net work line at the bottom of the circle separates the positive from the negative work in stance phase.

4.4 Results

Average net 6 DOF limb work, absolute 6 DOF limb work, stride length, and cost-of-transport are all reported in Table 4.1 for the left and right limbs of the unimpaired individuals (mean ± standard deviation) and the individual with amputation (hereafter noted as subject data). Fig. 4.2 depicts a typical clinical CLEW report. Fig. 4.2A summarizes the steps for systematically evaluating a subject's CLEW pie chart and a short interpretation of each variable. Fig. 4.2B provides an example of a typical CLEW report with reference data from the unimpaired individuals and a subject's data from the individual with a unilateral amputation. Table C.2 in Appendix C lists the relative constituent work values for the unimpaired individuals and the subject during stance and swing phases of gait.

Table 4.1: Net and absolute 6 DOF limb work, stride length, and cost-of-transport for average of a sample (n = 8) of unimpaired individuals (mean ± standard deviation), as well as for an individual subject (n = 1) with a unilateral amputation wearing an above-knee prosthesis.

	Unimpaired (n = 8)		**Subject (n = 1)**	
	Left	Right	Prosthetic	Intact
${}^{net}W_{limb}$ (J/kg)	0.05 ± 0.05	0.11 ± 0.09	0.02	-0.06
${}^{abs}W_{limb}$ (J/kg)	1.66 ± 0.31	1.62 ± 0.28	0.90	1.77
Stride length (m)	1.36 ± 0.14	1.36 ± 0.14	1.34	1.19
Cost-of-transport (J/kg/m)	1.22 ± 0.15	1.19 ± 0.14	0.67	1.49

A

CLEW Report: General Approach

Task: (e.g. walking, sit-to-stand)
Phase: (e.g. stance, swing)
Scale: (e.g. cost-of-transport scaled to area of pie)

Legend

+		—
	Hip	
	Knee	
	Ankle	
	Distal Foot	
	Ankle-Foot	

REFERENCE DATA

Examples of Reference data (left and/or right):
- Average data from individuals without impairments
- Average data from individuals with the same impairment as the Subject
- A prior assessment from the same Subject

Key for Constituents:
H: Hip, **K:** Knee, **A:** Ankle, **F:** Distal Foot, **AF:** Ankle-Foot*
Relative work not labeled for pie slices <2%

SUBJECT LIMBS

Steps	Interpretation	Figure
1a. The area (size) of the pie chart represents total cost-of-transport (CoT). Compare total CoT between limbs. **1b.** Compare the Subject's total CoT to the Reference.	**CoT:** Area corresponds to total burden of work for the limb **CoT$_{total}$:** Numerical presentation of total burden of work (sum of limbs)	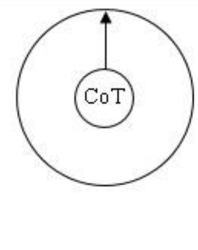
2a. Compare the portion of positive (+) and negative (-) relative work (RW) within the same limb (within or between stance and swing phase). **2b.** Compare the portion of summed (+) and (-) relative work between limbs and relative to the reference data.	(+): "Drivers" (−): "Brakers" **RW$_{limb}$:** Contribution of work performed by limb	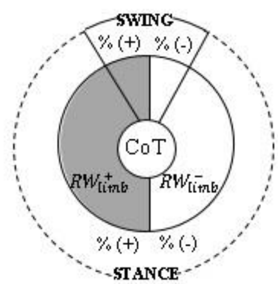
3. Compare positive and negative RW of constituents in each phase to respective constituents of opposite limb and to the Reference data.	**RW$_{constituent}$:** Percent work contributed by each constituent (hip; knee; ankle and distal foot or unified deformable ankle-foot)	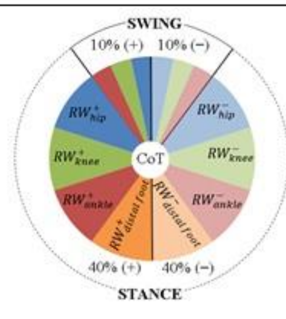

*See *Takahashi et al., 2012.*

Figure 4.2A: General approach for evaluating data from the CLEW report. This guide can be used to assess the CLEW pie charts systematically. Note, if unimpaired reference data are used, left and right limbs may be grouped together when appropriate.

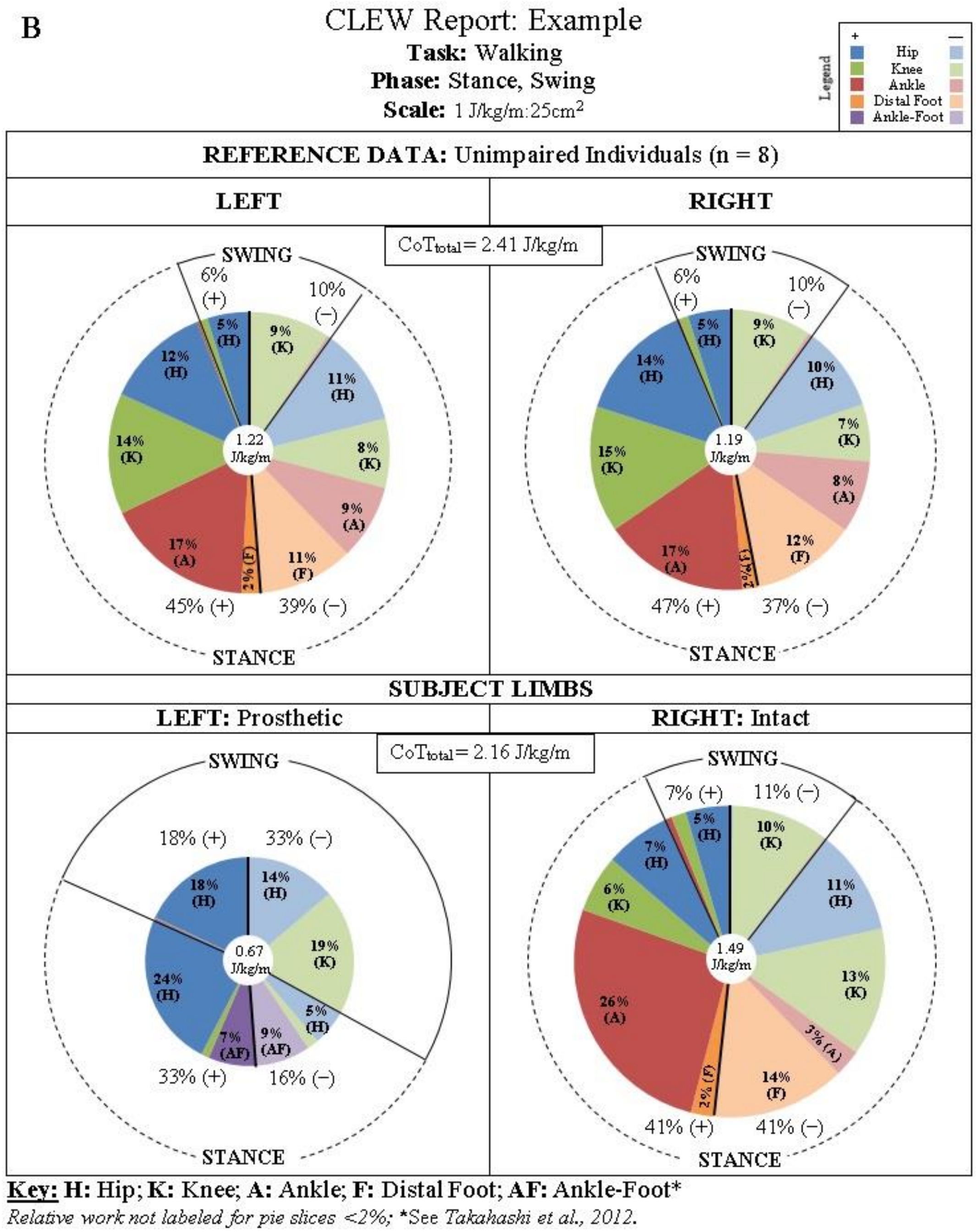

Figure 4.2B: Example CLEW report with average data from unimpaired individuals (n = 8) walking at 0.8 statures/s serving as reference data. Subject data are from an individual with a unilateral amputation (n = 1) walking at 0.8 statures/s. The unified deformable segment model (Takahashi et al., 2012) was used to characterize the work from the below-knee structures of the prosthetic limb during stance phase, noted here as ankle-foot (AF).

4.5 Discussion

The purpose of this study was to introduce the CLEW approach and demonstrate its utility in quantifying relative constituent work in a succinct and visually informative manner. The size of the pie charts, representing the mechanical cost-of-transport, provides a spatial relationship to interpret the total burden of work for the limb. The designation of positive and negative relative constituent work provides a way to readily compare the contribution of work from each constituent during the stance and swing phases of gait, thus identifying the primary "drivers" and "brakers" of the system.

The CLEW approach pie charts (as in Fig. 4.2B) may be clinically useful as a way to characterize the burden of work over an entire stride rather than an instant in time. For example, visual inspection of the size of the pie charts (scaled by cost-of-transport) appears to show greater burden of work (i.e., more absolute 6 DOF limb work) on the intact limb (1.49 J/kg/m) than on the prosthetic limb (0.67 J/kg/m) and compared to the unimpaired limbs (1.22 ± 0.15 J/kg/m on left and 1.19 ± 0.14 J/kg/m on right). On the prosthetic side, there is almost equal relative limb work (summed positive and negative) from stance (49%) and swing (51%), with a majority of the work from the positive hip (24% in stance, 18% in swing). A clinician may use this information to test a powered prosthetic device to reduce the burden of work on the intact limb and the hip work on the prosthetic limb, as may be hypothesized from the literature (Au et al., 2009).

Future clinical studies will be necessary to determine how a clinical treatment affects the work distribution of the limb. The CLEW approach may be applicable to the upper extremity as well, although this application was not explored here. This was a convenient sample of eight healthy, unimpaired adults, so the values represented here may not be representative of a larger population. A limitation of the 6 DOF approach is that it does not fully capture work due to soft tissue dissipation (Zelik et al., 2015).

The CLEW approach is a comprehensive data visualization tool for representing limb work over a cyclic task, such as over a stride in gait. In a single figure, the CLEW approach details the mechanical cost-of-transport, the percentage of positive and negative work performed in stance phase and swing phase, as well as the individual contributions of positive and negative work from each constituent. Furthermore, the approach can be used to compare the constituent-level adaptations occurring between limbs of individuals with impairments, or within a limb at different gait intensities.

4.6 Acknowledgments

This material is based upon work supported by the National Science Foundation Graduate Research Fellowship under Grant No. 1247394 and by the University of Delaware College of Health Sciences and Mechanical Engineering departments. Any opinions, findings, and conclusions or recommendations expressed in this material are those of the author(s) and do not necessarily reflect the views of the National Science Foundation. This project was also supported by the BADER consortium, a Department of Defense Congressionally Directed Medical Research Programs cooperative agreement (W81XWH-11-2-022). The views expressed do not necessarily reflect those of the Department of the Navy, Department of Defense or U.S. Government.

Chapter 5

A MATHEMATICAL ANALYSIS TO ADDRESS THE 6 DEGREE-OF-FREEDOM SEGMENTAL POWER IMBALANCE (PUB: 2018)

(Ebrahimi, Collins, Kepple, Takahashi, Higginson, and Stanhope, 2018)

5.1 Abstract

Segmental power is used in human movement analyses to indicate the source and net rate of energy transfer between the rigid bodies of biomechanical models. Segmental power calculations are performed using segment endpoint dynamics (kinetic method). A theoretically equivalent method is to measure the rate of change in a segment's mechanical energy state (kinematic method). However, these two methods have not produced experimentally equivalent results for segments proximal to the foot, with the difference in methods deemed the "power imbalance." In a 6 degree-of-freedom model, segments move independently, resulting in relative segment endpoint displacement and non-equivalent segment endpoint velocities at a joint. In the kinetic method, a segment's distal end translational velocity may be defined either at the anatomical end of the segment or at the location of the joint center (defined here as the proximal end of the adjacent distal segment). Our mathematical derivations revealed the power imbalance between the kinetic method using the anatomical definition and the kinematic method can be explained by power due to relative segment endpoint displacement. In this study, we tested this analytical prediction through experimental gait data from nine healthy subjects walking at a typical speed. The average absolute segmental power imbalance was reduced from 0.023 to 0.046

W/kg using the anatomical definition to ≤0.001 W/kg using the joint center definition in the kinetic method (95.56 – 98.39% reduction). Power due to relative segment endpoint displacement in segmental power analyses is substantial and should be considered in analyzing energetics flow into and between segments.

5.2 Introduction

A segmental power analysis is a useful biomechanical tool (Caldwell and Forrester, 1992), which has been used in analyzing human movement to indicate the source and net rate of energy transfer (flow) between the rigid bodies of biomechanical models (Aleshinsky, 1986; Robertson and Winter, 1980; van Ingen Schenau and Cavanagh, 1990). Segmental power calculations utilize segment endpoint dynamics (kinetic method), but a theoretically equivalent method is to measure changes in the segment's energy state (kinematic method) (Zajac et al., 2002). Several researchers have used independent measures of segmental power to explain how power flow between segments relates to changes in the energy state of the segments in activities like walking (Aleshinsky, 1986; Caldwell and Forrester, 1992; Robertson and Winter, 1980; Zelik et al., 2015), pedaling (Kautz et al., 1994; Kautz and Neptune, 2002), running (Caldwell and Forrester, 1992), wheelchair propulsion (Guo et al., 2003), lifting (de Looze et al., 1992), and various endurance sports (van Ingen Schenau and Cavanagh, 1990). Researchers have also used this mathematical equivalence to assess the accuracy of specific models (McGibbon and Krebs, 1998) based on how closely powers calculated using the kinetic method match with those using the kinematic method. Several investigators theorized the kinematic method is more accurate as it is based only on motion and anthropometric estimates (Caldwell and Forrester, 1992; Robertson and Winter, 1980).

The models and corresponding model assumptions used to analyze segmental power flow influence how results may be interpreted. A pin-joint model, which fixes segment ends at a coincident point, has been used for two- (i.e., sagittal plane) or three-dimensional gait analyses (de Looze et al., 1992; McGibbon and Krebs, 1998; Robertson and Winter, 1980). However, use of the pin-joint model may require segment lengths and inertial alignment (e.g., segment center of mass position) to change due to a shared joint center with adjacent segments, thus violating rigid body assumptions. Conversely, a 6 degree-of-freedom (6 DOF) model for three-dimensional gait analyses fixes segment characteristics, which can lead to relative displacement between adjacent segment ends, and thus non-equivalent segment endpoint velocities at a joint (Buczek et al., 1994; McGibbon and Krebs, 1998). While both models have limitations, the translational power resulting from the intersegmental joint force and the segment endpoint velocities in a 6 DOF model is valuable to include for a complete mechanical energy analysis of human gait (Buczek et al., 1994; Geil et al., 2000; Zelik et al., 2015).

Independent of chosen model, the kinetic and kinematic methods typically do not provide experimentally equivalent results, leading to a “power imbalance” (PI) (McGibbon and Krebs, 1998). Using a three-dimensional analysis, McGibbon and Krebs reported using the pin-joint model resulted in a mean absolute PI over stance ranging from 9.9 – 25.6 W for the shank and 6.8 – 23.4 W for the thigh. The mean absolute PI was reduced when segment lengths were fixed and radial velocities of the distal and proximal ends of the segment relative to the segment’s center of mass were accounted for (1.1 – 5.0 W and 0.7 – 4.1 W for the shank and thigh, respectively). However, while fixed segment lengths reduced the PI within a segment, there was a large power discrepancy between segment ends across a joint (e.g., 10.7 – 37.8 W at the knee), which was considered an “energy well” (McGibbon and Krebs, 1998).

Thus, identifying the source of the PI is important for effectively characterizing energetics measures in the study of human movement. To date, the foot is the only segment whose PI was computationally accounted for by the inclusion of a calculation for distal foot segmental power (Siegel et al., 1996).

The purpose of this study was to determine the source of PI by conducting a mathematical analysis to equate the kinematic and kinetic methods for a 6 DOF model. We theorized accounting for power due to relative displacement between the distal end of a segment and the joint center in the kinetic model (relative displacement power) would reduce the PI. We then experimentally characterized the PI with and without accounting for the relative displacement power.

5.3 Computational Development

Using Newton-Euler formulas (Siegler and Liu, 1997) in inverse dynamics calculations (Robertson et al., 2013), the general form for the proximal joint intersegmental force ($\vec{F}_{p,m}$) for any segment *m*, linked by *n* number of segments, is given by Equation 1, where m_m, $\vec{a}_m$, $\vec{g}$, and $\vec{F}_{grf}$ represent the segment mass, segment center of mass acceleration, gravity (9.81 m/s^2), and ground reaction force, respectively. Similarly, the proximal net joint moment ($\vec{M}_{p,m}$) is given by Equation 2 where I_m, $\vec{\alpha}_m$, $\vec{\omega}_m$, and $\vec{\tau}_{free}$ represent the moment of inertia, angular acceleration, angular velocity, and free moment, respectively. The $\vec{r}_{COM,n/m}$ and $\vec{r}_{COP,m}$ are vectors from the proximal end of the m^{th} segment end to the center of mass of the n^{th} segment and to the center of pressure, respectively (Fig. 5.1).

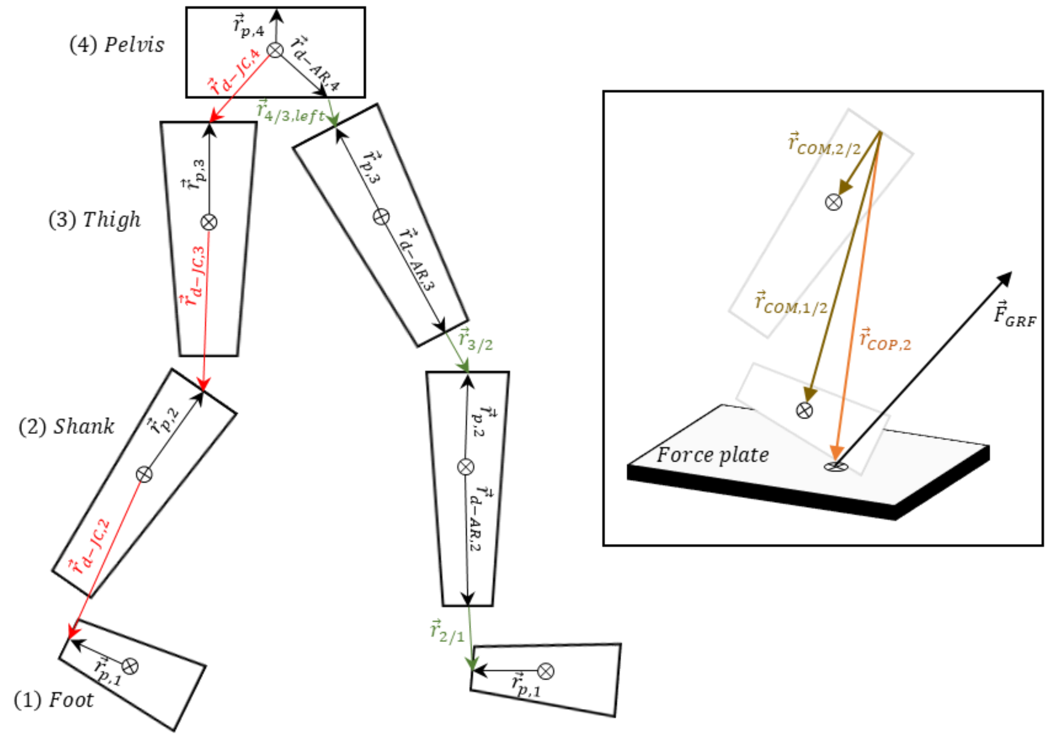

Figure 5.1: Visual representation of vectors used in inverse dynamics calculations for a 6 DOF multi-segment model. Here, segment *m* is numbered 1, 2, 3, and 4 which can represent the foot, shank, thigh, and pelvis, respectively. The model shows position vectors from a segment center of mass to the proximal segment end ($\vec{r}_{p,m}$) as well as to the distal segment end using the anatomically relevant (AR) definition ($\vec{r}_{d-AR,m}$) or the joint center (JC) definition ($\vec{r}_{d-JC,m}$). The displacement vector ($\vec{r}_{m/m-1}$) is defined from the AR distal end of the proximal segment *m* relative to the proximal end of the distal segment $m-1$ (i.e., joint center). Note that all segments are modelled equally, and representations being different on the two limbs are for clarity only. For the pelvis, the displacement vector is from the right or left hip joint center in the pelvis coordinate system (as defined by the static model pose) to the proximal end of the respective thigh. Inset shows notation for the position vectors $\vec{r}_{COM,n/m}$ and $\vec{r}_{COP,m}$ from the proximal segment end to the center of mass of the n^{th} segment (where *n* is less than or equal to *m*) and to the center of pressure, respectively.

$$\vec{F}_{p,m} = [\sum_{n=1}^{m}(m_n\vec{a}_n - m_n\vec{g})] - \vec{F}_{grf} \tag{1}$$

$$\vec{M}_{p,m} = [\sum_{n=1}^{m}(I_n\vec{\alpha}_n + \vec{\omega}_n \times I_n\vec{\omega}_n + \vec{r}_{COM,\mathrm{n/m}} \times (m_n\vec{a}_n - m_n\vec{g}))] - \vec{\tau}_{free} - \vec{r}_{COP,m} \times \vec{F}_{grf} \tag{2}$$

The proximal segment translational velocity is given by Equation 3 where $\vec{r}_{p,m}$ is the vector from the center of mass to the proximal (p) end of the segment, and the segment velocity is represented by $\vec{v}_m$.

$$\vec{v}_{p,m} = \vec{v}_m + \vec{\omega}_m \times \vec{r}_{p,m} \tag{3}$$

In an anatomically relevant (AR) definition, distal translational velocity is given by Equation 4 where $\vec{r}_{d-AR,m}$ is the vector from the center of mass to the distal (d) end of the segment.

$$\vec{v}_{d-AR,m} = \vec{v}_m + \vec{\omega}_m \times \vec{r}_{d-AR,m} \tag{4}$$

However, the AR definition of distal velocity is not always coincident with the point of force application (i.e., the joint center), which is defined here as the proximal end of the adjacent distal segment (Fig. 5.1). Therefore, there exists a displacement vector ($\vec{r}_{m/m-1}$) between the distal end of segment *m* and proximal end of segment *m−1* with a velocity given by Equation 5.

$$\vec{v}_{m/m-1} = \vec{\omega}_m \times \vec{r}_{m/m-1} \tag{5}$$

In a joint center (JC) definition, distal translational velocity is given by Equation 6 where $\vec{r}_{d-JC,m}$ is the vector from the center of mass to the joint center. This vector is equivalent to the sum of $\vec{r}_{d-AR,m}$and $\vec{r}_{m/m-1}$ (Fig. 5.1).

$$\vec{v}_{d-JC,m} = \vec{v}_m + \vec{\omega}_m \times \vec{r}_{d-JC,m} = \vec{v}_m + \vec{\omega}_m \times (\vec{r}_{d-AR,m} + \vec{r}_{m/m-1}) \tag{6}$$

Segmental power using the <u>kinetic method</u> can be calculated using the AR definition ($P_{AR,m}$) in Equation 7, where distal joint intersegmental force and net joint moment are represented by $\vec{F}_{d,m}$ and $\vec{M}_{d,m}$, respectively. The pelvis segment (*m* = 4) is calculated using proximal powers as well as left and right $\vec{F}_{d,4}$ and $\vec{M}_{d,4}$. The $\vec{r}_{d-AR,4}$ is from the center of mass to the left or right hip joint center positions in the pelvis coordinate system (as defined in the static model pose).

$$P_{AR,m} = \vec{M}_{p,m} \cdot \vec{\omega}_m + \vec{M}_{d,m} \cdot \vec{\omega}_m + \vec{F}_{p,m} \cdot \vec{v}_{p,m} + \vec{F}_{d,m} \cdot \vec{v}_{d-AR,m} \tag{7}$$

Segmental power calculated using the JC definition ($P_{JC,m}$) can be represented using Equations 6 and 7 as shown in Equation 8a. The power due to the displacement between segment ends of adjacent segments, or relative displacement power ($P_{m/m-1}$), is shown in Equation 8b.

$$P_{JC,m} = \vec{M}_{p,m} \cdot \vec{\omega}_m + \vec{M}_{d,m} \cdot \vec{\omega}_m + \vec{F}_{p,m} \cdot \vec{v}_{p,m} + \vec{F}_{d,m} \cdot \vec{v}_{d-JC,m} = P_{AR,m} + P_{m/m-1} \tag{8a}$$

where

$$P_{m/m-1} = \vec{F}_{d,m} \cdot \vec{v}_{m/m-1} \tag{8b}$$

Equations 1- 3 and 6 can be substituted into Equation 8a to achieve Equation 9 (see Derivation for complete details).

$$\begin{aligned} P_{JC,m} &= \vec{M}_{p,m} \cdot \vec{\omega}_m + \vec{M}_{d,m} \cdot \vec{\omega}_m + \vec{F}_{p,m} \cdot \vec{v}_{p,m} + \vec{F}_{d,m} \cdot \vec{v}_{d-JC,m} \\ &= (I_m\vec{\alpha}_m + \vec{\omega}_m \times I_m\vec{\omega}_m) \cdot \vec{\omega}_m + (m_m\vec{a}_m - m_m\vec{g}) \cdot \vec{v}_m - (\vec{r}_{COP,m} \times \vec{F}_{grf}) \cdot \\ &\quad \vec{\omega}_m + (\vec{r}_{COP,m-1} \times \vec{F}_{grf}) \cdot \vec{\omega}_m - \vec{F}_{grf} \cdot (\vec{\omega}_m \times \vec{r}_{p,m}) + \vec{F}_{grf} \cdot (\vec{\omega}_m \times \vec{r}_{d-AR,m}) + \\ &\quad \vec{F}_{grf} \cdot (\vec{\omega}_m \times \vec{r}_{m/m-1}) \end{aligned} \tag{9}$$

The rate of energy change ($\frac{d}{dt}E_m$) using the <u>kinematic method</u> is calculated in Equation 10, which sums the rotational kinetic, translational kinetic, and gravitational potential segmental energy. Note $\frac{d}{dt}E_m$ is computationally equivalent to $P_{JC,m}$ from Equation 9 because the vector $-\vec{r}_{COP,m}$ will cancel with the summed vectors -$\vec{r}_{p,m}$, $\vec{r}_{d-AR,m}$, $\vec{r}_{m/m-1}$and, $\vec{r}_{COP,m-1}$ using the properties of cross and dot products.

$$\frac{d}{dt}E_m = (I_m\vec{\alpha}_m + \vec{\omega}_m \times I_m\vec{\omega}_m) \cdot \vec{\omega}_m + m_m\vec{a}_m \cdot \vec{v}_m - m_m\vec{g} \cdot \vec{v}_m \qquad (10)$$

5.4 Experimental Method

Experimental data were derived from a coded database of nine healthy subjects (34 ± 10 years, 1.69 ± 0.10 m, 75.6 ± 16.2 kg), consented under an IRB approved protocol, walking with standard shoes on an instrumented treadmill (Bertec Corp., Columbus, OH). Kinematic data were collected using a seven-camera motion capture system (Motion Analysis, Santa Rosa, CA). Motion capture and force data were sampled at 240 Hz and 1200 Hz and low-pass filtered at 6 Hz and 25 Hz, respectively, and analyzed in Visual3D software (C-Motion, Inc. Germantown, MD). Reflective markers were placed on subjects using a modification to a previously reported marker configuration (Holden et al., 1997). Subjects walked at a height-scaled speed of 0.8 statures/s (approximately 1.4 m/s).

A minimum of 10 strides for the pelvis, left thigh, and left shank were analyzed. In the AR definition, the distal end of a segment was defined in the static model pose and tracked using marker clusters. In the JC definition, the location of the joint center, was determined on a frame-by-frame basis. All power terms were averaged across all subjects and scaled by body mass. Pelvis segmental power was the sum of powers at the left and right hip as well as the proximal pelvis. For each subject, the PI was calculated as the difference between the kinematic method and the kinetic method using the AR definition ($PI_{AR,m}$) or the JC definition ($PI_{JC,m}$) on a frame-by-frame basis across the gait cycle. Maximum and minimum PI were calculated along with the mean PI over the gait cycle for each subject and overall. Mean absolute PI was defined by the absolute value of the PI frame-by-frame averaged across the gait cycle. Mean absolute relative displacement power for the left and right hips are quantified in Table C.3 in Appendix C.

5.5 Results

The experimental segmental powers (Fig. 5.2) and PI (Figs. 5.3–5.4) revealed $P_{m/m-1}$ accounted for nearly all $PI_{AR,m}$. The average absolute segmental PI was reduced from 0.046 ± 0.015 W/kg, 0.034 ± 0.008 W/kg, and 0.023 ± 0.015 W/kg for the shank, thigh and pelvis, respectively, using the anatomical definition to ≤0.001 ± 0.000 W/kg using the joint center definition in the kinetic method. For context, the percent difference between these two measures was 98.4%, 95.7%, and 95.6% for the shank, thigh, and pelvis, respectively.

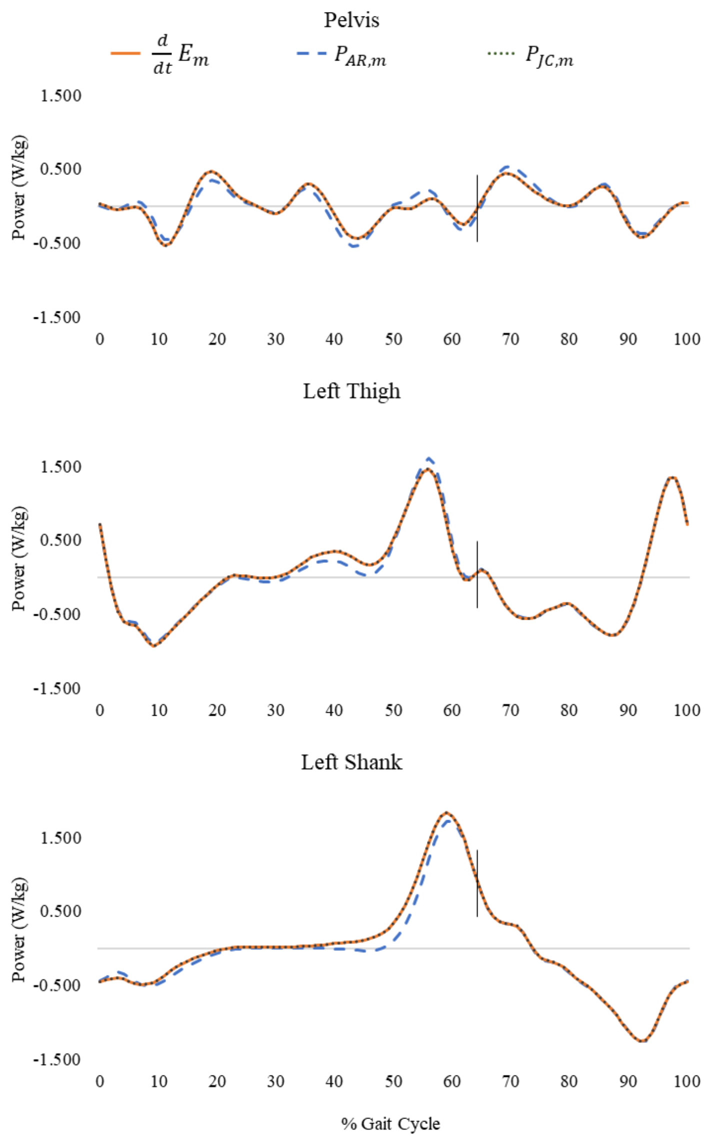

Figure 5.2: A noticeable power imbalance exists between segmental power using the anatomically relevant kinetic method ($P_{AR,m}$) and the rate of energy change using the kinematic method ($\frac{d}{dt}E_m$) over 100% of the gait cycle for a representative subject (where *m* represents the pelvis, left thigh, or left shank). The power imbalance is reduced between the segmental power using the joint center kinetic method ($P_{JC,m}$) and $\frac{d}{dt}E_m$. The power imbalance during swing phase (indicated to the right of the vertical black line at 64.3%) is much smaller than in stance phase due in part to the relatively small power during this phase where there is no ground reaction force.

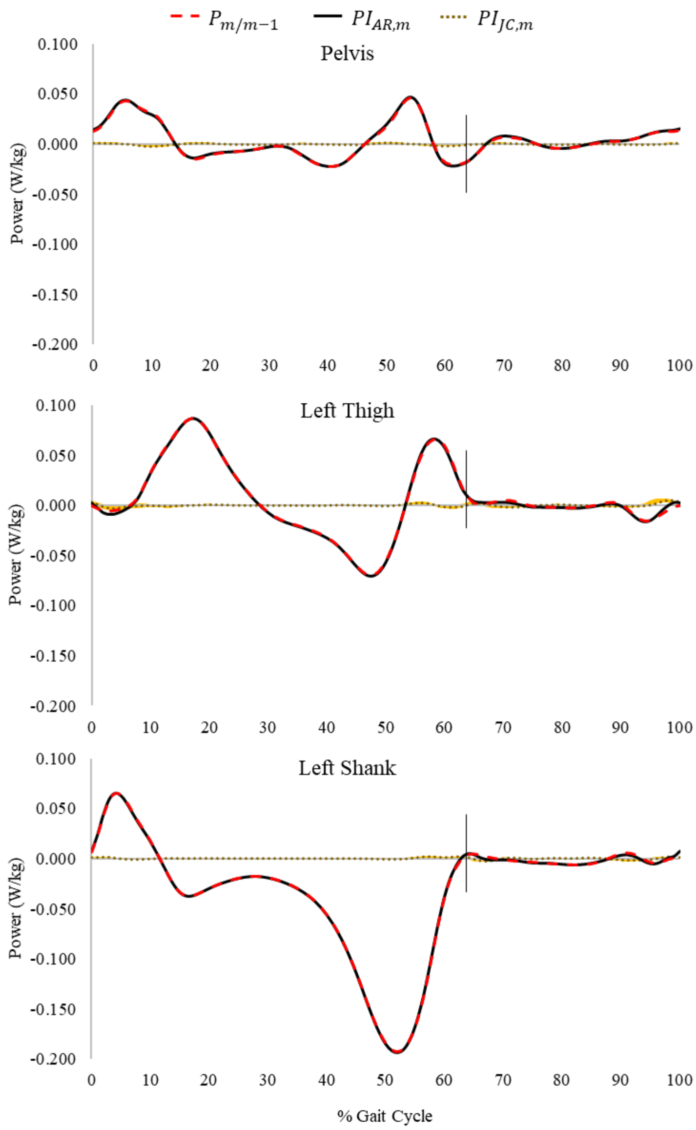

Figure 5.3: Average power imbalance between the segmental rate of energy change and the anatomically relevant kinetic method ($PI_{AR,m}$) is almost completely explained by the average power due to the relative segment endpoint displacement ($P_{m/m-1}$), as seen graphed over 100% of the gait cycle (where m represents the pelvis, left thigh, or left shank). Average (±1 standard deviation in yellow) power imbalance between the segmental rate of energy change and the joint center kinetic method ($PI_{JC,m}$) is relatively small in comparison to $PI_{AR,m}$. The range of $P_{m/m-1}$ is smaller in swing phase (indicated to the right of the vertical black line at 63%) than in stance for all three segments, and largest in the left shank compared to the thigh and pelvis over stance phase.

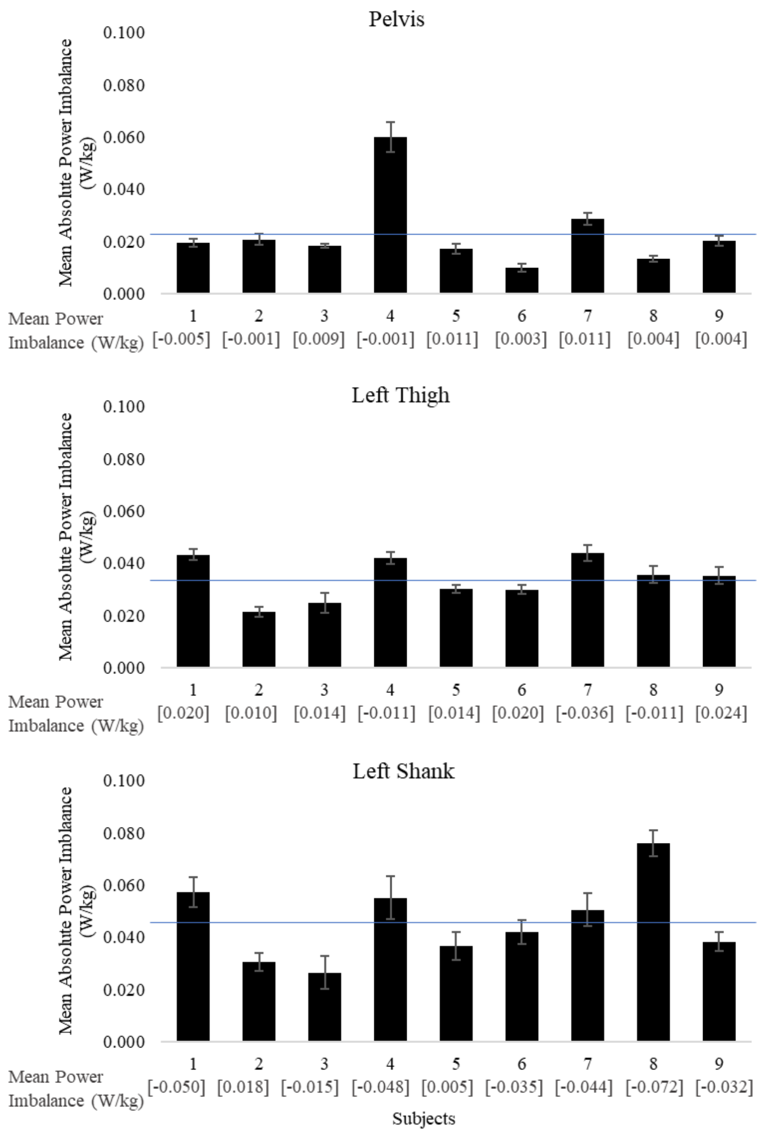

Figure 5.4: The mean (±1 standard deviation error bars) absolute power imbalance between the segmental rate of energy change and the anatomically relevant kinetic method ($|PI_{AR,m}|_{\text{mean}}$) averaged across a minimum of 10 gait cycles for each subject shows the inter-subject variability. Overall $|PI_{AR,m}|_{\text{mean}}$ across all subjects (indicated by the blue horizontal line) was 0.046 ± 0.015 W/kg, 0.034 ± 0.008 W/kg, and 0.023 ± 0.015 W/kg for the shank, thigh, and pelvis, respectively. The mean $PI_{AR,m}$ (bracketed numbers under subject data) further highlight the inter-subject variability, revealing no clear pattern in sign or magnitude of mean power imbalance across subjects.

5.6 Discussion

The mathematical analysis presented explains how the segmental PI between segmental power and rate of energy change is influenced by the definition of the distal translational velocity term. An AR definition of the distal translational velocity ignores the relative displacement of segment ends at a joint, resulting in a PI. A JC definition includes a relative displacement power ($P_{m/m-1}$) to accurately equate segmental power and rate of energy change mathematically.

The $P_{m/m-1}$ term computationally accounts for the $PI_{AR,m}$. The addition of the displacement vector $\vec{r}_{m/m-1}$ represents the magnitude of separation at the joint. The cross product of $\vec{\omega}_m$ and $\vec{r}_{m/m-1}$ is a result of relative motion physics (similar in concept to the previously derived distal foot velocity (Siegel et al., 1996)) which represents the relative translational velocity due to the separation of segment ends of the joint. While $P_{m/m-1}$ is included in the m^{th} segment because of our joint center definition, it is a result of imperfect modeling of the instantaneous joint center using marker based motion capture techniques.

Fig. 5.3 and 5.4 show the magnitude of $P_{m/m-1}$ – previously referred to as an "energy well" (McGibbon and Krebs, 1998) – is substantial. Interestingly, the pelvis had the lowest mean absolute PI. Table C.3 in Appendix C supports the possibility that relative displacement power at the left and right hips negate each other at parts of the gait cycle. 6 DOF joint power calculations use the JC definition of distal translational velocity (eq. 6), which inherently include the $P_{m/m-1}$ as originally intended when presented by Buczek and colleagues (Buczek et al., 1994). For explicit clarity, the 6 DOF joint powers include a change in velocity vector (Δv_{joint}) which denotes the difference in segment end velocities at the coincident location of the joint center (Buczek et al., 1994).

Irrespective of whether $\vec{r}_{m/m-1}$ is due to measurement artefact or physiological separation between segment ends at a joint, the translational velocity terms are a necessary inclusion for joint power calculations using 6 DOF models. If the source of $\vec{r}_{m/m-1}$ is due to measurement artefact (e.g., soft tissue movement), then $\vec{r}_{m/m-1}$ will affect segmental angular velocities used to calculate rotational powers. Thus, the true joint power is not better estimated by rotational terms alone. In fact, the results show $P_{m/m-1}$ would be equivalent to the $PI_{AR,m}$ if the primary source of error was joint displacement artefact. Furthermore, if $\vec{r}_{m/m-1}$ is physiological (rather than artefactual), then the same conclusion is reached – translational velocity terms in 6 DOF joint power calculations should not be disregarded.

Although the JC definition for the kinetic method theoretically equates the kinetic and kinematic methods, there remains a small (≤0.001 W/kg) average absolute experimental PI. All measures derived from motion and force data are estimates that contribute to errors not shared equally between the kinetic and kinematic methods. Regarding the tracking of motion data, errors may arise from accessory motion of skin-mounted markers due to soft tissue movement making segment endpoints inaccurate (violating rigid body assumptions) and missing axes of rotation (McGibbon and Krebs, 1998; van Ingen Schenau and Cavanagh, 1990; Zajac et al., 2002; Zelik et al., 2015). Regarding the measurement of force data, errors may arise from locating the center of pressure or from estimating the inertial properties of the segments. Furthermore, there may be numerical processing errors due to filtering of motion and force data. Noise in kinematic data due to a series of differentiations or estimates of segment position using least square calculations of retroreflective marker locations may all be factors for why a PI may be detected experimentally.

A limitation of the 6 DOF model is that traditional motion capture systems cannot precisely measure instantaneous joint translations from surface markers, which would be necessary to fully interpret $P_{m/m-1}$. Note that positive or negative powers at segment ends using the kinetic method produce computationally equivalent segmental energy values based on an assumed uniarticular muscle model to models using biarticular muscles. However, the net power does not identify the source of power generated or absorbed by uni- or biarticular muscles (Kautz et al., 1994; Prilutsky and Zatsiorsky, 1994; van Ingen Schenau and Cavanagh, 1990).

This study shows (1) the relative displacement power ($P_{m/m-1}$) mathematically accounts for the PI between the AR kinetic method and the kinematic method, and (2) the magnitude of $P_{m/m-1}$ is substantial. When tracking power and energy flow between the segments, it is important that the definition of the distal translational velocity is explicitly clear. In conclusion, $P_{m/m-1}$ must be included for the kinetic and kinematic analyses of segmental power to agree. These results support using both rotational and translational power terms to calculate joint powers for 6 DOF models.

5.7 Acknowledgments

This material was based upon work supported by the National Science Foundation (NSF) Graduate Research Fellowship Grant No. 1247394, the Center for Research in Human Movement Variability of the University of Nebraska at Omaha and the National Institute of Health (P20GM109090), the University of Delaware College of Health Sciences, and the Mechanical Engineering Department Helwig Fellowship. It was also supported by the BADER consortium, a Department of Defense Congressionally Directed Medical Research Programs cooperative agreement

(W81XWH-11-2-022). The views expressed do not necessarily reflect those of the Department of the Navy, Department of Defense or U.S. Government. Any opinions, findings, and conclusions or recommendations expressed in this material are those of the authors and do not necessarily reflect the views of the NSF.

5.8 Derivation

Equation 8a in the text can be parsed into two components based on the powers calculated from joint intersegmental forces proximally (Ia) and distally (Ib).

Ia. $\vec{F}_{p,m} \cdot \vec{v}_{p,m} = ([\sum_{n=1}^{m}(m_n\vec{a}_n - m_n\vec{g})] - \vec{F}_{grf}) \cdot (\vec{v}_m + \vec{\omega}_m \times \vec{r}_{p,m})$

$= [\sum_{n=1}^{m}(m_n\vec{a}_n - m_n\vec{g})] \cdot \vec{v}_m - \vec{F}_{grf} \cdot \vec{v}_m$

$+[\sum_{n=1}^{m}(m_n\vec{a}_n - m_n\vec{g})] \cdot (\vec{\omega}_m \times \vec{r}_{p,m}) - \vec{F}_{grf} \cdot (\vec{\omega}_m \times \vec{r}_{p,m})$

Ib. $\vec{F}_{d,m} \cdot \vec{v}_{d-JC,m} = -([\sum_{n=1}^{m-1}(m_n\vec{a}_n - m_n\vec{g})] - \vec{F}_{grf}) \cdot (\vec{v}_m + \vec{\omega}_m \times \vec{r}_{d-AR,m} + \vec{\omega}_m \times \vec{r}_{m/m-1})$

$= -[\sum_{n=1}^{m-1}(m_n\vec{a}_n - m_n\vec{g})] \cdot \vec{v}_m + \vec{F}_{grf} \cdot \vec{v}_m$

$-[\sum_{n=1}^{m-1}(m_n\vec{a}_n - m_n\vec{g})] \cdot (\vec{\omega}_m \times \vec{r}_{d-AR,m}) + \vec{F}_{grf} \cdot (\vec{\omega}_m \times \vec{r}_{d-AR,m})$

$-[\sum_{n=1}^{m-1}(m_n\vec{a}_n - m_n\vec{g})] \cdot (\vec{\omega}_m \times \vec{r}_{m/m-1}) + \vec{F}_{grf} \cdot (\vec{\omega}_m \times \vec{r}_{m/m-1})$

The summation of Ia and Ib can be simplified to the following (note the terms **bolded** will be noteworthy later):

Ic. $\vec{F}_{p,m} \cdot \vec{v}_{p,m} + \vec{F}_{d,m} \cdot \vec{v}_{d-JC,m}$

$= (m_m\vec{a}_m - m_m\vec{g}) \cdot \vec{v}_m$

$+[\sum_{n=1}^{m}(\boldsymbol{m_n\vec{a}_n - m_n\vec{g}})] \cdot\ (\boldsymbol{\vec{\omega}_m \times \vec{r}_{p,m}}) - [\sum_{n=1}^{m-1}(\boldsymbol{m_n\vec{a}_n - m_n\vec{g}})]$
$\cdot (\boldsymbol{\vec{\omega}_m \times \vec{r}_{d-AR,m}}) - [\sum_{n=1}^{m-1}(\boldsymbol{m_n\vec{a}_n - m_n\vec{g}})] \cdot (\boldsymbol{\vec{\omega}_m \times \vec{r}_{m/m-1}})$

$-\vec{F}_{grf} \cdot (\vec{\omega}_m \times \vec{r}_{p,m})\ ) + \vec{F}_{grf} \cdot (\vec{\omega}_m \times \vec{r}_{d-AR,m}) + \vec{F}_{grf} \cdot (\vec{\omega}_m \times \vec{r}_{m/m-1})$

Similarly, Equation 8a in the text can be parsed into two components based on powers calculated from net joint moments proximally (IIa) and distally (IIb).

IIa. $\vec{M}_{p,m} \cdot \vec{\omega}_m$

$= [[\sum_{n=1}^{m}(I_n\vec{\alpha}_n + \vec{\omega}_n \times I_n\vec{\omega}_n + \vec{r}_{COM,n/m} \times (m_n\vec{a}_n - m_n\vec{g}))] - \vec{\tau}_{free}$
$- \vec{r}_{COP,m} \times \vec{F}_{grf}]\ \cdot\ \vec{\omega}_m$

IIb. $\vec{M}_{d,m} \cdot \vec{\omega}_m$

$= -[[\sum_{n=1}^{m-1}(I_n\vec{\alpha}_n + \vec{\omega}_n \times I_n\vec{\omega}_n + \vec{r}_{COM,n/m-1} \times (m_n\vec{a}_n - m_n\vec{g}))] - \vec{\tau}_{free}$
$- \vec{r}_{COP,m-1} \times \vec{F}_{grf}]\ \cdot\ \vec{\omega}_m$

The summation of IIa and IIb can be simplified to the following (note the terms **bolded** will be noteworthy later):

IIc. $\vec{M}_{p,m} \cdot \vec{\omega}_m + \vec{M}_{d,m} \cdot \vec{\omega}_m$

$= (I_m\vec{\alpha}_m + \vec{\omega}_m \times I_m\vec{\omega}_m) \cdot \vec{\omega}_m + [\sum_{n=1}^{m}(\boldsymbol{\vec{r}_{COM,n/m} \times (m_n\vec{a}_n - m_n\vec{g})})] \cdot\ \boldsymbol{\vec{\omega}_m}$
$- [\sum_{n=1}^{m-1}(\boldsymbol{\vec{r}_{COM,n/m-1} \times (m_n\vec{a}_n - m_n\vec{g})})] \cdot\ \boldsymbol{\vec{\omega}_m}$
$- (\vec{r}_{COP,m} \times \vec{F}_{grf})\ \cdot\ \vec{\omega}_m + (\vec{r}_{COP,m-1} \times \vec{F}_{grf})\ \cdot\ \vec{\omega}_m$

Now, considering the terms bolded in IIc, $\boldsymbol{\vec{r}_{COM,n/m}}$ terms for each summation can be expanded. Here, some terms in these two summations will cancel such that the result of summing IId and IIe will be IIf.

IId. $[\sum_{n=1}^{m}(\vec{r}_{COM,n/m} \times (m_n\vec{a}_n - m_n\vec{g}))] \cdot \vec{\omega}_m$

where….

$$\vec{r}_{COM,m/m} = -\vec{r}_{p,m}$$

$$\vec{r}_{COM,m-1/m} = -\vec{r}_{p,m} + \vec{r}_{d-AR,m} + \vec{r}_{m/m-1} - \vec{r}_{p,m-1}$$

$$\vec{r}_{COM,m-2/m} = -\vec{r}_{p,m} + \vec{r}_{d-AR,m} + \vec{r}_{m/m-1} - \vec{r}_{p,m-1} + \vec{r}_{d-AR,m-1} + \vec{r}_{m-1/m-2} - \vec{r}_{p,m-2}$$

$etc.$

IIe. $-[\sum_{n=1}^{m-1}(\vec{r}_{COM,n/m-1} \times (m_n\vec{a}_n - m_n\vec{g}))] \cdot \vec{\omega}_m$

where….

$$\vec{r}_{COM,m-1/m-1} = -\vec{r}_{p,m-1}$$

$$\vec{r}_{COM,m-2/m-1} = -\vec{r}_{p,m-1} + \vec{r}_{d-AR,m-1} + \vec{r}_{m-1/m-2} - \vec{r}_{p,m-2}$$

IIf. $[\sum_{n=1}^{m}(\vec{r}_{COM,n/m} \times (m_n\vec{a}_n - m_n\vec{g}))] \cdot \vec{\omega}_m$

$$-[\sum_{n=1}^{m-1}(\vec{r}_{COM,n/m-1} \times (m_n\vec{a}_n - m_n\vec{g}))] \cdot \vec{\omega}_m$$

$$= [-\vec{r}_{p,m} \times \sum_{n=1}^{m}(m_n\vec{a}_n - m_n\vec{g})] \cdot \vec{\omega}_m + [\vec{r}_{d-AR,m} \times \sum_{n=1}^{m-1}(m_n\vec{a}_n - m_n\vec{g})] \cdot \vec{\omega}_m + [\vec{r}_{m/m-1} \times \sum_{n=1}^{m-1}(m_n\vec{a}_n - m_n\vec{g})] \cdot \vec{\omega}_m$$

$$= \mathbf{-1} * [[\sum_{n=1}^{m}(m_n\vec{a}_n - m_n\vec{g})] \cdot (\vec{\omega}_m \times \vec{r}_{p,m}) - [\sum_{n=1}^{m-1}(m_n\vec{a}_n - m_n\vec{g})] \cdot (\vec{\omega}_m \times \vec{r}_{d-AR,m}) - [\sum_{n=1}^{m-1}(m_n\vec{a}_n - m_n\vec{g})] \cdot (\vec{\omega}_m \times \vec{r}_{m/m-1})]$$

Rearranging the terms in IIf and using the properties of cross products, the result is actually the inverse of the bolded term in Ic. Thus, the summation of Ic and IIc will result in Equation 9 in the text.

5.9 Nomenclature

m_m	segment mass
$\vec{a}_m$	segment center of mass acceleration
$\vec{g}$	gravity
$\vec{F}_{grf}$	ground reaction force
$\vec{F}_{p,m}$	proximal joint intersegmental force
$\vec{F}_{d,m}$	distal joint intersegmental force
$\vec{M}_{p,m}$	proximal net joint moment
$\vec{M}_{d,m}$	distal net joint moment
I_m	segment moment of inertia
$\vec{\alpha}_m$	segment angular acceleration
$\vec{\omega}_m$	segment angular velocity
$\vec{\tau}_{free}$	free moment
$\vec{r}_{COM,n/m}$	position vector from proximal segment *m* to the center of mass of segment *n*
$\vec{r}_{COP,m}$	position vector from the proximal segment *m* to the center of pressure
$\vec{v}_{p,m}$	proximal segment velocity
$\vec{r}_{p,m}$	position vector from the center of mass to the proximal segment end
$\vec{r}_{d-AR,m}$	position vector from the center of mass to the anatomically relevant distal segment end
$\vec{r}_{d-JC,m}$	position vector from the center of mass to the joint center (defined as the proximal end of the adjacent distal segment)
$\vec{r}_{m/m-1}$	relative displacement vector between the distal end of segment *m* and proximal end of segment $m-1$
$\vec{v}_{d-AR,m}$	distal segment translational velocity from the anatomically relevant definition of $\vec{r}_{d-AR,m}$
$\vec{v}_{d-JC,m}$	distal segment translational velocity from the joint center definition of $\vec{r}_{d-JC,m}$
$\vec{v}_{m/m-1}$	relative displacement velocity associated with $\vec{r}_{m/m-1}$
$\vec{v}_m$	segment center of mass velocity
$P_{AR,m}$	segmental power using the anatomically relevant definition of $\vec{v}_{d-AR,m}$ using the kinetic method

$P_{JC,m}$	segmental power using the joint center definition of $\vec{v}_{d-JC,m}$ using the kinetic method
$\frac{d}{dt}E_m$	segment rate of energy change using the kinematic method
$PI_{AR,m}$	power imbalance between $\frac{d}{dt}E_m$ and $P_{AR,m}$
$PI_{JC,m}$	power imbalance between $\frac{d}{dt}E_m$ and $P_{JC,m}$
$P_{m/m-1}$	relative displacement power term between adjacent segments m and $m-1$
$\lvert PI_{AR,m}\rvert_{\text{mean}}$	mean absolute value of the $PI_{AR,m}$
$\lvert P_{m/m-1}\rvert_{\text{mean}}$	mean absolute value of the relative displacement power term

Chapter 6

COMPARING THE MECHANICAL ENERGETICS OF WALKING AT DIFFERENT SPEEDS USING WORK-ENERGY PROFILES

6.1 Abstract

Individuals adapt their gait strategy, or coordination of the joints and segments of the body to walk, based on different conditions (e.g., walking speed). A pervasive question in the field of gait analysis is how to determine if a strategy is "good" or "bad," which is partly due to the complexity in operationally defining such terms. However, mechanical energetics variables (like work and energy) can be used to quantify how humans achieve a certain gait strategy. Assessing if a strategy's energetics were more or less aligned with the theorized outcome of the gait tasks in one condition versus another can be done in an effort to better understand how and why certain gait mechanics are used under different conditions. For example, we hypothesize based on previous literature that the single support task in gait will result in pendular mechanics. We also hypothesize that minimal net work will be required over double support because negative work done by the leading limb will negate positive work done by the trailing limb to propel the body. The purpose of this chapter is to introduce and verify a novel Work-Energy Profiles approach to quantify and evaluate the energetics of gait strategies over a spectrum of conditions. Gait can be divided into sub-tasks relating to raising and lowering the body's center of mass (COM) in single support phase, and propelling the body in double support phase. Using motion and force data from 10 healthy subjects walking at slow, moderate, and

typical speeds, the mechanical work and changes in energy forms (e.g., gravitational potential [ΔGPE], translational kinetic [ΔTKE], and rotational kinetic energy [ΔRKE]) of the whole body were calculated. The calculations were verified using the work-energy relationship, showing only an average 1.0% difference in whole body mechanical work and change in energy. The sub-task of raising the COM in single support results in a positive displacement of height (i.e., positive ΔGPE) and the strategy at the slow speed behaved more like an inverted pendulum compared to the other speeds because negative ΔTKE and positive ΔGPE over this interval were closer in magnitude. The sub-task of lowering the COM in single support results in negative ΔGPE, but unexpectedly ΔTKE was minimal over all three speeds unlike an inverted pendulum. The sub-task of propelling the body in double support results in positive net work and change in velocity (i.e., positive ΔTKE), contrary to our hypothesis. Thus, when accounting for the energy of all segments of the body, human gait did not follow pendular mechanics. This data supports that gait is more of an assisted rise, damped fall, and active push by the constituents. These findings have important implications for fundamentally understanding gait energetics under different conditions.

6.2 Introduction

The purpose of gait analysis research is to understand a person's gait strategy, or how the joints and segments of the body coordinate to perform a task. Typical bipedal walking, as one of the most common human movements (Winter, 1991), has been well examined to utilize the most energetically economic coordination of limbs (Kuo and Donelan, 2010). Typical gait has been theorized to be most economical when adopting an inverted pendulum strategy in single support phase and a step-to-step transition in double support phase, referred to together as a dynamic walking model (Kuo, 2007). This corresponds with sub-tasks aimed primarily toward raising and lowering the center of mass (COM) during single support phase and propelling the body during double support phase. While individuals achieve these sub-tasks using different strategies (Inman et al., 1981), it is difficult to assess if one strategy is "better" than another, partly due to the unclear definition of the term. However, the expected energetics of the dynamic walking model can be used to hypothesize what may be the energetics of experimental gait data of the whole body under different conditions. Thus, a succinct approach to characterize gait strategy energetics is needed in an effort to better understand how and why certain gait mechanics are used under different conditions.

The causal relationship between energetics and movement (Winter, 2009) has been utilized to characterize gait strategies. During gait, mechanical work is done (primarily by muscles (Hof et al., 2002)) by the following joints and segments of the body, hereafter denoted as "constituents": bilateral hips, knees, ankles, distal feet (Siegel et al., 1996), and the grouped head-arms-trunk (HAT) (Perry, 1992). Unlike kinematic and kinetic measures (i.e., peak joint angles, moments, and powers) that are calculated at discrete instances in time, energetics (i.e., work and energy) metrics provide summary measures over an interval of time (Zajac et al., 2002). Furthermore, since mechanical energy forms (i.e., gravitational potential, translational kinetic, and rotational kinetic energies) are a result of changes in motion and position of the body, quantifying the change in energy forms during sub-tasks of gait can be interpreted as outcomes of a gait strategy. During walking, the whole body center of mass (COM) experiences changes primarily in two forms of energy: gravitational potential energy and translational kinetic energy, similar to an inverted pendulum (Buczek et al., 2000; Cavagna and Kaneko, 1977; Inman et al., 1981; Kuo, 2007; Perry, 1992). For example, the atypical exchange of kinetic and potential energy patterns of individuals with impairments has been used to characterize gait deviations of individuals post-stroke (Olney et al., 1986) and of children with cerebral palsy (Olney et al., 1987). While mechanical constituent work can be a method to quantify constituent efforts toward achieving a gait strategy, mechanical energy forms of the whole body can be interpreted as the net outcome of such efforts.

Assessing the energetics of a gait strategy is dependent on understanding the sub-tasks of gait. For example, the sub-tasks for walking change over the gait cycle, which may be divided into distinct intervals of gait (Cappozzo et al., 1976). During single support, the theoretically most economical strategy is to keep the stance limb relatively straight, so as to rotate upward in a semicircular arc like an inverted pendulum (Kuo, 2007). While the stance limb has been noted to follow more of an inverted pendulum pattern, the swing limb moves like a traditional pendulum (Kuo, 2007). Consequently, this leads to the COM rising to its peak height near midstance, where the stance limb's anterior-posterior ground reaction force changes direction from a braking force to a propulsive force (Griffin et al., 1999). After midstance, single support has been referred to as a "controlled fall" (Perry, 1992), as the COM loses height while the swing limb prepares for ground contact. In the dynamic walking model, this is the second half of the inverted pendulum. Then, double support occurs when both limbs are in contact with the ground, with the aim being to shift weight from the now trailing stance limb to the contralateral leading limb to continue forward progression. In this step-to-step transition, the velocity of the center of mass is redirected (Adamczyk and Kuo, 2009), thereby requiring effort to primarily change the kinetic energy of the body (Kuo et al., 2005). According to the dynamic walking model, negative work by the leading limb and positive work by the trailing limb negate each other during double support such that no net work is expected over double support (Kuo, 2007). The dynamic walking model is a simplified theory for gait which can provide initial hypotheses for energetics outcomes expected during experimental gait analysis.

The energetics of a gait strategy may change with different conditions. For example, gait biomechanists often seek to understand how gait strategies adapt across conditions of walking speed, because the ability to modulate walking speed is an important functional goal for individuals with gait impairments and there is a relationship between gait speed and quality of life (Winter, 1991). Several researchers have looked at joint work across speeds comparing effects of age (Buddhadev and Martin, 2016; Frost et al., 1997; Mian et al., 2006), hemiparesis (Detrembleur et al., 2003), and amputation (Safaeepour et al., 2014). Over the entire gait cycle, researchers have found that whole body and limb mechanical work increases with walking speed (Cavagna et al., 2000; Cavagna and Kaneko, 1977; Ebrahimi et al., 2017a; Ortega and Farley, 2005; Willems et al., 1995). However, there has been a discrepancy between mechanical work and metabolic cost. Previously, researchers have noted that less mechanical work is done at slow speeds (Alexander, 1991), but the greater mechanical work at typical speeds aligns with more efficient metabolic output by the muscles such that a typical speed is less metabolically costly (Cavagna et al., 1976). However, these energetics metrics only observe the mechanical work done over the entire gait cycle and not over sub-tasks. Elucidating the energetics of gait strategies during specific sub-tasks could help the field better understand the mechanism for gait strategy adaptations across conditions.

Based on the physical principle that net mechanical work is equivalent to the change in mechanical energy (ignoring other forms of energy like heat, sound, etc.), the energetics of gait strategies using constituent work and energy forms can be assessed. To easily visualize and interpret mechanical work and energy forms, a graphical “Work-Energy Profiles” approach was created. The objective of this chapter is to introduce and verify the Work-Energy Profiles approach, which can be used to quantify and evaluate gait energetics under different conditions. The applicability of the approach was demonstrated by comparing the gait energetics of healthy individuals walking at slow, moderate, and typical speeds.

6.3 Computational Development

The Work-Energy Profiles approach is a tool to assess the energetics of gait strategies across conditions at specific intervals, corresponding to sub-tasks, of gait. Because the work-energy relationship is used to develop this approach, both calculations for work and energy metrics must be first verified that they are executed correctly, in accordance with the definition of verification by Hicks and colleagues (Hicks et al., 2015). Data from the Work-Energy Profiles approach are visually represented as bar charts of work and energy forms during intervals of gait.

6.3.1 Verification

6.3.1.1 Constituent Power-Rate of Energy Change

Using the summed segmental energies approach (Winter, 1979), 6 DOF constituent powers, and the work-energy relationship, mechanical work done about constituents can be mathematically related to the change in energy of the whole body in all its forms (i.e., potential and kinetic). A 6 DOF 10-segment rigid body model (bilateral feet, shanks, thighs, arms; pelvis; trunk) should be used to include all segments of the body. The relationship between segmental power-rates of change in energy is stated in Equation 1(A-C) using the joint center method described by Ebrahimi and colleagues (Ebrahimi et al., 2018). The variable *m* denotes the segment, P denotes the segmental power, while $\vec{F}$ denotes the joint force and $\vec{M}$ denotes the segment torque for the respective distal (d) or proximal (p) segment ends. Segment translational velocity $\vec{v}$ is denoted with the subscript *p* for proximal end or *d-JC* for distal end calculated in the segment coordinate system at the location of the joint center (proximal end of the adjacent distal segment) (Ebrahimi et al., 2018). Segment angular velocity $\vec{\omega}$ is about the segment center of mass. The rate of change in gravitational potential energy (GPE), rotational kinetic energy (RKE), and translational kinetic energy (TKE) are taken with respect to time *t*. The rate of change in energy of the segment is denoted ΔE_m. Note that due to the assumption of rigid body segments, elastic potential energy is zero and is therefore not included in the calculations.

(1) A) $P_m = \vec{M}_{p,m} \cdot \vec{\omega}_m + \vec{M}_{d,m} \cdot \vec{\omega}_m + \vec{F}_{p,m} \cdot \vec{v}_{p,m} + \vec{F}_{d,m} \cdot \vec{v}_{d-JC,m}$

B) $\frac{d}{dt} E_m = \frac{d}{dt} GPE_m + \frac{d}{dt} RKE_m + \frac{d}{dt} TKE_m$

C) $P_m = \frac{d}{dt} E_m$

Mechanical energy forms of the segments are calculated as follows (equations 2A-C):

(2) A) $\frac{d}{dt} GPE_m = -m_m \vec{g} \cdot \vec{v}_m$

B) $\frac{d}{dt} RKE_m = (I_m \vec{\alpha}_m + \vec{\omega}_m \times I_m \vec{\omega}_m) \cdot \vec{\omega}_m$

C) $\frac{d}{dt} TKE_m = m_m (\frac{d}{dt} \vec{v}_{m+treadmill}) \cdot \vec{v}_{m+treadmill}$

Where m_m is segment mass, $\vec{g}$ is gravity, I_m is segment moment of inertia, $\vec{\alpha}_m$ is segment angular acceleration, and $v_{m+treadmill}$ is segment translational velocity ($\vec{v}_m$) summed with the treadmill velocity in the anterior-posterior direction. Note that the addition of this treadmill velocity to $\vec{v}_m$ in Equation 2C is to transform the data into the reference frame of the treadmill.

The summed segmental powers equate to the summed rate of change in energy of all 10 segments, which is equivalent to the total rate of change in energy of the whole body (wb) (Equation 3).

$$(3)\ P_{wb} = \sum_{n=1}^{10}\left(\vec{M}_{p,n} \cdot \vec{\omega}_n + \vec{M}_{d,n} \cdot \vec{\omega}_n + \vec{F}_{p,n} \cdot \vec{v}_{p,n} + \vec{F}_{d,n} \cdot \vec{v}_{d-JC,n}\right)$$
$$= \frac{d}{dt}E_{wb} = \sum_{n=1}^{10}\left(\frac{d}{dt}GPE_n + \frac{d}{dt}RKE_n + \frac{d}{dt}TKE_n\right)$$
$$= \frac{d}{dt}GPE_{wb} + \frac{d}{dt}RKE_{wb} + \frac{d}{dt}TKE_{wb}$$

6.3.1.2 Constituent Work-Change in Energy Forms

Using the 6 DOF joint power calculations (Buczek et al., 1994), segmental powers are used to calculate constituent powers (P_i) where *i* denotes the joint between the distal end of segment *m* and the proximal end of segment *m−1* (Equation 4).

$$(4)\ P_i = \vec{M}_{p,m-1} \cdot \vec{\omega}_{m-1} + \vec{M}_{d,m} \cdot \vec{\omega}_m + \vec{F}_{p,m-1} \cdot \vec{v}_{p,m-1} + \vec{F}_{d,m} \cdot \vec{v}_{d-JC,m}$$
$$= \vec{M}_{p,m-1} \cdot (\vec{\omega}_{m-1} - \vec{\omega}_m) + \vec{F}_{p,m-1} \cdot (\vec{v}_{p,m-1} - \vec{v}_{d-JC,m})$$

If the center of each joint is located perfectly, the distal joint force power of the proximal segment ($\vec{F}_{d,m} \cdot \vec{v}_{d-JC,m}$) and the proximal joint force power of the distal segment ($\vec{F}_{p,m-1} \cdot \vec{v}_{p,m-1}$) should be equal and opposite to each other (Winter, 2009). However, there is some error in defining a joint center, which can be accounted for by multiplying the joint force by the change in respective distal and proximal translational velocities at each joint (Buczek et al., 1994). The joint force power and distal foot power are calculated using previously reported calculations (Siegel et al., 1996; Takahashi and Stanhope, 2013). Therefore, Equation 5 can be rewritten using P_i for the ipsilateral (I) and contralateral (C) legs and summed head-arms-trunk (HAT) as shown in Equation 5.

(5) $$P_{distal\ foot,I} + P_{ankle,I} + P_{knee,I} + P_{hip,I} + P_{distal\ foot,C} + P_{ankle,C} + P_{knee,C} + P_{hip,C} + P_{HAT} = \frac{d}{dt}GPE_{wb} + \frac{d}{dt}RKE_{wb} + \frac{d}{dt}TKE_{wb}$$

The rates of change in energy forms of the body are then integrated in each of their forms, as are the constituent powers of the ipsilateral and contralateral limb and HAT over intervals defined in the next section, to attain change in energy forms and constituent work measures.

6.3.2 Work-Energy Profiles

Graphical representations of work and energy data have been presented previously in flow charts for a sit-to-stand task (Figs. 1, 3 and 5 in Pai et al., 2006) and bar charts in accelerated and decelerated walking (Fig. 5 in Qiao and Jindrich, 2016). These profiles can be used to determine the positive (or negative) constituent work done to generate (or absorb) whole body energy (Pai et al., 2006). The flow charts used in previous literature made it difficult to visually compare the magnitude of the joint work and the energy forms (Pai et al., 2006). The bar charts presented previously were effective in achieving this, although the sum of the mechanical work and change in energy was not shown to equate exactly (Qiao and Jindrich, 2016).

Thus, the Work-Energy Profiles were created and represented as bar charts for each condition, an example of which is shown in Fig. 6.1. Gait sub-tasks were analyzed based on intervals corresponding to ipsilateral stance phase: (1) initial double support – ipsilateral heel strike to contralateral toe off, (2) single support rise – contralateral toe off to ipsilateral midstance, (3) single support fall – ipsilateral midstance to contralateral heel strike, (4) terminal double support – contralateral heel strike to ipsilateral toe off, and (5) swing – ipsilateral toe off to ipsilateral heel strike. Constituents with a positive or negative constituent work after integration over the interval of interest are shown in a stacked positive (${}^{+}W_{wb}$) or negative (${}^{-}W_{wb}$) bar chart, respectively. An adjacent bar chart represents net work (${}^{net}W_{wb}$), which is the sum of ${}^{+}W_{wb}$ and ${}^{-}W_{wb}$. Four adjacent bars representing the integrated energies over the interval of interest are included (ΔE_{wb}, ΔGPE_{wb}, ΔTKE_{wb}, and ΔRKE_{wb}), where the sum of ΔGPE_{wb}, ΔTKE_{wb}, and ΔRKE_{wb} is denoted as ΔE_{wb} (Fig. 6.1). Note that using the work-energy relationship, ΔE_{wb} is theoretically equivalent to ${}^{net}W_{wb}$.

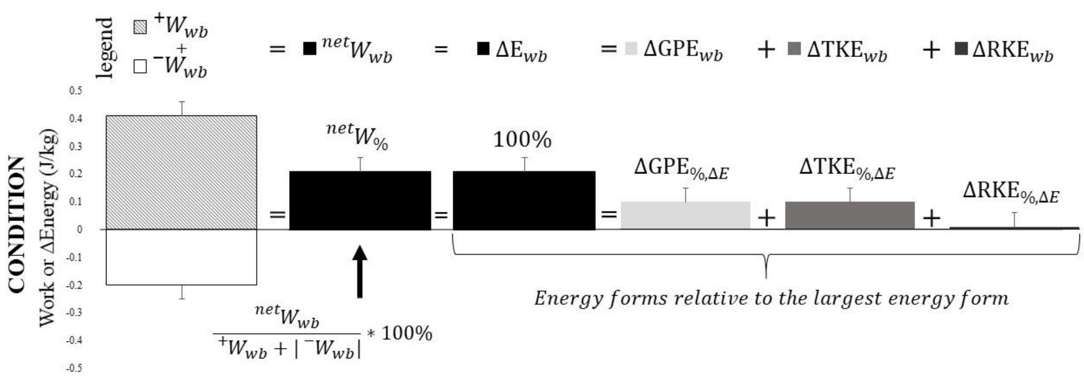

Figure 6.1: Example data of Work-Energy Profiles bar charts for any condition over a specific sub-task. Relative net work and relative energy forms were calculated in order to standardize comparisons across conditions (see section 6.3.3). Column data are presented as averages with standard deviation bars.

6.3.3 Evaluating Energetics

Before assessing the experimental energetics of the gait strategy, consider that the magnitude of work and energy metrics differ based on the gait speed. Thus, relative measures of work and energy were used in order to standardize metric comparisons across speeds (Fig. 6.1). The relative net work (${}^{net}W_{\%}$), defined as the amount of ${}^{net}W_{wb}$ relative to the sum of the absolute resulting work done over that interval ($|{}^{+}W_{wb}| + |{}^{-}W_{wb}|$), was calculated as a percentage. This is a measure of the amount of remaining work relative to the absolute net positive and net negative work over the sub-task. The energies (ΔE_{wb}, ΔGPE_{wb}, ΔTKE_{wb}, and ΔRKE_{wb}) were also analyzed in relation to the largest energy form as a percentage. For example, if the ΔGPE_{wb} was the largest energy form, the relative energy forms would be written as the following: $\Delta E_{\%,\Delta GPE}$, $\Delta TKE_{\%,\Delta GPE}$, and $\Delta RKE_{\%,\Delta GPE}$.

Then, the relative net work and energy forms in the Work-Energy Profiles were compared across conditions and compared to the theoretical resulting energetics based on models in previous literature, like the dynamic walking model. Assessing energetics of one strategy versus another is dependent on defining the sub-tasks of each interval of gait. As discussed in the introduction, a sub-task for single support rise is to raise the COM, for single support fall to lower the COM, and for double support to propel the body. It must be acknowledged these are not the only tasks of walking. For example, while the stance limb is in single support, another task besides lifting and lowering the COM is to successfully swing the opposite limb from its position as a trailing limb through to a leading limb. However, the Work-Energy Profiles are comprehensive in that it is possible to assess the constituent work done over single support by the swing limb (specifically the swing limb hip and knee work). If the body acted as a conserved inverted pendulum during single support, the ΔTKE_{wb} would be equal in magnitude and opposite in sign to the ΔGPE_{wb}, such that no net constituent work was done (Kuo and Donelan, 2010). While previous literature has shown there is some net constituent work done (Inman et al., 1981), a less mechanically costly strategy may be one where work is minimal. Previous literature supports that constituents help control the fall of the COM, suggesting the magnitude of relative ΔGPE_{wb} to be greater than ΔTKE_{wb} during single support fall. During double support, the dynamic walking model theorizes no net work over the double support interval. It is theorized the negative work primarily by the leading limb will negate the positive work by the trailing limb (Kuo, 2007).

6.4 Experimental Methods

A subset of previously recorded data collected on 10 healthy, unimpaired individuals (height 1.73 ± 0.07 m, mass 72.1 ± 13.6 kg) was used for analysis (Goldberg and Stanhope, 2013). Force data were collected while subjects walked on a dual-belted instrumented treadmill (Model TM-06-B, Bertec Corp., Columbus, OH) at three velocities – slow (0.4 statures/s), moderate (0.6 statures/s), and typical (0.8 statures/s) – while motion capture data were collected using a six-camera system (Vicon, Los Angeles, CA). All subjects provided informed consent under an IRB-approved protocol. Reflective markers were placed on subjects using a 6 DOF marker configuration (Holden et al., 1997), where clusters of markers were placed on the feet, shanks, thighs, pelvis, trunk, and upper arms. All conditions were randomized, and subjects were given sufficient time to acclimate to each condition (approximately 1.5 – 2 minutes) (Donelan and Kram, 1997). Motion capture data were sampled at 120 Hz and low-pass filtered at 6 Hz, and treadmill force data were sampled and low-pass filtered at 1040 Hz and 10 Hz, respectively.

Visual3D software (C-Motion Inc., Germantown, MD) was used to model a 6 DOF 10-segment (bilateral feet, shanks, thighs, arms; pelvis; trunk) body for all calculations. The mass of the head was included in the trunk segment, and each arm was modeled as a rigid segment which accounted for the weight of the upper arm, forearm, and hand. Heel strike and toe off were determined based on the first (> 20 N) and last (< 20 N) instance of ground reaction force and midstance was determined by the zero crossing of the anterior-posterior ground reaction force (Griffin et al., 1999). Work-Energy Profiles were calculated as addressed in section 6.3 above.

For verification of the Work-Energy Profiles approach, the absolute difference between power (P_{wb}) and rate of energy change ($\frac{d}{dt}E_{wb}$) for the whole body was calculated and integrated over the gait cycle. The percent difference was calculated as the absolute difference divided by the absolute change in energy of the whole body as a percentage.

Work-Energy Profiles for initial double support phase and swing phase were not presented since healthy, able-bodied individuals have symmetrical gait patterns (Seeley et al., 2008); the roles of the ipsilateral constituents during initial double support and ipsilateral swing phase were represented by the contralateral limb during terminal double support and over both single support intervals (rise and fall).

Using SPSS software (IBM Corp., Armonk, NY), differences in ${}^{net}W_{\%}$ and relative changes in energy forms were compared for the three walking speeds using several one-way repeated measures ANOVAs with Bonferroni corrections for each interval. Constituent work (ipsilateral and contralateral foot, ankle, knee, hip, and HAT) and change in energy (ΔE_{wb}, ΔGPE_{wb}, ΔTKE_{wb}, and ΔRKE_{wb}) were compared separately across the three intervals and three walking speeds using several two-way repeated measures ANOVAs with Bonferroni corrections to assess the interval-by-speed interaction ($p < 0.05$) as supplemental data. For the one-way ANOVA, a value more than 1.5 times the interquartile range from a boxplot of the data was considered an outlier. For the two-way ANOVA, studentized residuals greater than ±3 were considered outliers. Shapiro-Wilk's test of normality on the studentized residuals ($p < 0.05$) were used to assess normality, although violations of normality did not halt the test as ANOVA analyses are robust to violations of normality (Schmider et al., 2010). If Mauchly's test of sphericity was significant ($p < 0.05$), the Greenhouse-Geisser correction was reported. If there was a significant interaction, simple main effects of speed were examined with post hoc Bonferroni corrections for pairwise comparisons ($p < 0.05$). If no interaction was found, the main effect of speed was reported ($p < 0.05$).

6.5 Results

6.5.1 Verification

The difference in whole body power and rate of mechanical energy change over an entire gait cycle was minimal (Fig. 6.2). The average percent difference over the 10 subjects was 1.0 ± 0.2 % over the gait cycle (see Table C.4 in Appendix C for percent differences by subject and interval). The whole body, lower limbs, and HAT energies (Figs. D.1 and D.2 in Appendix D) match that of previous literature (Cappozzo et al., 1976; Inman et al., 1981).

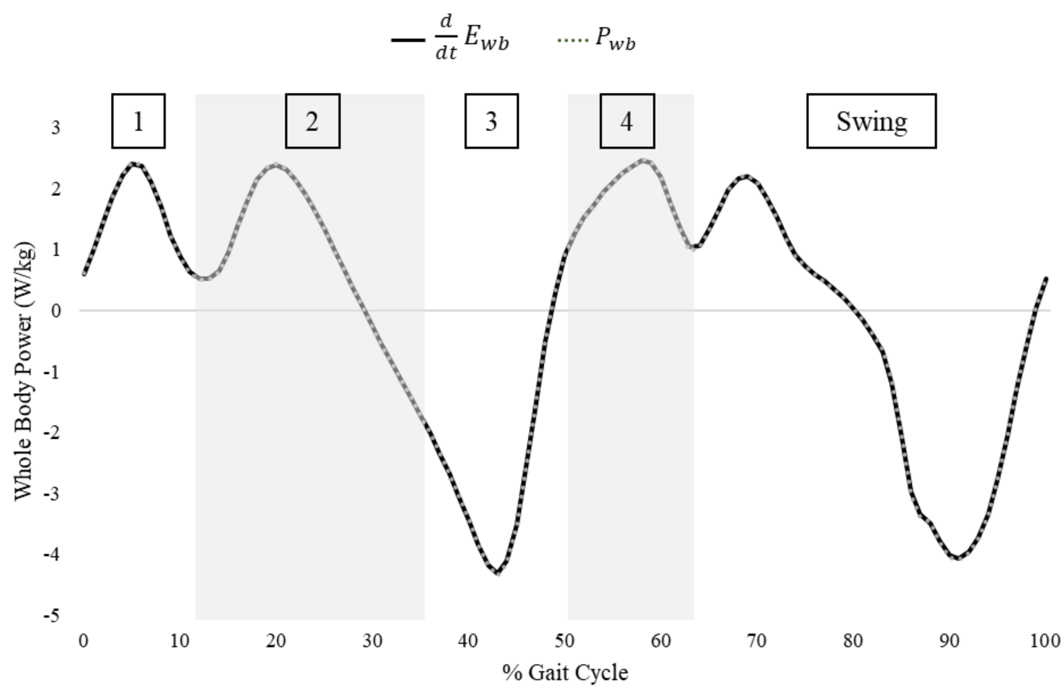

Figure 6.2: Whole body power calculated using the rate of energy change ($\frac{d}{dt}\text{E}_{wb}$) and mechanical power using the joint center kinetic method (P_{wb}) is nearly equivalent, shown here for a representative subject. Intervals marked with shading: (1) initial double support, (2) single support rise, (3) single support fall (4) terminal double support, and swing phase in reference to the ipsilateral limb gait cycle.

6.5.2 Work-Energy Profiles

Within each interval across speeds, the roles of the constituent work or energy forms (as determined by their signs) did not change in general (Table C.5 in Appendix C). Over all intervals, ΔRKE was minimal and the difference between ${}^{net}W_{wb}$ and ΔE_{wb} was less than 0.00 J/kg. (Fig. 6.3 – 6.5). In analyzing the Work-Energy Profiles, first the ${}^{net}W_{\%}$ and then the relative changes in energies are assessed, as discussed in section 6.3.3.

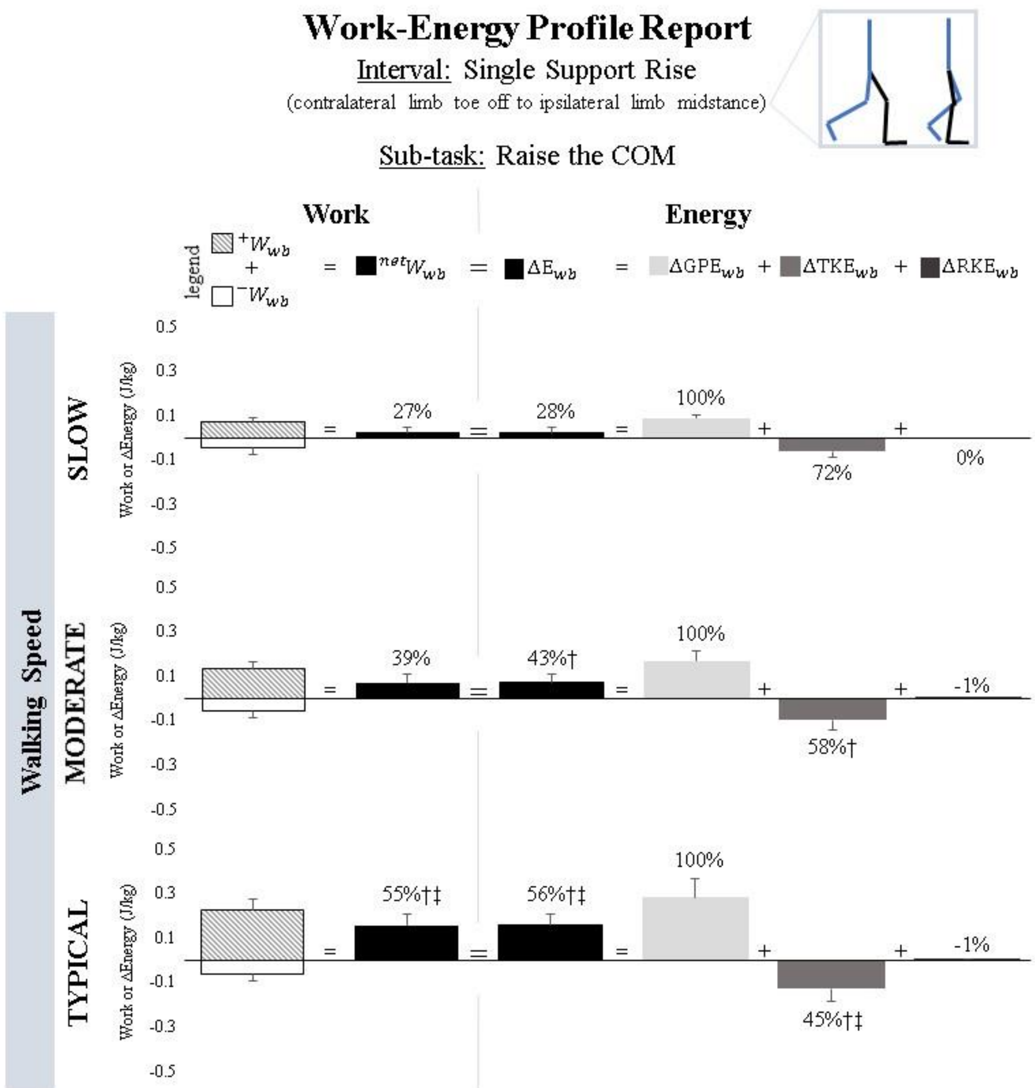

Figure 6.3: Over the single support rise interval, a functional sub-task of the whole body (wb) is to raise the COM, which is observed by a positive ΔGPE_{wb}. The slow speed shows characteristic patterns more expected of a conserved inverted pendulum than the other speeds, where negative ΔTKE_{wb} is closer in magnitude to positive ΔGPE_{wb}. There is minimal net work (${}^{net}W_{wb}$) performed as a percentage of summed positive (${}^{+}W_{wb}$) and absolute negative (${}^{-}W_{wb}$) work. Two subjects at the slow speed and one subject at the moderate speed showed work-energy patterns which did not follow the average pattern. The reader is referred to the text for detail. A † and ‡ denote the values are significantly different from the values at the slow and moderate speeds, respectively (p < 0.05).

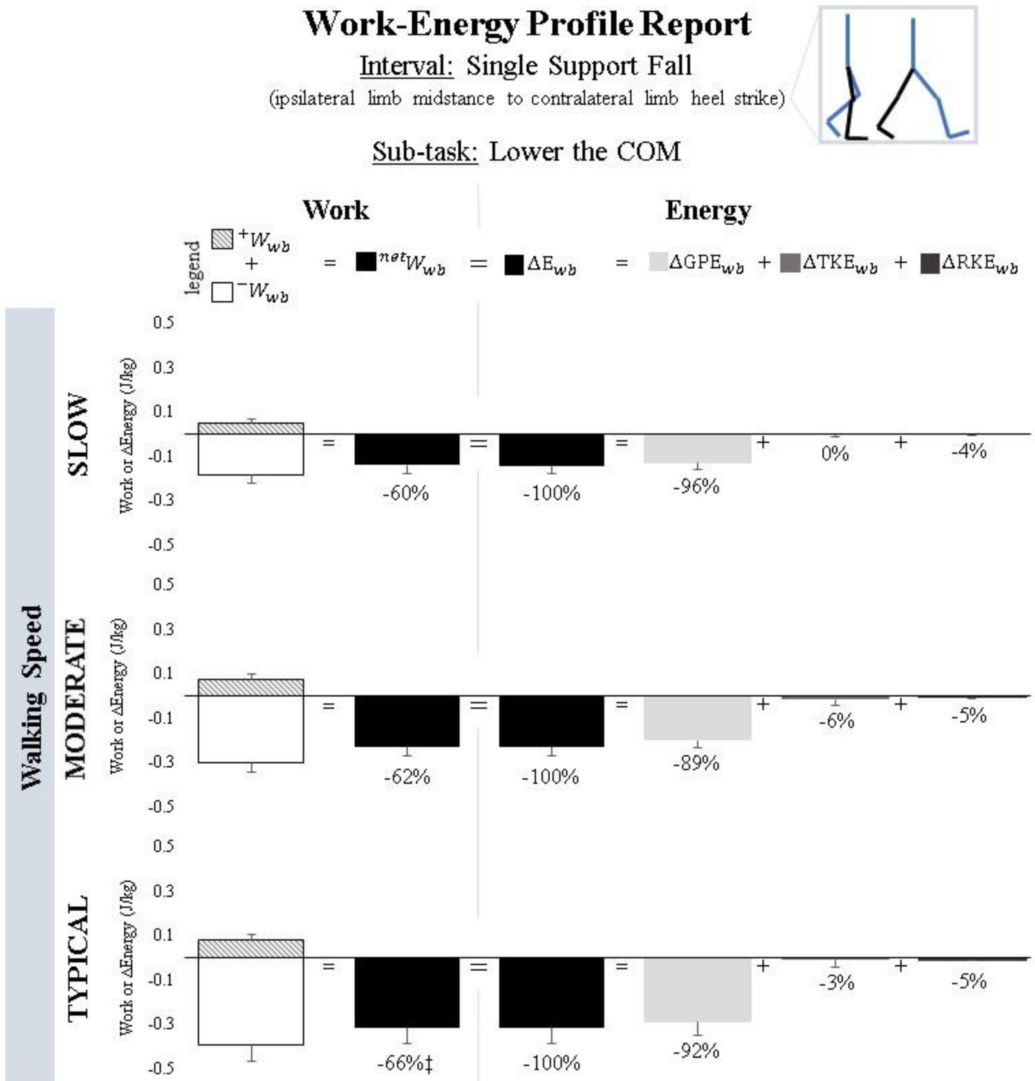

Figure 6.4: Over the single support fall interval, a functional sub-task of the whole body (wb) is to lower the COM, which is observed by a negative ΔGPE_{wb}. All three walking speeds achieve this by using mechanical work to control the fall of the COM. More than 62% of the net work ($^{net}W_{wb}$) performed as a percentage of summed positive ($^{+}W_{wb}$) and absolute negative ($^{-}W_{wb}$) work is negative, and almost all of the net energy is in the form of negative ΔGPE_{wb}. Interestingly, there is not a net positive change in translational kinetic energy (ΔTKE_{wb}), which would be expected for characteristic patterns of a conserved inverted pendulum. A † and ‡ denote the values are significantly different from the values at the slow and moderate speeds, respectively ($p < 0.05$).

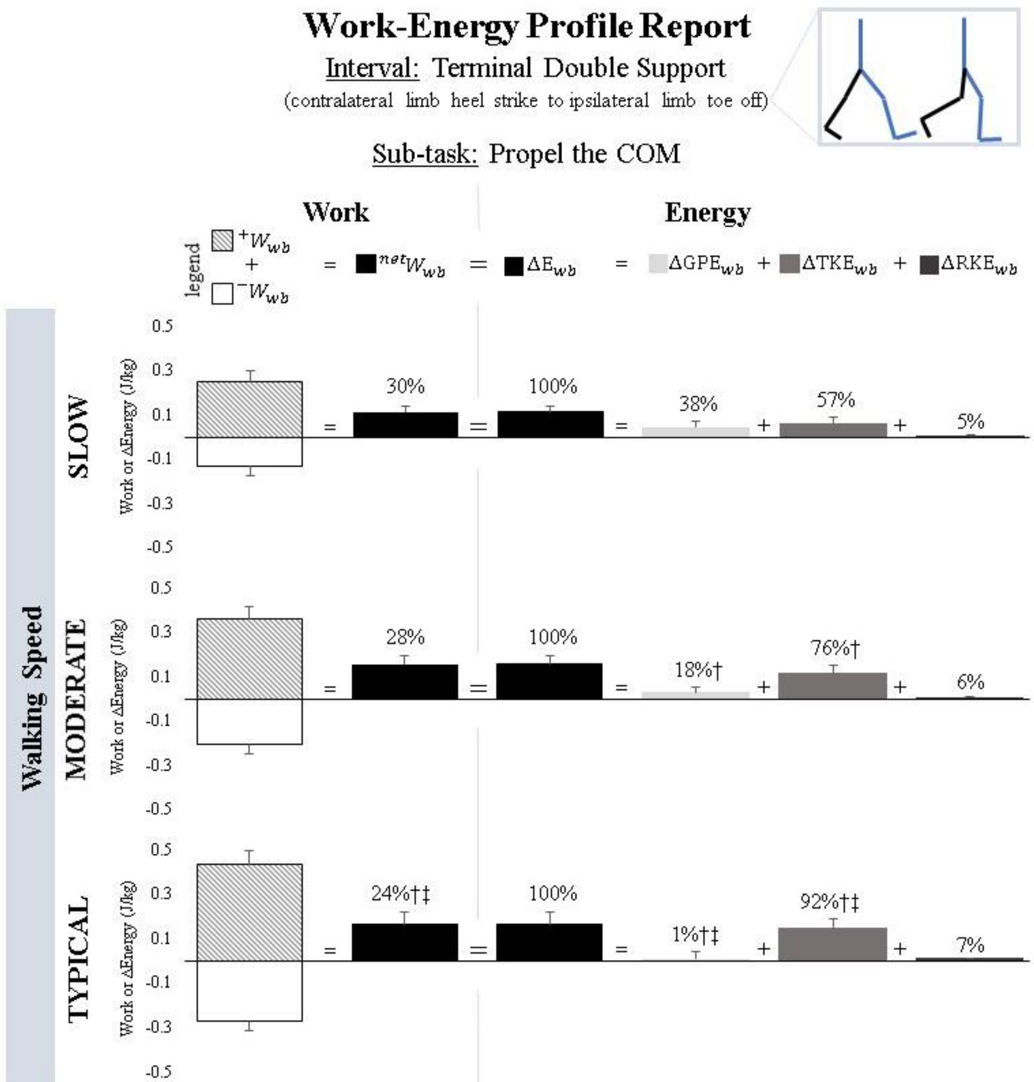

Figure 6.5: Over the terminal double support interval, a functional sub-task of the whole body (wb) is to propel the COM. Minimal net work was hypothesized over this interval, but instead results show a positive ΔTKE_{wb}. More net work ($^{net}W_{wb}$) performed as a percentage of summed positive ($^{+}W_{wb}$) and absolute negative ($^{-}W_{wb}$) work occurs at the slow speed (30%). At the typical speed, where ΔGPE_{wb} is minimal, almost all energy is in the form of ΔTKE_{wb}. Thus, the typical speed may be more effective at propelling the COM because positive ΔTKE_{wb} is 92% of the ΔE_{wb}, which is significantly larger than at the other speeds. A † and ‡ denote the values are significantly different from the values at the slow and moderate speeds, respectively ($p < 0.05$).

Over the single support rise interval, a functional sub-task is to raise the COM, which is observed by a positive change in ΔGPE_{wb} (Fig. 6.3). On average over the three conditions, the gait strategy was characterized by positive ${}^{net}W_{wb}$ done by the constituents and a net positive ΔGPE_{wb} indicating the COM increased in height. Net negative ΔTKE_{wb} was not equal in magnitude to ΔGPE_{wb}, yielding a net positive ΔE_{wb}. The ${}^{net}W_{\%}$ was significantly larger at the typical speed (average 55%) than the slow (27%, p = 0.036) and moderate (39%, p = 0.014) speeds. When considering energy values, two subjects at the slow speed and one subject at the moderate speed showed a strategy resulting in a net negative ΔE_{wb} but were still included in the analysis as these data were not outliers. The magnitude of positive ΔGPE was larger than ΔE_{wb}, ΔTKE_{wb}, and ΔRKE_{wb} so the percentage of energies was assessed relative to the ΔGPE_{wb} (i.e., $\Delta E_{\%,\Delta GPE}$, $\Delta TKE_{\%,\Delta GPE}$, and $\Delta RKE_{\%,\Delta GPE}$). The $\Delta TKE_{\%,\Delta GPE}$ was significantly largest at the slow speed (72%, main effect p < 0.001), while $\Delta E_{\%,\Delta GPE}$ was significantly smallest (28%, main effect p < 0.001) relative to the other speeds. These results support that more pendular mechanics were used at the slow speed, in which there was a larger portion of translational kinetic energy transferred to gravitational potential energy, requiring minimal net mechanical work by the body. Relative to the other speeds, the task of raising the COM at the slow speed was accomplished using a strategy more akin to an inverted pendulum.

Over the single support fall interval, a functional sub-task is to lower the COM, which is observed by a negative change in ΔGPE_{wb} (Fig. 6.4). On average over the three conditions, the gait strategy was characterized by negative ${}^{net}W_{wb}$, which resulted in net negative ΔGPE_{wb}, indicating the COM decreased in height. The magnitude of the ΔTKE_{wb} was small for each speed and did not significantly differ (p

= 0.109), while the resulting net negative ΔGPE_{wb} and ΔE_{wb} significantly increased in magnitude from slow to typical speeds (main effect p < 0.001 for both) (Table C.5 in Appendix C). Negative ${}^{net}W_{\%}$ was only significantly larger at the typical speed (-66%) compared to the moderate speed (-60%, p = 0.01). The magnitude of ΔE_{wb} was larger than the other energies, so the percentage of energies was assessed relative to the ΔE_{wb} (i.e., $\Delta GPE_{\%,\Delta E}$, $\Delta TKE_{\%,\Delta E}$, and $\Delta RKE_{\%,\Delta E}$). There were no significant differences in relative energies across speeds (p > 0.05 for all). These results do not support pendular-like mechanics, but instead show the strategy used in single support fall is like a damped fall in which negative constituent work controls the lowering of the COM.

Over the terminal double support interval, a functional sub-task is to propel the body (Fig. 6.5). On average over the three conditions, the gait strategy was characterized by positive ${}^{net}W_{wb}$, which resulted in net positive ΔTKE_{wb}, indicating the whole body translational velocity increased. The positive ${}^{net}W_{\%}$ was significantly smaller at the typical speed (24%) compared to the slow (30%, p = 0.013) or moderate (28%, p = 0.001) speeds. The $\Delta GPE_{\%,\Delta E}$ became significantly smaller with speed (38%, 18%, 1% for slow, moderate, and typical speeds, respectively), while $\Delta TKE_{\%,\Delta E}$ became larger (57%, 76%, 92% for slow, moderate, and typical speeds, respectively; p < 0.01 for all pairwise comparisons). Thus, these results do not support our hypothesis that no net work would be done during the transition between steps, as in the dynamic walking model. Instead, the strategy used in double support is more like an active push in which positive constituent work is propelling the body.

The average net constituent work maintains the same pattern over the three walking speeds, but the constituents change roles over each interval (Fig. 6.6). The stance knee, HAT, and swing hip contribute primarily to positive work during single support rise, while the stance foot, ankle and hip, HAT, and swing knee do negative work during single support fall. During double support the trailing ankle, leading knee, and bilateral hips do positive work to propel the body while all other constituents do negative work, which has a braking effect.

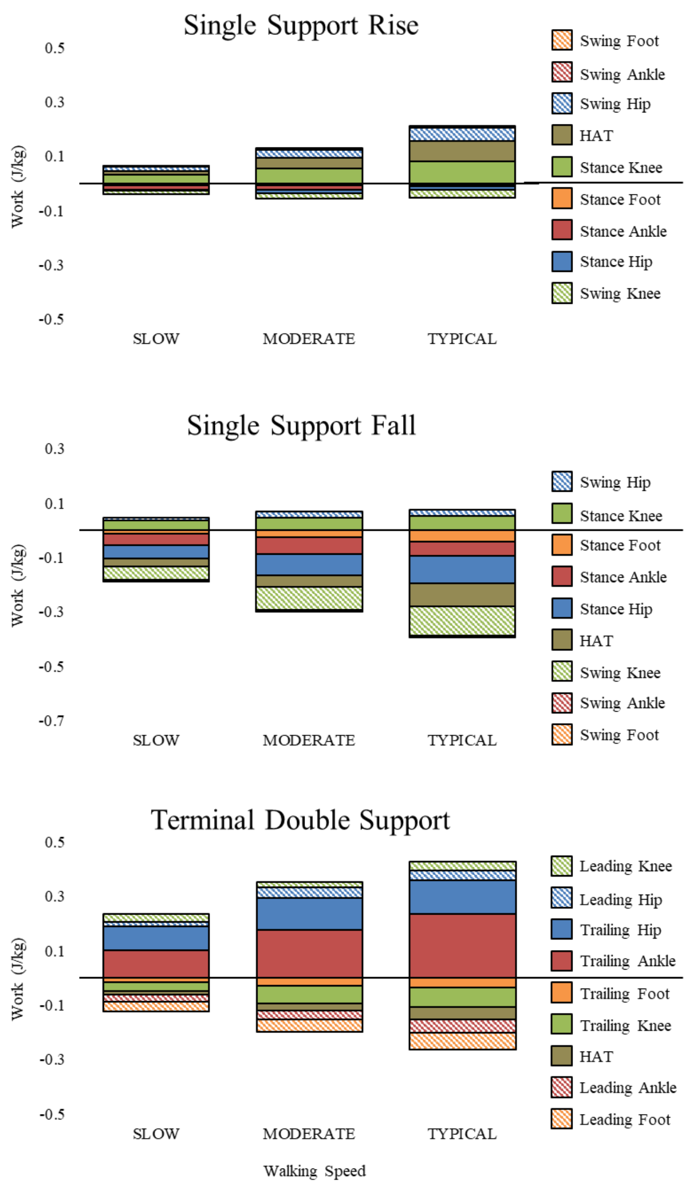

Figure 6.6: The average net constituent work maintains the same pattern over the three walking speeds, but the constituents change roles over each interval (except for the swing limb hip which is net positive for all intervals shown). The stance knee, HAT, and swing hip do net positive work during single support rise to raise the COM. All but the swing hip and stance knee do negative work during single support fall to control the lowering of the COM. The trailing ankle and hip primarily do net positive work that helps to propel the body during terminal double support. Statistically significant differences are reported in Table C.5 in Appendix C.

A table with the averages and ranges [max to min] for the ${}^{net}W_{\%}$, relative energies, and results of the statistical tests for each interval corresponding to Figs. 6.3 – 6.5 is in Table C.6 in Appendix C. A comprehensive table of the constituent work (corresponding to Fig. 6.6) and changes in energy values (corresponding to Figs. 6.3 – 6.5), along with the results of the statistical two-way repeated measures ANOVAs, is in Table C.5 in Appendix C.

6.6 Discussion

The Work-Energy Profiles is a novel, visual approach which, in presenting the constituent work and resulting changes in energy forms side-by-side, can be used to assess the energetics of the employed gait strategy over a task. The stacked bar charts of net positive and negative constituent work reveal the roles and relative magnitude of the constituents to generate or absorb energy over a task interval (i.e., the energetics of the gait strategy). The ΔGPE_{wb}, ΔTKE_{wb}, and ΔE_{wb} reveal the resulting change in energy state of the whole body over the task interval (i.e., the task outcome). The relative net work done by the constituents compared to the absolute resulting work was calculated, and the change in energy forms compared to the largest energy form. These metrics were used to compare the energetics from healthy individuals walking at slow, moderate, and typical speeds to each other and to the theorized energetics from previous literature, like the dynamic walking model. Unlike an inverted pendulum and a step-to-step transition in the dynamic walking model, this data supports that gait is more of an assisted rise, damped fall, and active push by the constituents.

6.6.1 Verification

The Work-Energy Profiles are dependent on the equivalence of all summed constituent work and changes in energy forms. Our results (Fig. 6.2, Table C.4 in Appendix C) verify that the calculations to create these profiles were executed correctly. Although the two measures of power are theoretically equivalent, differences can be expected using experimental data based on an analysis at the segmental level (Ebrahimi et al., 2018). These experimental errors can be a result of errors in tracking motion data, in accuracy of force and center of pressure data, or in filtering (Ebrahimi et al., 2018). Errors at the segmental level can compound when summing all the segments together in a whole body analysis, such that an average 1.0% difference in the power and rate of energy change measures is not unreasonable.

6.6.2 Work-Energy Profiles

When accounting for the energy of all segments of the body, human gait did not follow pendular mechanics. Instead, work done by the body actively controlled the gait mechanics from assisting in raising the body and dampening the lowering of the body in single support to actively propelling the body in double support. We hypothesized the body's potential and kinetic energy would exchange like an inverted pendulum during single support phase. However, experimental data showed that while there was partial exchange of potential and kinetic energy to raise the body during single support, a portion of positive net work assisted this task with more net work required as walking speed increased. There was no evidence of pendular-like mechanics in lowering the body in single support. Nearly all the negative net work was in the form of negative potential energy, with no significant differences in potential energy relative to net work as walking speed increased. During double support, zero net work was expected to transition between steps. However, positive net work done by the body was observed, with the majority of energy in the form of translational kinetic energy which increased with walking speed.

The Work-Energy Profiles summarize and compile findings of constituent work and energy that add new insight into the assessment of the energetics of gait strategies. First, the stacked positive and negative work bar charts reveal the magnitude of work from all constituents of the body together, as opposed to focusing on the stance limb. Previous literature that has only evaluated the stance limb work (Qiao and Jindrich, 2016) misses the positive work of the swing limb hip during single support rise and the negative work of the swing limb knee during single support fall. Second, the analysis of whole body energy forms assures that all the energy is accounted for over the interval. Previous studies that have focused on the change in energy forms of the COM alone would miss the additional translational kinetic energy contribution from the swing limb in single support, for example (Inman et al., 1981). Finally, the percentage of each energy form relative to the largest energy form provides a novel method for comparing experimental energetic values to theoretical models. Greater constituent work and energy with speed can be expected since stride length (Ebrahimi et al., 2017a) and, subsequently, COM displacement (Orendurff et al., 2004) increases with walking speed. However, the ratio of an energy form or work over an interval scales the data in such a way as to reduce the influence of greater inherent energy due to walking speed. Thus, these profiles presented with data from healthy individuals walking at different speeds demonstrate advantages from previous energetics metrics and provide new insight into assessing the energetics of gait strategies.

Mimicking pendular mechanics requires less work as evidenced more at the slow speed. A completely conserved inverted pendulum, where ΔTKE_{wb} is equal in magnitude and opposite in sign to the ΔGPE_{wb}, is not entirely expected in human gait as there is some work done by the constituents (Inman et al., 1981). While raising the body in single support phase, the mechanics more closely matched those of an inverted pendulum at the slow speed than the other two speeds (Fig. 6.3). During this sub-task, the stance knee is doing positive work (Fig. 6.6) where there is a resulting positive knee extension moment to support the body (Winter and Robertson, 1978). Individuals with muscle weakness, especially weakness leading to reduced knee extension moment, have been found to reduce walking speeds (Allen et al., 2010). Our results support that slower walking speed with muscle weakness may mechanically be a compensation for reducing the requirement of the joints and segments to do work to raise the body during single support. Instead, the body can take advantage of pendular mechanics during this sub-task.

Interestingly, typical gait energetics at all three speeds did not take advantage of pendular mechanics while lowering the body, but instead used negative work to control the fall of the center of mass. The concept of stance hip and ankle controlling the fall of the center of mass has been established for the stance limb (Hof et al., 2007). However, the bar charts in Fig. 6.6 show all joints and segments (except for stance knee and swing hip) are doing negative work. The work done to lower the body during this sub-task could be an important design factor for lower extremity assistive devices. Research has shown individuals with lower extremity amputations are prone to falls (Miller et al., 2001). Our results may provide evidence that individuals with impairments who lack the ability to control the body during this sub-task based on their injury (e.g. limitations from the prosthetic device or eccentric muscle weakness) may be more prone to falls as well.

Typical gait energetics also did not do zero net work during the step-to-step transition during double support as theorized in the dynamic walking model. This finding, however, is in accordance with the net negative work done during the single support fall. Net positive work is needed during double support so that net work over the entire gait cycle remains near zero (Bertram and Hasaneini, 2013; Cavagna et al., 2000; DeVita et al., 2007; Farris and Sawicki, 2012; Kuo, 2007; Miller and Verstraete, 1996; Zelik and Kuo, 2010). Previously, researchers have investigated the "push-off" phase, which generally overlaps with double support (Kuo et al., 2005). Researchers have identified the ankle plantar flexors to be the primary contributor to the progression of the body specifically during the push-off task in double support (e.g., Kepple et al., 1997; Neptune et al., 2001). However, previous research has not quantified the energetics of the whole body along with the work done by all the constituents. In this study, the ankle work did significantly increase with speed (Table C.5 in Appendix C). If positive work is necessary to propel the body into its next step, then it would be more successful to have the positive net work in the form of positive ΔTKE_{wb}. The $\Delta TKE_{\%,\Delta E}$ was largest at the typical speed, which provides support to why healthy individuals walk at typical speeds. The positive work done by the constituents is going into a positive change in ΔTKE_{wb}, indicating an increase in velocity (which is primarily in the forward direction during gait). Thus, the profiles of single support fall and terminal double support together can help to explain the gait strategy used at different conditions.

6.6.3 Limitations

The Work-Energy Profiles approach has notable limits to the extent with which results may be interpreted. By summing the energy forms of all segments in the body model, the Work-Energy Profiles approach allows transfer of energy between segments. Therefore, it is possible that positive and negative constituent work may be done during a sub-task that is negated and not shown in the net result. Several researchers have discussed energy transfer (Cavagna and Kaneko, 1977; Frost et al., 1997; McDowell et al., 2002; Van de Walle et al., 2012), and while it is not possible to know the true transfer of energy with rigid body models, the data with the presented model account for complete energy transfer. This is considered one extreme, where no energy transfer would be the other extreme.

There are some experimental limitations of this work. A constant treadmill speed was used, where previous literature may suggest variations in power with treadmill belt speed (Crétual and Fusco, 2011). However, because treadmill speed was used for both kinetic and kinematic measures, the relationship between constituent work and energies at each interval are unlikely to be affected by the constant speed, while the magnitude might. Furthermore, constituent work in rigid body inverse dynamics is a net effect of multiple muscles. Muscle work is not accurately represented by constituent values because of co-contraction and work done by biarticular muscles (Neptune and Van Den Bogert, 1998).

Also of note is the range of patterns exhibited by the subjects, as seen in detail in Table C.6 in Appendix C. Data in this table highlight the variability in task strategy even over a healthy sample population. For example, not all subjects followed the same pattern of relative percent changes in energy forms during single support rise at slow (n=2) and moderate (n=1) speeds. The Work-Energy Profiles display averages, and more data will be necessary in the future to determine if the instances where gait strategies did not follow the average pattern are meaningful.

6.6.4 Future Directions

The Work-Energy Profiles can be used to evaluate the energetics of tasks performed by a range of patient populations or at different conditions. This article demonstrates how profiles of healthy gait energetics data from walking at slow, moderate, and typical speeds can be used to compare and contrast with findings from several research studies with simple models of gait. Profiles investigating greater than typical speeds may reveal constituent work thresholds. In the future, these profiles can be used to analyze the energetics of compensatory strategies that develop when one or more constituents are impaired.

While the sum of constituent work is equivalent to the sum of energy forms mathematically, there cannot be claims of causality. A power flow analysis (Siegel et al., 2004) or induced acceleration analysis (Siegel et al., 2006) would be necessary for such claims. Some of the negative work or energy could be stored and returned as positive work or energy later in the gait cycle and would not be captured by these profiles. However, while these profiles cannot show the path for how energy was transferred within the interval, they do provide the resulting effect of work done over the interval. In the future, an approach could be developed that tracks how the constituent work contributed to certain energy forms precisely, but that would require knowledge of muscle activations (Crompton et al., 1998) to be modeled in a simulation.

6.7 Conclusion

This article presents the Work-Energy Profiles, a new approach to visualize and interpret the energetics of gait over specific sub-tasks. The calculations for the profiles were verified, and the utility of the profiles were demonstrated over three sub-tasks of gait across slow to typical walking speeds. When accounting for the energy of all segments of the body, human gait did not follow pendular mechanics. Unlike an inverted pendulum and a step-to-step transition in the dynamic walking model, this data supports that gait is more of an assisted rise, damped fall, and active push by the constituents. Profiles presented here for healthy individuals walking may be used as a normative sample data set to compare the energetics of compensatory strategies used by individuals walking with impairments in the future.

Chapter 7

CHANGES IN RELATIVE CONSTITUENT WORK WITH ARTIFICIAL ANKLE IMPAIRMENT

7.1 Abstract

The rehabilitation field is limited by the inability to fully predict the formation of compensatory strategies when individuals have impairments. To begin probing if there is a predictable interaction in the formation of compensatory strategies, this study induced an artificial impairment at the ankle unilaterally and bilaterally in healthy subjects. We theorized that the compensatory strategy due to bilateral ankle impairment would be the combination (interaction) of two compensatory strategies due to unilateral ankle impairment. Motion capture and force data were collected on 17 healthy subjects as they walked with standard shoes, with an ankle-foot orthotic unilaterally (RiAFO), and with an ankle-foot orthotic bilaterally (BiAFO) that impaired ankle motion in dorsiflexion and plantar flexion. Absolute mechanical work and relative constituent work were calculated to assess the gait strategy used under each condition. The AFO was successful in partially impairing ankle function (average 37 – 40% reduction in ankle work in RiAFO and BiAFO). Subjects walked at the same speed with similar temporal-spatial measures as without ankle impairment. Despite walking in a similar manner, the increase in mechanical constituent work by the hip and knee did not equal the amount reduced by the ankle, leading to a significant decrease in absolute limb work in the RiAFO and BiAFO conditions compared to Shoes (*p* < 0.001 for both). With unilateral ankle impairment, the

impaired limb’s relative knee work increased, whereas with bilateral ankle impairment, both the relative hip and knee work increased. Thus, these results indicate the compensatory strategy with bilateral ankle impairment is not simply the addition of two unilateral ankle impairment strategies.

7.2 Introduction

Individuals who have experienced a lower limb amputation (one million individuals in the United States (Ziegler-Graham et al., 2008)), stroke (over four million individuals (Kelly-Hayes et al., 1998)), or other lower limb impairment may require use of assistive devices in order to perform one of the most basic human movements: walking. Ankle musculature serves a primary function in gait and has been shown to play a key role in providing support and propelling the body forward (Neptune et al., 2008). Individuals with ankle weakness or loss of ankle musculature may rely on other joints of the limb to compensate, leading to compensatory gait strategies to walk at the same speed as an individual without impairment. However, the rehabilitation field is limited by the inability to fully understand if a causal or predictable relationship exists between an individual’s level of impairment and the formation of compensatory gait strategies, which could be useful for optimizing the care and quality of life for these individuals.

Mechanical work can be used to quantify compensatory gait strategies, because it is a summary measure of energy generated (positive) and absorbed (negative) at the joints and segments over an interval of time (Winter, 2009). Even in the case of an impairment, the net mechanical work of the limb is theoretically zero over the gait cycle as it is a cyclic task (Huang et al., 2015). However, the strategy to maintain net work near zero is unclear when one joint (e.g., ankle) is impaired such that work at that joint is significantly decreased. To investigate compensatory gait strategies, the magnitude of work distributed among the lower extremity "constituents" (i.e., hip, knee, ankle, distal foot (Siegel et al., 1996)) can be analyzed. David Winter, for example, found "equivalent load sharing," where the support moment (summed ankle, knee, and hip moment) was similar across walking speeds while individual joint moments varied (Winter, 1984). Mechanical cost-of-transport, or absolute limb work per unit distance traveled, may reveal a similar "equivalent work sharing" concept, where the sum of constituent work of the limb is constant despite variability in the magnitude of work from each constituent. Furthermore, relative constituent work (or constituent work as a percentage of absolute limb work) reveals the proportion of constituent work within a limb when an impairment exists. A constituent compensation is defined as a significant change in relative constituent work while walking with an impairment compared to typical, unimpaired walking.

Currently, predicting the form of interaction between constituent impairments and the resulting compensatory gait strategy is difficult. This idea has been postulated for decades, including by Ralston and colleagues who theorized that after finding an increase in energy expenditure when immobilizing one typical constituent of a healthy individual that immobilization of two or more constituents would have a summative effect (Inman et al., 1981). However, the compensatory gait strategy when more than one constituent is impaired may not be a simple "additive interaction," where the resulting strategy from multiple constituent impairments is the sum of unilateral constituent compensatory strategies. Researchers restricted the ankle joints of healthy individuals and found increased bilateral hip power generation with unilateral ankle restriction (Wutzke et al., 2012), but increased knee work primarily (and some increased hip work) with bilateral ankle restriction (Huang et al., 2015). This suggests that an additive interaction does not exist, but the compensatory strategies in these two studies are difficult to compare since the level of impairment and method used to restrict the ankle were inconsistent between studies. Therefore, it is yet unclear if there is an additive interaction between compensatory strategies when examining mechanical constituent work with one or more constituents impaired.

The objective of this study was to explore the form of interaction that governs compensatory strategies due to impaired ankle function. A cohort of typical, unimpaired individuals walked at a fixed speed with and without an artificial ankle impairment unilaterally and bilaterally. We hypothesized that the limb would exhibit equivalent work sharing across conditions such that absolute limb work would not significantly change when walking with one or both ankles impaired compared to walking without impairment. We also hypothesized that the compensatory strategy with bilateral ankle impairment would be the addition of two unilateral ankle impairment strategies (i.e., an additive interaction).

7.3 Methods

Seventeen healthy subjects (8M/9F, height 1.7 ± 0.2 m, mass 75.7 ± 15.1 kg, 33 ± 9 years) were fitted for rigid ankle foot orthotics (AFOs) for each limb (Fig. 7.1). All subjects provided informed consent under an IRB-approved protocol. Reflective markers were placed on subjects using a 6 degree-of-freedom (DOF) marker configuration (Holden et al., 1997), where clusters of markers were placed on the feet, shanks, thighs, pelvis, trunk, and upper arms. Breath-by-breath metabolic response was recorded using the Oxycon™ Mobile metabolic system (CareFusion, Reston, VA). Subjects walked on an instrumented split-belt treadmill (Bertec Corp., Columbus, OH) at 0.8 statures/s (1.36 ± 0.09 m/s) for 10 minutes to ensure metabolic stabilization as well as acclimation with the AFO. Motion (Motion Analysis Corp., Santa Rosa, CA) and force data were collected in the last three minutes of the trial. The subjects walked with standard shoes in all three conditions: without an AFO (Shoes), with an AFO on their right limb (RiAFO), and with AFOs on both limbs (BiAFO). Subjects were given a minimum of five minutes rest to ensure return to baseline conditions before beginning the next trial. All conditions were randomized. Motion capture data were sampled at 120 Hz and low-pass filtered at 6 Hz, and treadmill force data were sampled and low-pass filtered at 1200 Hz and 25 Hz, respectively.

Figure 7.1: Ankle foot orthotic (AFO) used to partially restrict the ankle joint only. AFOs were custom fitted to each subject by a certified orthotist and manufactured by the same technician for all subjects. The camber axis joint was locked at neutral and a plantar flexion stop was placed at the back. The foot plate was cut to three-quarters length to allow for toe extension.

Using Visual3D software, 6 DOF powers of each constituent (hip, knee, ankle, distal foot) were calculated bilaterally using methods described elsewhere (Buczek et al., 1994; Ebrahimi et al., 2018; Siegel et al., 1996). Positive or negative constituent work was calculated as the integration of the respective portions of the power curve over stance and swing phases and scaled by body mass. Note, when the ankle was restricted with an AFO, any work done by the AFO was accounted for in the resulting ankle work. Net limb work was the sum of the four positive and negative constituent work values. Absolute limb work was the sum of the positive constituent work values and absolute value of the four negative constituent work values. Mechanical cost-of-transport was computed as absolute limb work divided by stride length. Relative constituent work was calculated as the positive ($^{+}RW_{constituent}$) or negative ($^{-}RW_{constituent}$) constituent work divided by the absolute limb work, as a percentage in both stance and swing phase of gait (Ebrahimi et al., 2017a).

Differences in absolute limb work and relative constituent work were compared using several two-way repeated measures ANOVAs comparing the interaction of limb (left, right) and condition (Shoes, RiAFO, BiAFO) ($p < 0.05$) using SPSS software (IBM Corp., Armonk, NY). Outliers were assessed if studentized residuals were greater than ±3. Shapiro-Wilk's test of normality on the studentized residuals ($p < 0.05$) was used to assess normality. If Mauchly's test of sphericity was significant ($p < 0.05$), the Greenhouse-Geisser correction was reported. If there was a significant limb-by-condition interaction, simple main effects of condition were examined with post hoc Bonferroni corrections for pairwise comparisons ($p < 0.05$). If no interaction was found, the main effect of condition was reported ($p < 0.05$).

7.4 Results

Subjects walked at the same height-scaled speed and did not significantly change their step lengths (main effect $p = 0.065$). Net work was small (less than an average of 0.05 J/kg) across conditions (Table 7.1). Temporal-spatial parameters like cycle time, step length, and step width are reported in Table C.7 in Appendix C. The AFO was successful in partially reducing the ankle work, as positive ankle work went from 0.26 ± 0.04 J/kg in the Shoes condition to 0.16 ± 0.04 J/kg (37 ± 14% reduction) on the right limb in the RiAFO condition, and to 0.16 ± 0.04 J/kg (38 ± 15% reduction) on the right limb and 0.15 ± 0.04 J/kg (40 ± 9% reduction) on the left limb in the BiAFO condition (Table 7.2). Ankle plantar flexion and dorsiflexion were also restricted (Fig. D.3 in Appendix D). The shape of all power curves appears to be maintained across conditions as well (Fig. 7.2).

Table 7.1: Stride length, net limb work ($^{net}W_{limb}$), absolute limb work ($^{abs}W_{limb}$), and cost-of-transport (COT) metrics over the gait cycle (mean ± standard deviation). The limb-by-condition interactions and main effect of condition were not significant for stride length. Violations in normality are denoted with an "*," and Greenhouse-Geisser corrections for violations of sphericity are noted with superscripted "G-G" (all $p < 0.05$).

Metric	**Limb**	**Condition**			***p*-values**				
		Shoes	**RiAFO**	**BiAFO**	**Inter-action**	**Main effect**	**Sh-Ri**	**Sh-Bi**	**Ri-Bi**
Stride length (m)	Left	1.42 ± 0.13	1.42 ± 0.13	1.42 ± 0.13	0.423$^{G\text{-}G}$	0.065$^{G\text{-}G}$			
	Right	1.42 ± 0.13	1.42 ± 0.13	1.42 ± 0.13					
$^{net}W_{limb}$ (J/kg)	Left	0.03 ± 0.04	0.05 ± 0.05	0.04 ± 0.06	0.202	0.013	0.106	0.038	0.590
	Right	0.03 ± 0.05	0.02 ± 0.05	0.03 ± 0.06					
$^{abs}W_{limb}$ (J/kg)	Left	1.61 ± 0.24	1.63 ± 0.24*	1.54 ± 0.22	<0.001	0.001	0.720	0.055	0.003
	Right	1.61 ± 0.20	1.49 ± 0.21	1.51 ± 0.21		<0.001	<0.001	<0.001	0.142
COT (J/kg/m)	Left	1.12 ± 0.09	1.15 ± 0.09	1.08 ± 0.08	<0.001	0.001	0.217	0.086	0.002
	Right	1.10 ± 0.07	1.05 ± 0.08	1.06 ± 0.07		<0.001	<0.001	<0.001	0.460

Table 7.2: Magnitude of positive and negative constituent work ($^{+}W_{constituent}$, $^{-}W_{constituent}$) used to derive relative work values (mean ± standard deviation).

Variable	Phase	Limb	Shoes	RiAFO	BiAFO
$^{+}W_{hip}$ (J/kg)	Stance	Left	0.20 ± 0.06	0.22 ± 0.07	0.22 ± 0.07
		Right	0.21 ± 0.05	0.20 ± 0.04	0.22 ± 0.04
	Swing	Left	0.12 ± 0.03	0.13 ± 0.04	0.15 ± 0.03
		Right	0.12 ± 0.02	0.14 ± 0.02	0.14 ± 0.02
$^{-}W_{hip}$ (J/kg)	Stance	Left	-0.22 ± 0.06	-0.22 ± 0.05	-0.22 ± 0.06
		Right	-0.20 ± 0.06	-0.19 ± 0.05	-0.20 ± 0.05
	Swing	Left	-0.00 ± 0.00	-0.00 ± 0.00	-0.00 ± 0.00
		Right	-0.00 ± 0.00	-0.00 ± 0.00	-0.00 ± 0.00
$^{+}W_{knee}$ (J/kg)	Stance	Left	0.19 ± 0.06	0.20 ± 0.06	0.22 ± 0.07
		Right	0.19 ± 0.05	0.20 ± 0.05	0.21 ± 0.05
	Swing	Left	0.01 ± 0.01	0.01 ± 0.01	0.01 ± 0.01
		Right	0.01 ± 0.01	0.01 ± 0.01	0.01 ± 0.01
$^{-}W_{knee}$ (J/kg)	Stance	Left	-0.13 ± 0.04	-0.13 ± 0.04	-0.15 ± 0.04
		Right	-0.12 ± 0.03	-0.13 ± 0.04	-0.13 ± 0.04
	Swing	Left	-0.16 ± 0.03	-0.17 ± 0.02	-0.18 ± 0.03
		Right	-0.16 ± 0.02	-0.18 ± 0.02	-0.18 ± 0.03
$^{+}W_{ankle}$ (J/kg)	Stance	Left	0.26 ± 0.05	0.24 ± 0.03	0.15 ± 0.04
		Right	0.26 ± 0.04	0.16 ± 0.04	0.16 ± 0.04
	Swing	Left	0.00 ± 0.00	0.00 ± 0.00	0.00 ± 0.00
		Right	0.00 ± 0.00	0.00 ± 0.00	0.00 ± 0.00
$^{-}W_{ankle}$ (J/kg)	Stance	Left	-0.13 ± 0.04	-0.14 ± 0.04	-0.08 ± 0.03
		Right	-0.15 ± 0.03	-0.09 ± 0.02	-0.09 ± 0.02
	Swing	Left	-0.01 ± 0.00	-0.01 ± 0.00	-0.00 ± 0.00
		Right	-0.01 ± 0.00	-0.00 ± 0.00	-0.00 ± 0.00
$^{+}W_{foot}$ (J/kg)	Stance	Left	0.03 ± 0.01	0.04 ± 0.01	0.04 ± 0.01
		Right	0.03 ± 0.01	0.04 ± 0.01	0.04 ± 0.01
$^{-}W_{foot}$ (J/kg)	Stance	Left	-0.13 ± 0.03	-0.12 ± 0.02	-0.11 ± 0.02
		Right	-0.15 ± 0.04	-0.14 ± 0.03	-0.13 ± 0.03

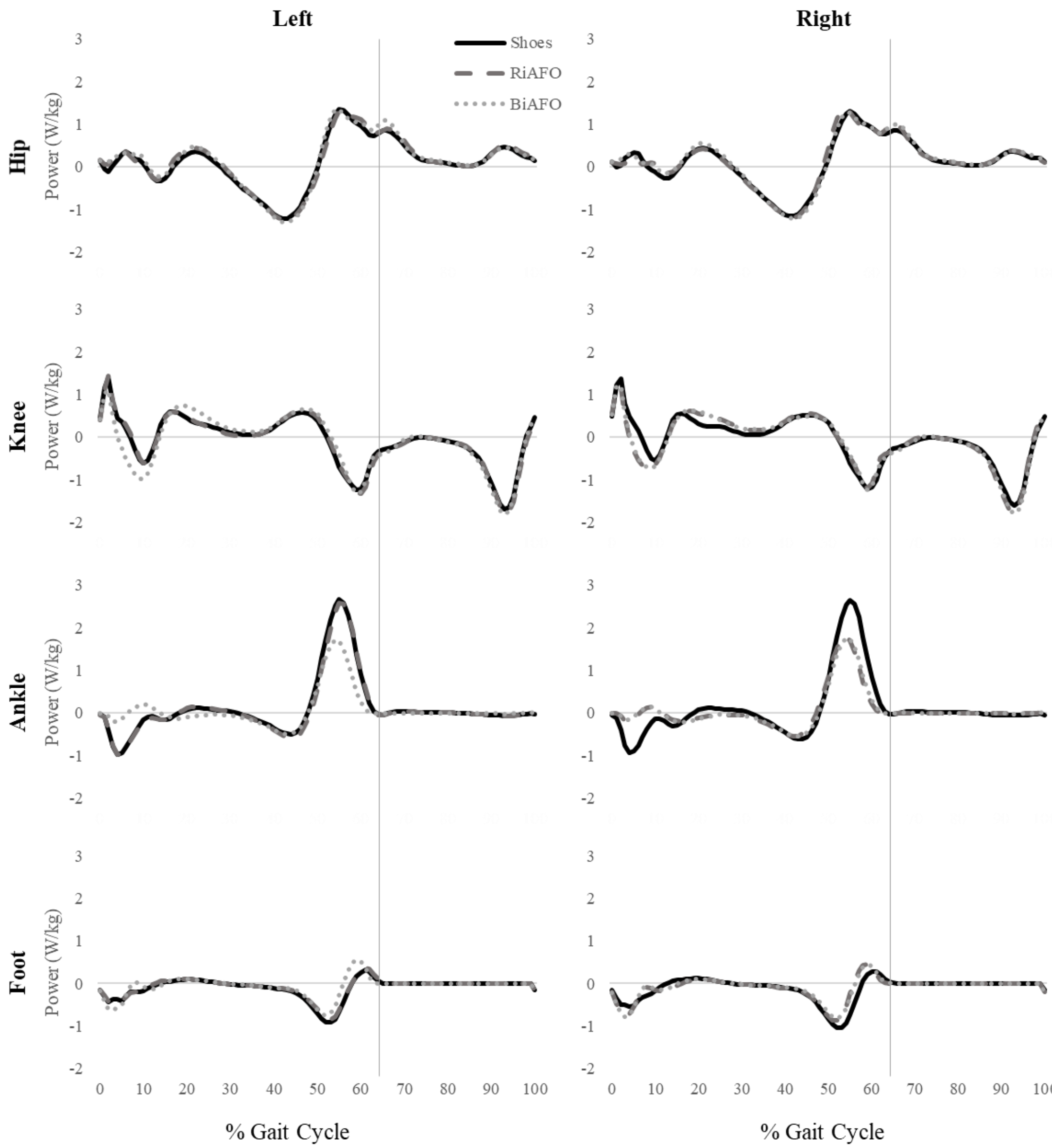

Figure 7.2: Constituent power curves averaged across all subjects for the left and right limbs appear to maintain their shape across conditions. Vertical line indicates end of stance (62% of the gait cycle).

The hip, knee, and foot did not fully compensate for reduced ankle work in the RiAFO and BiAFO conditions, leading to non-equivalent work sharing compared to the Shoes condition. On the right limb, absolute limb work and cost-of-transport both significantly decreased from Shoes in the RiAFO ($p < 0.001$) and BiAFO ($p < 0.001$) conditions (Table 7.1). However, the absolute limb work and cost-of-transport did not significantly differ between the right limb RiAFO and BiAFO conditions ($p = 0.142$ and $p = 0.460$, respectively). These limb work metrics show that, over the gait cycle, partial ankle impairment results in less limb work overall compared to without ankle impairment, such that there is not equivalent work sharing.

In the RiAFO condition compared to the Shoes condition, the right and left positive relative hip work only significantly increased in swing phase, while right relative knee work increased in stance and swing (Fig. 7.3). In stance, right $^{+}RW_{ankle}$ significantly decreased from an average of 15.9% to 10.8% ($p < 0.001$) and $^{-}RW_{ankle}$ decreased from an average of 9.3% to 6.4% ($p < 0.001$) (Table C.8 in Appendix C). There was a compensatory increase of relative work by 1 – 2% each in the $^{+}RW_{knee}$ and $^{-}RW_{knee}$ in stance, right $^{-}RW_{knee}$ and $^{+}RW_{hip}$ in swing, and the left $^{+}RW_{ankle}$ (Fig. 7.3, Table C.8 in Appendix C). Thus, there was a relative compensation by the right knee during stance phase, while both the knee and hip compensated during swing, despite an overall decrease in cost-of-transport.

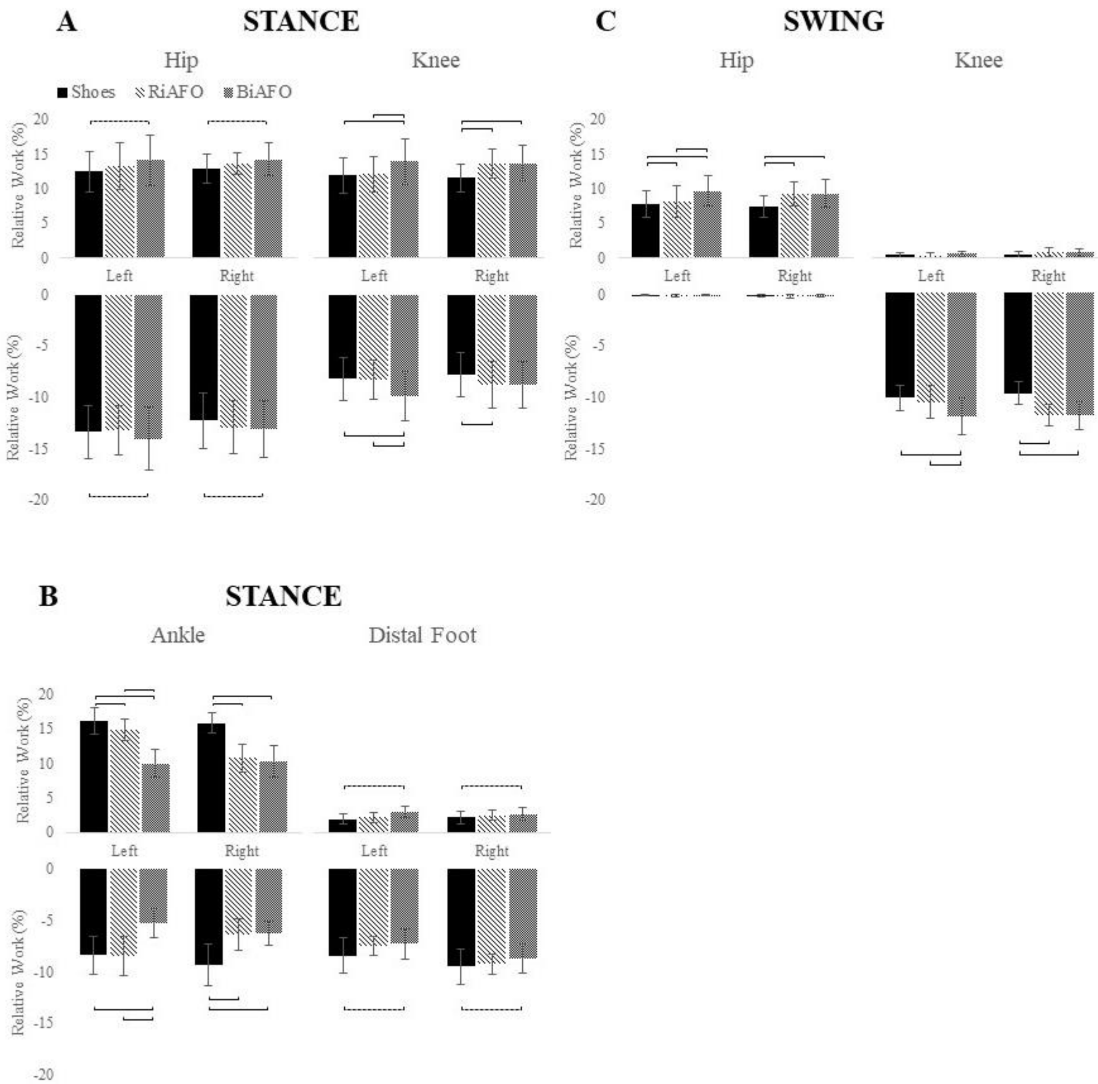

Figure 7.3: Relative constituent work for the hip and knee in stance (A), ankle and distal foot in stance (B), and hip and knee in swing (C) are presented for the Shoes, RiAFO, and BiAFO conditions. Dashed bars indicate a significant pairwise main effect of condition after a non-significant limb-by-condition interaction. Solid bars indicate a significant pairwise simple effect of condition after a significant limb-by-condition interaction ($p <$ 0.05).

The constituent compensations in the RiAFO condition were observed bilaterally in the BiAFO condition, but the BiAFO condition had additional constituent compensations (e.g., increased relative hip work and decreased relative distal foot work in stance phase) (Fig. 7.3). In the BiAFO condition, the $^{+}RW_{ankle}$ and $^{-}RW_{ankle}$ significantly decreased and the $^{+}RW_{knee}$ and $^{-}RW_{knee}$ significantly increased in stance, while the $^{+}RW_{hip}$ and $^{-}RW_{knee}$ significantly increased in swing bilaterally with similar magnitudes as changes in the right limb for the RiAFO condition ($p < 0.05$) (Fig. 7.3). There were no significant limb-by-condition interactions for the $^{+}RW_{hip}$, $^{-}RW_{hip}$, $^{+}RW_{foot}$, or $^{-}RW_{foot}$ ($p > 0.05$), although these four variables did have a significant main effect of condition with a significant pairwise comparison between Shoes and BiAFO ($p < 0.05$) (Table C.8 in Appendix C). Thus, the compensations from unilateral to bilateral ankle impairment do not show an additive interaction.

Although there were significant differences observed in the $^{-}RW_{hip}$, $^{+}RW_{knee}$, $^{+}RW_{ankle}$, and $^{-}RW_{ankle}$ in swing, these relative constituent work values were less than 1% and were thus not considered meaningful in this analysis.

7.5 Discussion

This study systematically induced a unilateral and bilateral ankle impairment on healthy individuals and found that the form of interaction that governs compensatory strategies with ankle impairment is complex. The AFOs were successful in reducing the ankle work by similar amounts in both the RiAFO and BiAFO conditions, and subjects walked in a similar manner with unilateral and bilateral ankle impairment (i.e., same speed and step length). Interestingly, there was non-equivalent work sharing between the Shoes and the AFO conditions, such that the hip, knee, and foot did not increase in work to the same magnitude as was reduced at the ankle work due to the AFO. Primarily, a unilateral ankle impairment strategy resulted in an increase in relative knee work on the impaired limb. If there was an additive interaction between compensatory strategies, an increase in relative knee work on both limbs in the BiAFO condition would be observed. This would mean the compensatory strategy for the BiAFO condition was the sum of two compensatory strategies observed in the RiAFO condition. However, the results do not support such an additive interaction from unilateral to bilateral ankle impairment; the hip and foot in stance compensated in the BiAFO condition along with the knee.

Fig. 7.2 can be used to interpret generally when the constituents compensated for ankle impairment. The increase in relative knee work during stance appears to have occurred during early single support when the knee extends to raise the COM because there is reduced eccentric control of ankle dorsiflexion due to ankle impairment. Changes in relative hip and foot work appear to occur during early and late stance in order to compensate for decreased ankle push-off power to propel the body forward. The increase in positive hip work in swing appears to occur early during concentric hip flexion, and the increase in negative knee work in swing appears to occur late to control eccentric knee extension. The AFO was lightweight and there was no discernable change in an individual’s body mass when wearing the AFOs, so it is unlikely the distal mass had a factor in swing limb energetics, as is supported by previous literature (Geboers et al., 2002).

Previous literature shows similar compensatory strategies with ankle impairment. Huang and colleagues systematically decreased ankle plantar flexion using steel cables at varying lengths. Specifically, a post hoc analysis revealed the peak ankle power was reduced from approximately 10% to 50%. Our results show on average a 34% reduction in peak ankle power, which appears to be in the middle range of the data from Huang and colleagues. Both Huang et al. and the present study found an increase in knee and hip work bilaterally with reduced ankle function (Huang et al., 2015). Previously, Wutzke and colleagues found healthy individuals walking with unilateral restriction of the ankle joint increased bilateral hip power generation in late stance with an approximate 36% decrease in peak ankle power (Wutzke et al., 2012). Note, peak ankle power reduction is different from the reduced work done over the gait cycle reported in Table 7.2. However, both of these previously published studies are difficult to compare to the current findings, not only because of the varying level of impairment, but also because of the varying methodology in restricting the ankle. The AFOs used by previous researchers had a full foot plate that restricted both the ankle and distal foot compared to the AFOs used in the present study that allowed toe extension with a three-quarters foot plate (Fig. 7.1).

The strengths of this study include the repeated measures design to methodically restrict the ankle joint using the same strategy (i.e., an AFO) both unilaterally and bilaterally and compare the constituent compensations against a control (i.e., no AFO). Several measures were taken to standardize the execution of the data collection. All subjects wore standardized shoes and walked at the same height-scaled walking speed for all three randomized conditions (Shoes, RiAFO, BiAFO). The same certified orthotist fitted all subjects for bilateral ankle foot orthotics, and the orthotics were manufactured by the same technician.

Despite controlling for the AFO design, there was notably large variability in the actual impairment these AFOs provided to the subjects. Recall, for example, the 37 ± 14% reduction in ankle work on the right limb in the RiAFO condition. In this study, the orthotist created the AFOs in a similar manner (e.g., casted all ankles at neutral, pulled the plastic to similar thicknesses, and cut plastic to allow toe extension). Previous literature has found the AFO to be stiffer during plantar flexion than dorsiflexion (Convery et al., 2004). However, studies have found that a ±20% difference in AFO stiffness did not considerably affect overall joint work (Harper et al., 2014). An alternative study design could involve providing different AFOs to individuals that equally reduced the amount of ankle work. However, the results from such a study would be difficult to parse if changes in gait were due to the device or due to the amount of reduced ankle work.

Some outliers were observed, although data were found to be genuine rather than due to measurement error, such that outliers were included in the data set. Because the statistical significance was comparable with and without the inclusion of the outlier data, only *p*-values from data with the outliers included is presented (noted in Table C.8 in Appendix C). Although there were some violations of normality via the Shapiro-Wilk's test, ANOVA tests are robust against violations of normality and were thus not expected to alter the findings (Schmider et al., 2010).

Further investigations that systematically control for level of impairment and number of constituents impaired will be necessary to explore if there is any predictable pattern to compensatory strategies. Exploring the interaction between impairment level and constituents impaired could revolutionize the design of rehabilitation and assistive devices. While this study isolated the impairment to the ankle joint, it is more likely that individuals with ankle weakness, such as individuals post-stroke, will have additional impairments that will affect more than one constituent (Jonkers et al., 2009; Peterson et al., 2010). In future studies, data presented here can be used in a

Constituent Lower Extremity Work (CLEW) report as presented in Chapter 4. Data in the CLEW pie charts from patients with ankle impairments may be compared to data presented in this chapter from healthy individuals with an induced ankle impairment. Fig. D.4 in Appendix D shows the relative work data from Fig. 7.3 in CLEW pie charts.

In conclusion, this study quantified and compared the compensatory strategies that are exhibited with unilateral and bilateral ankle impairment, where healthy subjects served as their own controls. There was non-equivalent work sharing with artificial ankle impairment (average 37 – 40% reduction in ankle work) compared to without ankle impairment, but subjects were able to walk in the same manner despite doing less absolute limb work. Relative constituent work analyses revealed that compensatory strategies may not be additive such that the sum of two unilateral ankle impairment compensatory strategies is not equivalent to a bilateral ankle impairment strategy. The relative constituent work approach presented here can be used to create a landscape for compensatory strategy options in the future that will take into account both the level of impairment and the number of constituents impaired.

7.6 Acknowledgments

The authors thank Teresa Ferrara, Michael Christensen, and Independence Prosthetics and Orthotics for assistance with data collection.

Chapter 8

COMPENSATORY GAIT STRATEGIES DUE TO ARTIFICIAL ANKLE IMPAIRMENT ARE AS EFFECTIVE AS UNIMPAIRED GAIT

8.1 Abstract

A long-standing interest in rehabilitation biomechanics is to determine if a compensatory gait strategy following impairment is effective. An objective method for assessing the effectiveness of a compensatory gait strategy is by determining if the strategy used mechanical energetics (i.e., gravitational potential, translational kinetic, and rotational kinetic energy) that are not significantly different from the energetics of a typical, unimpaired gait strategy. Using data collected during this dissertation that artificially impaired the ankle unilaterally and bilaterally, the purpose of this study was to use the Work-Energy Profiles approach developed in Chapter 6 to assess the effectiveness of compensatory strategies with artificial ankle impairment. Unimpaired gait energetics during three sub-tasks can be expected based on previous literature. First, net positive work by the body actively propels the body in double support, resulting in a positive change in translational kinetic energy. Second, minimal net positive work by the body assists the pendular mechanics in raising the center of mass in single support (i.e., single support rise), resulting in a primarily negative change in translational kinetic energy and positive change in gravitational potential energy. Third, net negative work by the body dampens the fall of the center of mass in single support (i.e., single support fall), resulting in a primarily negative change in gravitational potential energy. Relative measures of work and energy were calculated

in order to standardize metric comparisons across conditions. The experimental results revealed that both the unilateral and bilateral ankle impairment conditions were effective during double support where there were no significant differences in relative translational kinetic energy compared to the unimpaired condition. With bilateral ankle impairment, however, more relative mechanical work was done to change the gravitational potential energy during single support rise, which was less effective in using pendular mechanics to raise the center of mass than the unimpaired or unilateral ankle impairment conditions. With unilateral ankle impairment, less relative gravitational potential energy was observed while lowering the body during single support fall, which was less effective in dampening the fall of the body than the unimpaired or bilateral ankle impairment conditions. In terms of mechanical energetics, the compensatory strategies with both unilateral and bilateral impairment appeared effective in propelling the body in double support, but less effective in raising and lowering the body in single support. Future studies may explore how changes in constituent work in a compensatory strategy affect the changes in energy of the whole body more directly.

8.2 Introduction

Individuals with an impairment or weakness at one joint will often develop compensations in the other lower limb joints and segments in order to walk at a typical, unimpaired speed, thus developing a compensatory gait strategy. This is especially true for individuals with ankle weakness due to the important role of the ankle musculature in propelling the body forward and providing upright support (Neptune et al., 2001). In biomechanics research, several parameters are often used to describe the complex coordination of limbs that produce a gait strategy, from kinetic and kinematic measures like joint angles, moments, and powers, to temporal-spatial variables like stride length and stride time (Winter, 2009). David Winter formulated a "support moment synergy" in which he found that despite some variability in ankle, knee, and hip moments during gait across walking speeds, the support moment (summed joint moments) was consistently positive (Winter, 2009). Similar fundamental characteristics of gait may be true for individuals with impairments in determining a compensatory gait strategy, but these "rules" that govern the formation of compensatory gait strategies are not well understood.

Several research studies have focused on characterizing the mechanisms for the formation of compensatory strategies of individuals with ankle weakness, like individuals post-stroke (e.g., Cruz et al., 2009). However, this mechanism is complicated to measure, as it varies based on the number of lower limb joints impaired (Jonkers et al., 2009) and the magnitude of impairment (Allen et al., 2011; Chen et al., 2003; Mahon et al., 2015). Instead, researchers have controlled the magnitude of impairment by inducing a synthetic ankle impairment and characterizing the resulting compensation. While procedures like a tibial-nerve block can be useful in identifying the compensatory gait strategy due to the lack of plantar flexor activity (Sutherland et al., 1980), a less invasive technique is to restrict the ankle using an external device (Huang et al., 2015; Vanderpool et al., 2008; Wutzke et al., 2012). These studies have either artificially impaired one ankle or both ankles, but a comparison between unilateral and bilateral ankle impairment (i.e., increasing the number of constituents impaired) has yet to be shown.

A compensatory strategy can be deemed "effective" if the mechanical energetics of the strategy align with the energetics of a typical, unimpaired gait strategy during the sub-tasks of gait. Soo and Donelan probed the center of mass (COM) work requirements by bracing the ankle and knee of the leading or trailing limb in a rocking step-to-step transition movement, finding that more COM work was required when one limb was braced (Soo and Donelan, 2010). In Chapter 6, a Work-Energy Profiles approach was developed to assess the energetics of gait strategies by healthy, unimpaired individuals. The constituent (i.e., hip, knee, ankle, distal foot (Siegel et al., 1996), and head-arms-trunk (HAT)) mechanical work was used to understand how a gait strategy was performed, while the change in energy forms (gravitational potential and translational kinetic energy) described the resulting movement outcome of the strategy. The sub-tasks of gait were defined based on the functional roles of the body relating to raising and lowering the body's center of mass (COM) in single support phase, and propelling the body in double support phase.

The Work-Energy Profiles approach relies on the mechanical principle that net work over a sub-task is equivalent to the change in energy, which was experimentally verified (Chapter 6). Briefly, gait can be sectioned into four sub-tasks: initial double support, single support as the COM rises, single support as the COM falls, and terminal double support. During single support rise and fall, the COM moves through a semicircular arc, such that a net positive and a net negative gravitational potential energy of the body during each of these intervals is expected, respectively (Cappozzo et al., 1976; Inman et al., 1981). During double support, the aim is to transfer the weight of the trailing limb to the leading limb and redirect the velocity of the COM to progress forward (Donelan et al., 2002), resulting in a net positive translational kinetic energy (Chapter 6). Data from Chapter 6 support that gait is an assisted rise and controlled fall in single support, and an active push by the constituents in double support. Using this approach to determine the effectiveness of compensatory strategies with ankle impairment compared to without impairment can be beneficial in learning not only how the constituents compensate, but also why this compensatory strategy is implemented.

Thus, a systematic approach to explore the rules that govern the formation of compensatory adaptations is to artificially impair one constituent unilaterally and then bilaterally and compare the strategies to unimpaired gait. Using data collected during this dissertation impairing the ankle unilaterally and bilaterally (Chapter 7), the Work-Energy Profiles approach can reveal if the compensatory strategies with ankle impairment were effective, as assessed by the energy forms compared to the unimpaired ankle condition. Unimpaired gait energetics during three sub-tasks can be expected based on previous literature. First, net positive work by the body actively propels the body in double support, resulting in a positive change in translational kinetic energy. Second, minimal net positive work by the body assists the pendular mechanics in raising the center of mass in single support (i.e., single support rise), resulting in a primarily negative change in translational kinetic energy and positive change in gravitational potential energy. Third, net negative work by the body dampens the fall of the center of mass in single support (i.e., single support fall), resulting in a primarily negative change in gravitational potential energy. The purpose of this study was to assess the effectiveness of compensatory strategies when the ankle is partially impaired unilaterally and bilaterally in terms of mechanical energetics.

8.3 Methods

Data were analyzed from a data set presented previously (Chapter 7). Briefly, 17 healthy subjects (8M/9F, height 1.7 ± 0.2 m, mass 75.7 ± 15.1 kg, 33 ± 9 years) were fitted for rigid ankle foot orthoses (AFOs) for each limb. All subjects provided informed consent under an IRB-approved protocol. Reflective markers were placed on subjects using a 6 degree-of-freedom (DOF) marker configuration (Holden et al., 1997), where clusters of markers were placed on the feet, shanks, thighs, pelvis, trunk, and upper arms. Subjects walked on an instrumented split-belt treadmill (Bertec Corp., Columbus, OH) at 0.8 statures/s (1.36 ± 0.09 m/s) for 10 minutes while motion (Motion Analysis Corp., Santa Rosa, CA) and force data were collected. The subjects walked with standard shoes in all three conditions: without an AFO (Shoes), with an AFO on their right limb (RiAFO), and with AFOs on both limbs (BiAFO). All conditions were randomized. Motion capture data were sampled at 120 Hz and low-pass filtered at 6 Hz, and treadmill force data were sampled and low-pass filtered at 1200 Hz and 25 Hz, respectively.

Using Visual3D software, 6 DOF powers of each constituent (hip, knee, ankle, distal foot) were calculated bilaterally using methods described elsewhere (Buczek et al., 1994; Ebrahimi et al., 2018; Siegel et al., 1996). Work-Energy Profiles were created as described previously (Chapter 6). Constituent power (P_i) for the left (L) and right (R) legs and summed head-arms-trunk (HAT) is equivalent to the summed rate of change in energy forms of the whole body (wb), where GPE is gravitational potential energy, RKE is rotational kinetic energy, and TKE is translational kinetic energy (Equation 1).

$$(1)\quad P_{distal\ foot,L} + P_{ankle,L} + P_{knee,L} + P_{hip,L} + P_{distal\ foot,R} + P_{ankle,R} + P_{knee,R} + P_{hip,R} + P_{HAT} = \frac{d}{dt}GPE_{wb} + \frac{d}{dt}RKE_{wb} + \frac{d}{dt}TKE_{wb}$$

The rate of change in energy of the body was integrated in each of its forms as were the constituent powers of the left and right limb and HAT over the following intervals, corresponding with right stance phase: (1) initial double support – right heel strike to left toe off, (2) single support rise – left toe off to right midstance, (3) single support fall – right midstance to left heel strike, and (4) terminal double support – left heel strike to right toe off. Heel strike and toe off were determined based on the first (> 20 N) and last (< 20 N) instance of ground reaction force, and midstance was determined by the zero crossing of the anterior-posterior ground reaction force (Griffin et al., 1999).

Work-Energy Profiles for each interval were created where constituents with a resulting net positive (${}^{+}W_{wb}$) or negative (${}^{-}W_{wb}$) constituent work after integration over the interval of interest were shown in a stacked positive or negative bar chart, respectively, with an adjacent bar chart representing net work (${}^{net}W_{wb}$), which is the sum of ${}^{+}W_{wb}$ and ${}^{-}W_{wb}$. Four adjacent bars representing the integrated energies over the interval of interest are included (ΔE_{wb}, ΔGPE_{wb}, ΔTKE_{wb}, and ΔRKE_{wb}), where the sum of $\Delta GPE_{wb}, \Delta TKE_{wb}, \Delta RKE_{wb}$ is denoted as ΔE_{wb}. Note, using the work-energy relationship, ΔE_{wb} is theoretically equivalent to ${}^{net}W_{wb}$.

Before assessing the relative effectiveness of the gait strategies, consider that the magnitude of work and energy metrics would differ based on the different conditions. Thus, relative measures of work and energy were calculated in order to standardize metric comparisons across conditions. The relative net work (${}^{net}W_{\%}$), defined as the amount of ${}^{net}W_{wb}$ relative to the sum of the absolute resulting work done over that interval ($|{}^{+}W_{wb}| + |{}^{-}W_{wb}|$), was calculated as a percentage. This is a measure of the amount of remaining work relative to the absolute net positive and net negative work over the sub-task. The energies (ΔE_{wb}, ΔGPE_{wb}, ΔTKE_{wb}, and ΔRKE_{wb}) in relation to the largest energy form were also calculated as a percentage.

For example, if the ΔGPE_{wb} was the largest energy form, the relative energy forms would be written as the following: $\Delta E_{\%,\Delta GPE}$, $\Delta TKE_{\%,\Delta GPE}$, and $\Delta RKE_{\%,\Delta GPE}$.

Then, the relative net work and energy forms in the Work-Energy Profiles were compared across conditions to the resulting energetics of unimpaired gait (Shoes). For single support rise, raising the COM is assisted by net positive constituent work. Thus, the AFO conditions were effective if the $\Delta E_{\%,\Delta GPE}$ and $\Delta TKE_{\%,\Delta GPE}$ were not significantly different from Shoes. For single support fall, lowering the COM is controlled by net negative constituent work. The AFO conditions were effective if the negative $\Delta GPE_{\%,\Delta E}$ was not significantly different from Shoes. For double support, propelling the COM is an active push by net positive constituent work. The AFO conditions were effective if $\Delta TKE_{\%,\Delta E}$ was not significantly different from Shoes.

Using SPSS software (IBM Corp., Armonk, NY), differences in ${}^{net}W_{\%}$ and relative changes in energies were compared for the three walking speeds using several one-way repeated measures ANOVAs with Bonferroni corrections for each interval. For the one-way ANOVA, a value more than 1.5 times the interquartile range from a boxplot of the data was considered an outlier. If Mauchly's test of sphericity was significant ($p < 0.05$), the Greenhouse-Geisser correction was reported. If there was a significant interaction, simple main effects of speed were examined with post hoc Bonferroni corrections for pairwise comparisons ($p < 0.05$). If no interaction was found, the main effect of speed was reported ($p < 0.05$).

8.4 Results

As reported in detail in Chapter 7, individuals walked in a similar manner (e.g., walking speed and temporal-spatial parameters) in the three conditions, and the AFO was successful in reducing the amount of ankle work by an average of 37 – 40% in both the RiAFO and BiAFO conditions. The changes in energy forms showed a similar pattern when individuals walked with unilateral (RiAFO) or bilateral (BiAFO) ankle impairment as with no ankle impairment (Shoes) (Figs. 8.1 – 8.4). ΔRKE_{wb} is minimal through each interval. All relative changes in energies are quantified in Table C.9 in Appendix C. Column data are presented as averages with standard deviation bars.

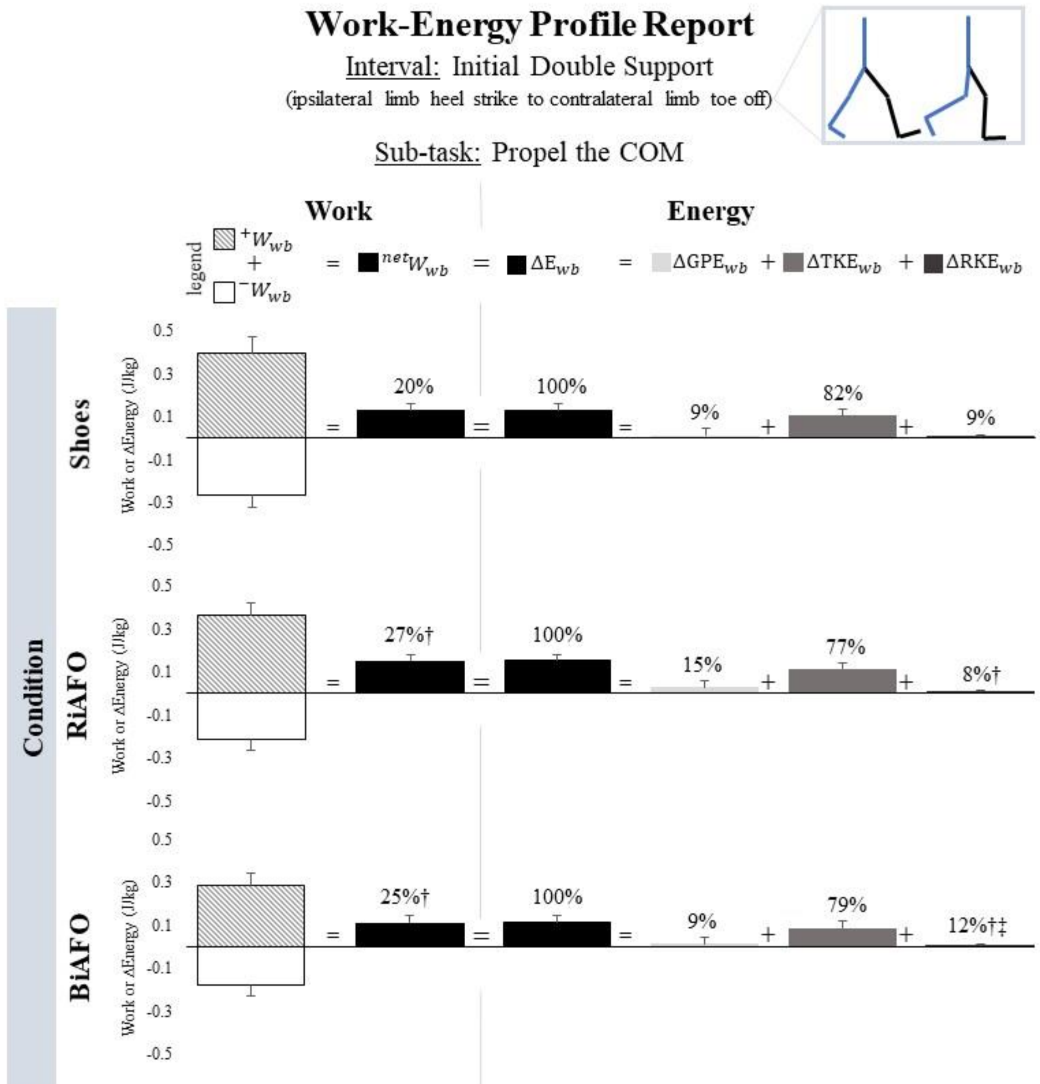

Figure 8.1: Over the initial double support interval, a functional sub-task of the whole body (wb) is to propel the COM, which is observed by a positive ΔTKE_{wb}. The strategy in the RiAFO and BiAFO conditions used more net work ($^{net}W_{wb}$) as a percentage of summed positive ($^{+}W_{wb}$) and absolute negative ($^{-}W_{wb}$) work (27% and 25% compared to 20%). The proportion of ΔTKE_{wb} did not significantly differ with condition, so that AFO conditions were effective compared to Shoes. A † and ‡ denote the values are significantly different from the values at the Shoes and RiAFO conditions, respectively ($p < 0.05$).

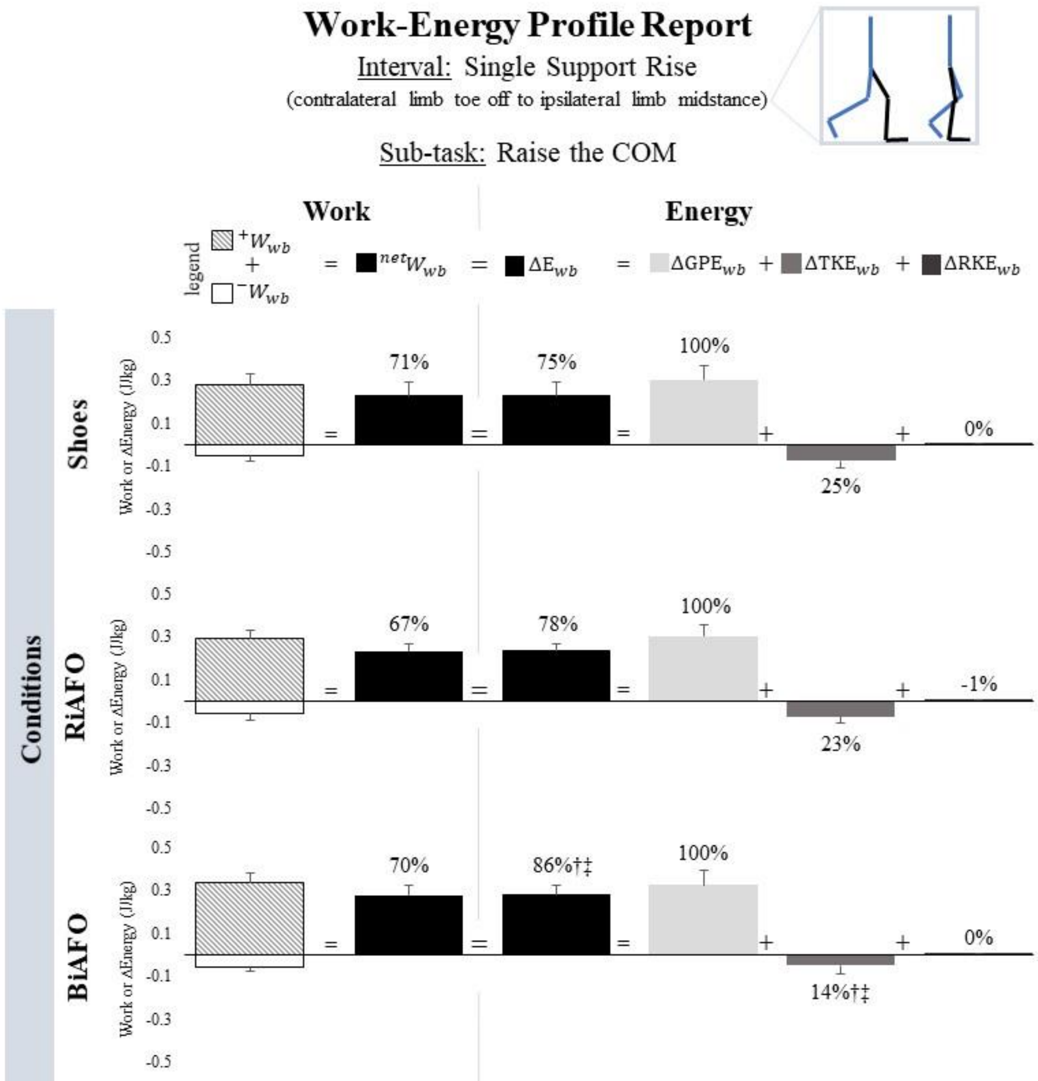

Figure 8.2: Over the single support rise interval, a functional sub-task of the whole body (wb) is to raise the COM, which is observed by a positive ΔGPE_{wb}. The net work $^{net}W_{wb}$ performed as a percentage of summed positive ($^{+}W_{wb}$) and absolute negative ($^{-}W_{wb}$) work did not change across conditions. The BiAFO condition was less effective because significantly more of the proportion of ΔE_{wb} was used (86%) to raise the COM relative to the other conditions. This shows the strategy in the BiAFO condition used less pendular-like mechanics than the Shoes condition. A † and ‡ denote the values are significantly different from the values at the Shoes and RiAFO conditions, respectively ($p < 0.05$).

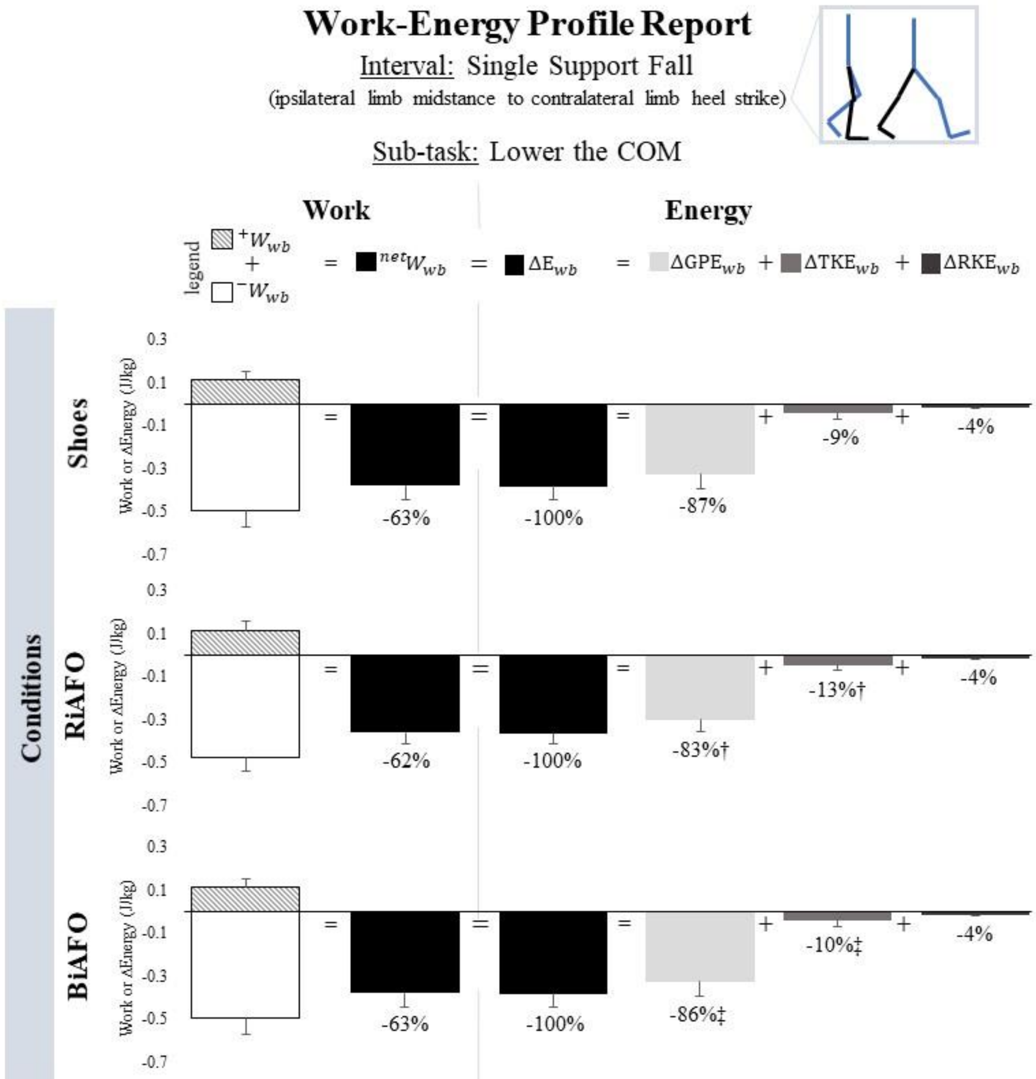

Figure 8.3: Over the single support fall interval, a functional sub-task of the whole body (wb) is to lower the COM, which is observed by a negative ΔGPE_{wb}. More than 62% of the net work ($^{net}W_{wb}$) performed as a percentage of summed positive ($^{+}W_{wb}$) and absolute negative ($^{-}W_{wb}$) work was negative, and almost all of the energy was negative ΔGPE_{wb}. The strategy in the RiAFO condition had a significantly lower proportion of ΔGPE_{wb} (-83%) than in Shoes or BiAFO, but the majority of energy took the form of ΔGPE_{wb} in all three conditions. A † and ‡ denote the values are significantly different from the values at the Shoes and RiAFO conditions, respectively ($p < 0.05$).

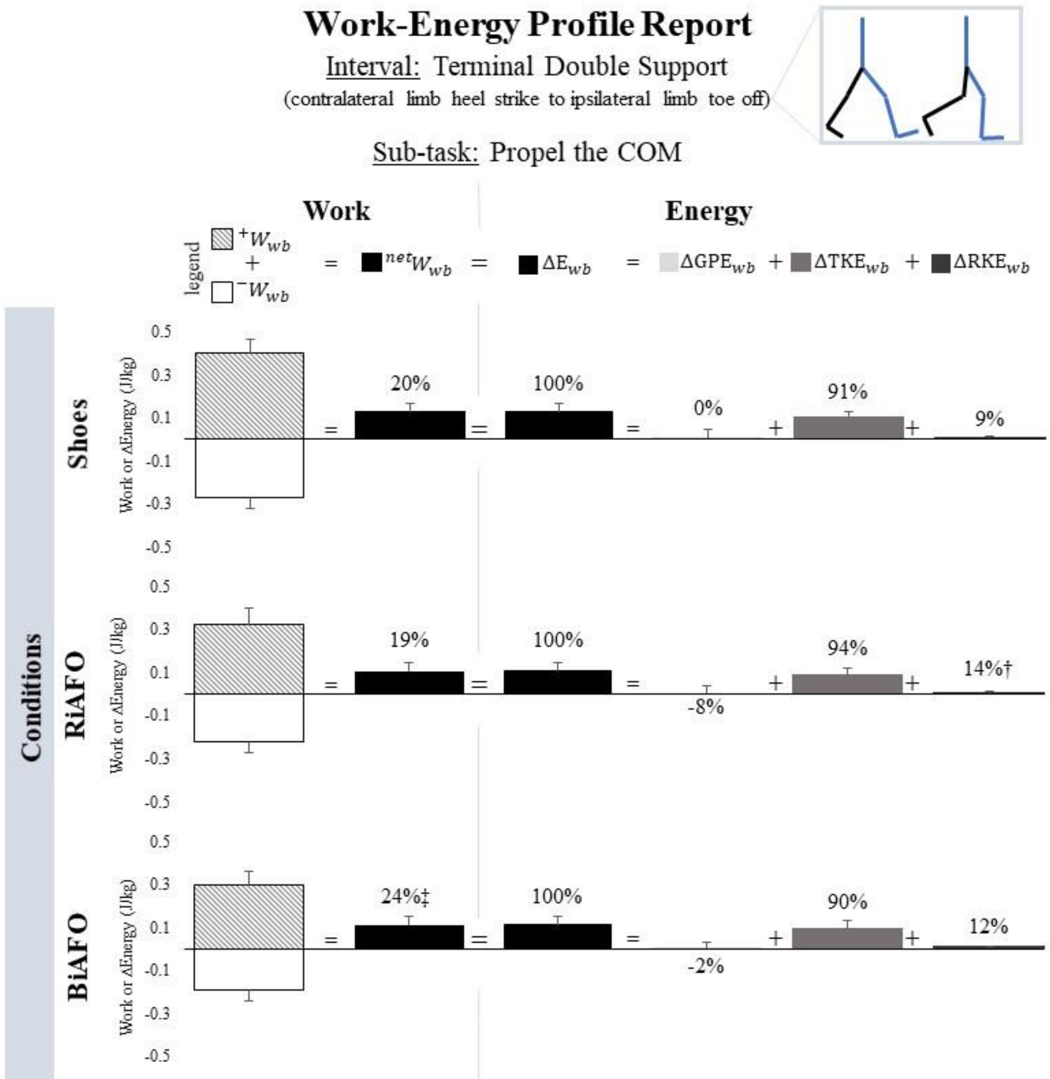

Figure 8.4: Over the terminal double support interval, a functional sub-task of the whole body (wb) is to propel the COM, which is observed by a positive $\Delta\mathrm{TKE}_{wb}$. There was more net work (${}^{net}W_{wb}$) performed as a percentage of summed positive (${}^{+}W_{wb}$) and absolute negative (${}^{-}W_{wb}$) work in the BiAFO condition. The proportion of $\Delta\mathrm{TKE}_{wb}$ did not significantly differ with condition, so that AFO conditions were effective compared to Shoes. A † and ‡ denote the values are significantly different from the values at the Shoes and RiAFO conditions, respectively ($p < 0.05$).

During double support, the sub-task to propel the body results in a majority of energy in the form of positive ΔTKE_{wb} for typical gait. In initial (Fig. 8.1) and terminal (Fig. 8.4) double support, all three conditions used a strategy that achieved positive ΔTKE_{wb}, with $\Delta TKE_{\%,\Delta E}$ greater than 77% and with no significant difference across conditions (p = 0.302 in initial and p = 0.391 in terminal double support). In the RiAFO condition, when the AFO was on the leading limb in initial double support, there was an increase in positive ${}^{net}W_{wb}$ compared to Shoes (p = 0.003) (Table 8.1). However, when the AFO was on the trailing limb in terminal double support, there was a decrease in positive ${}^{net}W_{wb}$ compared to Shoes (p = 0.002). With both limbs impaired in the BiAFO condition, the ${}^{net}W_{wb}$ did not significantly change with Shoes in either double support conditions, but the ${}^{net}W_{\%}$ was significantly larger compared to Shoes in initial double support (p = 0.023) and compared to the RiAFO in terminal double support (p = 0.033). By compensating for the ankle impairment (as observed by the changes in ${}^{net}W_{wb}$), the RiAFO and BiAFO conditions were effective in propelling the body compared to Shoes since there were no significant differences in $\Delta TKE_{\%,\Delta E}$ across conditions.

Table 8.1: Summed positive and negative work by all the constituents ($^{+}W_{wb}$ and $^{-}W_{wb}$) and net, gravitational potential, translational kinetic, and rotational kinetic energies of the whole body (ΔE_{wb}, ΔGPE_{wb}, ΔTKE_{wb}, and ΔRKE_{wb}, respectively) are presented (mean ± standard deviation). All work and changes in energy forms had significant interval-by-condition interactions based on several two-way repeated measures ANOVAs. Violations in normality are denoted with an "*," and Greenhouse-Geisser corrections for sphericity are noted with superscripted "G-G" (all $p < 0.05$). Intervals correspond to initial double support (Init DS), single support rise (SS Rise), single support fall (SS Fall), and terminal double support (Term DS) of the right gait cycle.

Metric	**Interval**	**Shoes (J/kg)**	**RiAFO (J/kg)**	**BiAFO (J/kg)**	***p*-values**				
					Inter-action	**Main effect**	**Sh-Ri**	**Sh-Bi**	**Ri-Bi**
$^{+}W_{wb}$	Init DS	0.39 ± 0.07*	0.36 ± 0.06*	0.29 ± 0.06*^	<0.001	<0.001	0.005	<0.001	<0.001
	SS Rise	0.25 ± 0.05	0.29 ± 0.04	0.33 ± 0.05		<0.001	0.094	<0.001	<0.001
	SS Fall	0.11 ± 0.04	0.11 ± 0.04	0.11 ± 0.04		0.567			
	Term DS	0.40 ± 0.06	0.32 ± 0.07	0.30 ± 0.06		<0.001	<0.001	<0.001	0.050
$^{-}W_{wb}$	Init DS	-0.26 ± 0.06	-0.21 ± 0.05	-0.17 ± 0.05*	<0.001	<0.001	<0.001	<0.001	<0.001
	SS Rise	-0.05 ± 0.03	-0.06 ± 0.03	-0.06 ± 0.02		0.033	0.171	0.073	1.000
	SS Fall	-0.47 ± 0.07	-0.47 ± 0.06	-0.49 ± 0.08		0.009	1.000	0.015	0.094
	Term DS	-0.27 ± 0.05	-0.22 ± 0.05*	-0.19 ± 0.05		<0.001	<0.001	<0.001	0.017
$^{net}W_{wb}$	Init DS	0.13 ± 0.03*	0.15 ± 0.03	0.11 ± 0.03	<0.001	<0.001	0.003	0.096	<0.001
	SS Rise	0.23 ± 0.06	0.23 ± 0.04	0.28 ± 0.05		<0.001	1.000	<0.001	<0.001
	SS Fall	-0.36 ± 0.06	-0.36 ± 0.06	-0.38 ± 0.07		0.010	1.000	0.050	0.018
	Term DS	0.13 ± 0.04	0.11 ± 0.04	0.11 ± 0.04		$0.005^{G\text{-}G}$	0.002	0.102	0.687
ΔGPE_{wb}	Init DS	0.01 ± 0.03	0.03 ± 0.03	0.01 ± 0.03	<0.001	0.003	0.009	1.000	0.006
	SS Rise	0.30 ± 0.07	0.30 ± 0.06	0.32 ± 0.07		0.001	1.000	0.003	0.002
	SS Fall	-0.31 ± 0.06	-0.30 ± 0.06	-0.33 ± 0.07		<0.001	0.131	0.074	<0.001
	Term DS	0.01 ± 0.04	0.00 ± 0.03	0.00 ± 0.03		0.079			
ΔTKE_{wb}	Init DS	0.11 ± 0.03	0.11 ± 0.03*	0.09 ± 0.03	<0.001	<0.001	0.168	0.031	<0.001
	SS Rise	-0.08 ± 0.03	-0.07 ± 0.03	-0.05 ± 0.04		<0.001	1.000	0.003	0.007
	SS Fall	-0.03 ± 0.03	-0.05 ± 0.02	-0.04 ± 0.03		0.053			
	Term DS	0.11 ± 0.02	0.09 ± 0.03	0.10 ± 0.04		<0.001	<0.001	0.127	0.092
ΔRKE_{wb}	Init DS	0.01 ± 0.00	0.01 ± 0.00	0.01 ± 0.00	N/A				
	SS Rise	0.00 ± 0.00	0.00 ± 0.00	0.00 ± 0.00					
	SS Fall	-0.01 ± 0.00	-0.01 ± 0.00	-0.01 ± 0.00					
	Term DS	0.01 ± 0.00	0.01 ± 0.00	0.01 ± 0.00					

During single support rise, the sub-task to raise the COM results in a majority of energy in the form of positive ΔGPE_{wb} for typical gait. All three conditions used a strategy that achieved positive ΔGPE_{wb} and negative ΔTKE_{wb}. Only in the BiAFO condition (0.32 ± 0.07 J/kg) was ΔGPE_{wb} significantly larger than Shoes (0.30 ± 0.07 J/kg) and RiAFO (0.30 ± 0.06 J/kg) (Table 8.1). There was a significantly larger $\Delta E_{\%,\Delta GPE}$ and a significantly smaller $\Delta TKE_{\%,\Delta GPE}$ as a portion of ΔGPE_{wb} in the BiAFO condition than both Shoes and RiAFO (Fig. 8.2). Thus, the BiAFO condition was less effective in using pendular mechanics to raise the COM compared to Shoes.

During single support fall, the sub-task to lower the COM results in a majority of energy in the form of negative ΔGPE_{wb} for typical gait. All three conditions used a strategy that achieved negative ΔGPE_{wb} and minimal ΔTKE_{wb}. There were no significant differences in ΔGPE_{wb} in RiAFO or BiAFO compared to Shoes (p = 0.131 and 0.074, respectively). The gait strategy in the RiAFO condition did result in significantly less negative $\Delta GPE_{\%,\Delta E}$ (average -83%) and increase in negative $\Delta TKE_{\%,\Delta E}$ (-13%) compared with Shoes (-87% and -9%, respectively) and BiAFO (-86% and -10%, respectively) (Fig. 8.3). Thus, the RiAFO condition was less effective in controlling the fall of the COM compared to Shoes.

Constituent work appeared to generally maintain the same roles over each interval but at different magnitudes (Table C.10 in Appendix C). In initial double support (Fig. 8.5A) and terminal double support (Fig. 8.5B), the trailing ankle and hip do positive work, while the trailing knee and leading ankle and foot do negative work. In single support rise (Fig. 8.6A), the stance knee, HAT, and swing hip do positive work, while in single support fall (Fig. 8.6B), the stance ankle, hip, HAT, and swing knee do negative work.

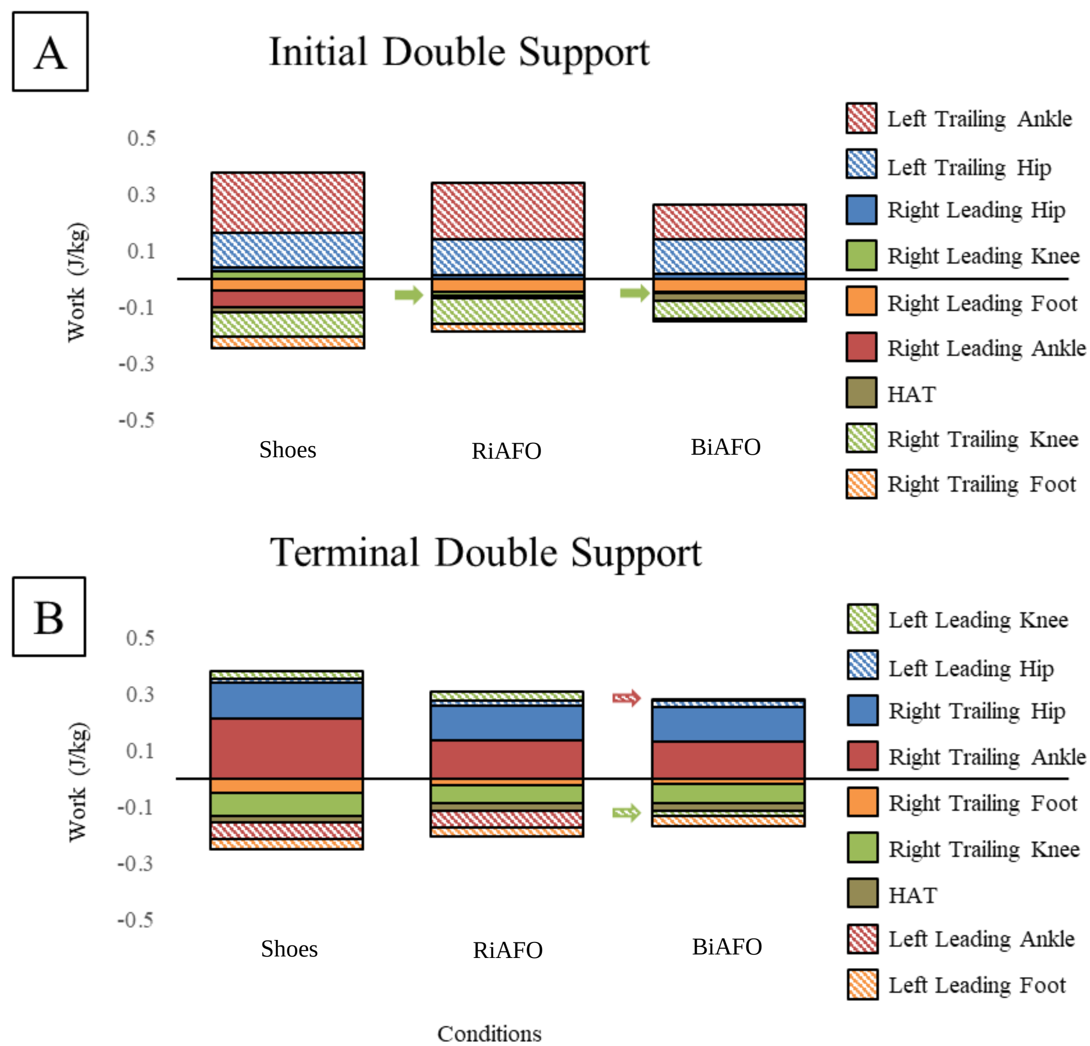

Figure 8.5: The average net constituent work generally maintains the same pattern over the three conditions (except where noted in color coordinated arrows) for (A) initial double support and (B) terminal double support. The trailing ankle and hip primarily do net positive work to propel the COM during double support.

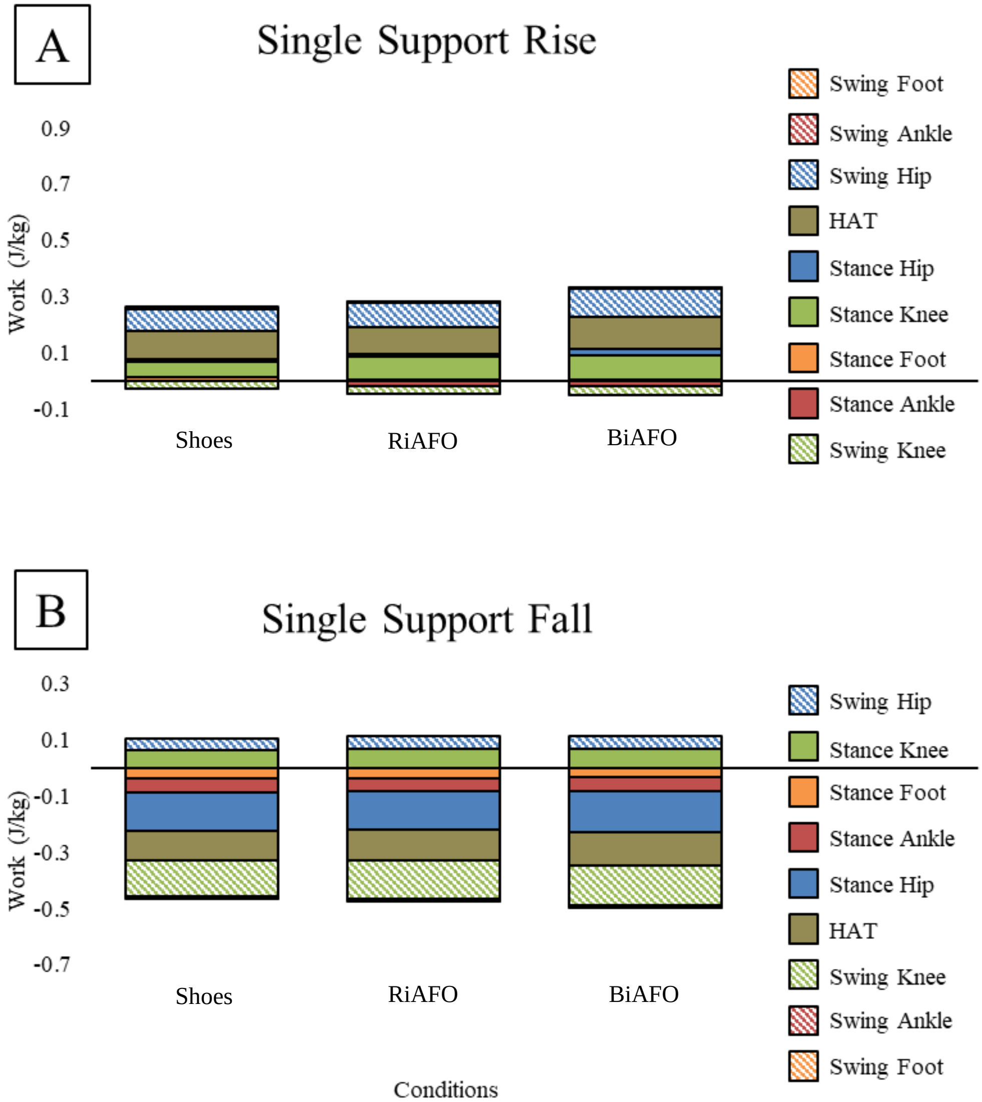

Figure 8.6: The average net constituent work maintains the same pattern over the three conditions, but the constituents change roles over (A) single support rise and (B) single support fall. The stance knee, HAT, and swing hip do net positive work during single support rise to raise the COM. All but the swing hip and stance knee do negative work during single support fall to control lowering the COM.

8.5 Discussion

Using mechanical energetics, data from individuals walking with unilateral and bilateral partial ankle impairment revealed where in the gait cycle compensatory strategies were effective compared to typical, unimpaired gait. In double support phase, individuals were effective in compensating for ankle impairment, as evidenced by no significant differences in a positive $\Delta TKE_{\%,\Delta E}$ to propel the body compared to unimpaired gait. However, in single support phase, individuals walking with bilateral ankle impairment were less effective in using pendular mechanics (as evidenced by a smaller $\Delta TKE_{\%,\Delta GPE}$) to raise the COM compared to unimpaired gait. Also in single support, individuals walking with unilateral ankle impairment were less effective in controlling the fall of the COM (as evidenced by less negative $\Delta GPE_{\%,\Delta E}$) compared to unimpaired gait. These compensatory strategies and the resulting energy forms of the body were assessed using Work-Energy Profiles, which were developed in Chapter 6. The generally similar patterns of changes in energy forms across conditions further support that individuals walked in a similar manner across walking speeds, as first reported in Chapter 7, where there was no difference in step length as individuals walked at the same speed in all conditions. However, an analysis of the relative changes in energies and ${}^{net}W_{\%}$ helps explain how the compensatory strategy in the presence of reduced ankle work was effective in double support to propel the body but less effective in single support to raise and lower the body.

In the RiAFO condition during double support, the compensatory strategy was as effective in propelling the COM as in the Shoes condition based on no significant differences in positive $\Delta TKE_{\%,\Delta E}$ compared to Shoes, despite changes in ${}^{net}W_{wb}$ and ${}^{net}W_{\%}$. During initial double support, there was a decrease in ${}^{-}W_{wb}$ compared to Shoes because the impaired ankle was on the leading limb, which has a "braking" role.

During terminal double support, when the impaired ankle was on the trailing limb which has a "propulsive" role, there was less ${}^{+}W_{wb}$ and a decrease in ${}^{net}W_{wb}$. Thus, with a partial ankle impairment unilaterally (average 37 – 40% reduction in ankle work), healthy individuals were able to perform a compensatory adaptation to walk with similar energy forms despite changes in constituent and whole body net work during this sub-task. However, during single support fall, the RiAFO condition was less effective in lowering the COM than the Shoes condition. Net mechanical constituent work was distributed primarily to the negative $\Delta GPE_{\%,\Delta E}$ in all conditions, but there was significantly less $\Delta GPE_{\%,\Delta E}$ in the RiAFO condition compared to Shoes. While this is considered less effective based on the definition presented in this chapter, a majority of the energy is still in the form of $\Delta GPE_{\%,\Delta E}$ (>80%), which must be considered in the determination of effectiveness.

In the BiAFO condition, while the compensatory strategy was also effective in propelling the COM in double support, more mechanical work went into raising the COM during single support rise than the Shoes or RiAFO conditions. With both ankles impaired, there was less ${}^{+}W_{wb}$ and ${}^{-}W_{wb}$ during double support than Shoes, but this did not significantly change the ${}^{net}W_{wb}$ or the relative $\Delta GPE_{\%,\Delta E}$ or $\Delta TKE_{\%,\Delta E}$. However, the $\Delta E_{\%,\Delta GPE}$ to raise the COM in single support rise was larger, meaning that more of the mechanical work done by the constituents went into raising the COM, and less came from a pendular-like mechanism of transferring negative ΔTKE_{wb} to positive ΔGPE_{wb} (Chapter 6). During single support rise, the sub-task to raise the COM is achieved through some transfer of negative ΔTKE_{wb} to positive ΔGPE_{wb} and additional mechanical constituent work (ΔE_{wb}). Previous research has supported that significant muscle mechanical work is required to raise the COM during this interval (Neptune et al., 2004). Also during this interval, the stance knee and swing hip are doing positive work. So, despite achieving the sub-task, requiring more work to raise the COM may theoretically be more metabolically taxing over time, based on evidence that increased mechanical work by the knee and hip is less efficient and may show an increased metabolic cost (Farris and Sawicki, 2012).

Previous literature supports the importance of the hip muscles concentrically contracting during double support to move the body forward. Wutzke and colleagues found that reducing peak ankle plantar flexion power by an average of 36% unilaterally resulted in an increase in peak hip power bilaterally in terminal stance (Wutzke et al., 2012). In a review of secondary compensatory mechanisms due to primary pathologies, researchers found that ankle plantar flexor weakness results in a compensatory mechanism by the hip flexors to concentrically contract in pre-swing (Schmid et al., 2013). Furthermore, lower functioning subjects with hemiparesis were unable to increase walking speed due to a limited ability to generate hip and ankle power (Jonkers et al., 2009). In this study, the partial ankle impairment was successful in reducing peak ankle power by an average of 34%. This may have been small enough not to affect the hip power in stance, thus maintaining the subjects' ability to achieve an effective walking strategy during double support. Previous literature with data from subjects walking with an average 14% decrease in peak ankle power also found no change in hip mechanics (Lewis and Ferris, 2008). While the direct claims between constituent work and changes in energy forms cannot be made with this analysis, it is worth exploring thresholds for how larger decreases in trailing ankle and/or hip work will alter the gait strategy, which may in turn affect the positive ΔTKE_{wb} output over double support.

There are several advantages to the Work-Energy Profiles report and the positive and negative constituent work analysis over traditional gait analyses. Previous research using this data set revealed the compensatory strategy in the RiAFO condition involved increasing stance relative knee work on the involved limb, and the compensatory strategy in the BiAFO condition involved increasing both stance relative knee and hip work bilaterally (Chapter 7). By defining intervals of gait, there is evidence for where these compensations occur in stance. The constituent graphs (Figs. 8.5 – 8.6) and Table 8.1 show that the increase in stance knee work likely occurred during single support rise, while the increase in stance hip work likely occurred during double support where the knee and ankle constituent work decreased, which would result in a larger relative percentage of hip work.

Several measures were taken to standardize the execution of the data collection. All subjects wore standardized shoes and walked at the same height-scaled walking speed for all three conditions (Shoes, RiAFO, BiAFO). The same certified orthotist fitted all subjects for bilateral ankle foot orthoses, and the orthoses were manufactured by the same technician.

While AFOs were used in this population to partially impair the ankles of healthy individuals, there may be limitations in applying these findings to individuals with ankle weakness. Specifically, individuals walking after a stroke may have several motor control issues that prevent them from increasing their hip work due to impaired ankle function (Jonkers et al., 2009; Peterson et al., 2010). Some outliers were included in the data (noted in Table C.9 in Appendix C) because they were found to be genuine data points and not due to measurement error. The ANOVA test is robust against violations of normality, so data that did not pass the Shapiro-Wilk's test for normality were still included (Schmider et al., 2010).

While mechanical constituent work and energy can be measured, the Work-Energy Profiles approach cannot alone link the cause-effect relationship between the two measures. A power flow analysis can be a useful tool to track how constituent moments transfer mechanical energy across the leg and trunk segments (Siegel et al., 2004). Future research using induced acceleration analyses will also be critical to directly relate the efforts of constituents to the acceleration of the body. At the joint level, Siegel and colleagues used induced acceleration analyses to assess the effectiveness of different compensatory strategies used by individuals to walk with hip (Siegel et al., 2007) or knee (Siegel et al., 2006) weakness. At the muscle level, Neptune and colleagues used forward simulation and an induced acceleration analysis to separate the specific contributions of the gastrocnemius and the soleus to forward propulsion and upright support during gait (Neptune et al., 2001).

This study found that partial ankle impairment unilaterally and bilaterally induced compensatory strategies resulting in changes in net work done by the constituents during double support, but were as effective at propelling the body during this sub-task as without ankle impairment. While bilateral ankle impairment resulted in a less effective strategy to raise the COM, the unilateral ankle impairment condition resulted in a less effective strategy to control lowering the COM during single support. This is the first study to use work and energy metrics to objectively assess the effectiveness of compensatory strategies. Future studies may explore more directly how changes in constituent work in a compensatory strategy affect the changes in energy of the whole body.

8.6 Acknowledgments

The authors thank Teresa Ferrara, Michael Christensen, and Independence Prosthetics and Orthotics for assistance with data collection.

Chapter 9

CONCLUSION

9.1 Major Findings

The overall goal of this dissertation was to develop and implement a general framework to understand the mechanism for gait adaptations across a spectrum of conditions using mechanical work and energy. This goal was achieved by developing and using the Constituent Lower Extremity Work (CLEW) approach to measure gait strategy adaptations of the typical lower extremity limb across a range of walking speeds (Aim 1). Then, the mechanical energetics of gait strategies used by typical individuals to walk at a range of speeds was assessed by creating the Work-Energy Profiles approach (Aim 2). The CLEW and Work-Energy Profiles approaches created the Gait Energetics Adaptations Resource (GEAR) framework, which was then used to identify the interaction that governs how compensatory adaptations are formed due to impaired ankle function (Aim 3).

In Aim 1, measures of absolute limb work and relative constituent work were used to quantify gait strategy adaptations in healthy individuals walking at slow, moderate, and typical speeds (Chapter 3). The relative work contributions of the constituents to the absolute limb work revealed that the ankle-foot complex adapts to increasing walking speed from slow to typical speeds whereas the hip and knee do not. The Constituent Lower Extremity Work (CLEW) approach was developed as a comprehensive data visualization tool for representing limb work over a cyclic task, such as over a stride in gait (Chapter 4). In a single figure, the CLEW approach details the mechanical cost-of-transport, the percentage of positive and negative work performed in stance phase and swing phase, as well as the individual contributions of positive and negative work from each constituent. The absolute limb work and cost-of-transport variables indicate the level of limb effort over a stride and limb effort per unit distance, respectively. The relative constituent work variable identified the comparative amount each constituent's work contributed to absolute limb work during the stance and swing phases of gait. Thus, the CLEW approach was developed to quantify how the constituents coordinated to achieve a gait strategy and was implemented to find that typical individuals adapt relative work of the ankle-foot complex to walk from slow to typical walking speeds while the relative knee and hip work do not change.

In Aim 2, the work-energy relationship was used to relate constituent work to the resulting energy forms of the body in order to assess the mechanical energetics of gait strategies. However, previous literature had not shown the experimental equivalence of work and change in energy, or power and rate of change in energy, in biomechanical models. Thus, a mathematical proof was derived and presented to verify the work-energy relationship could be used in 6 degree-of-freedom model calculations of work and energy (Chapter 5). The proof reveals that a relative displacement power should be mathematically accounted for in 6 DOF models in order to have segmental power and energy agreement. Using this proof, the Work-Energy Profiles approach was then developed to visualize and interpret the mechanical energetics of gait strategies by typical individuals walking at slow to typical speeds (Chapter 6). The profiles synthesized and corroborated findings from previous literature, and further explained how healthy individuals, on average, use a walking pattern that is more pendular during single support rise at slow speeds, but is more effective at propelling the center of mass during double support at typical speeds.

In Aim 3, the CLEW and Work-Energy Profiles were applied to probe the form of interaction that governs how compensatory strategies are formed due to impaired ankle function and how these strategies are effective. The CLEW approach was used to explore how compensatory strategies change with additional impaired constituents by partially impairing healthy ankle motion unilaterally and bilaterally (Chapter 7). There was non-equivalent work sharing with ankle impairment (average 37 – 40% reduction in ankle work) compared to typical gait, meaning individuals walked with decreased absolute limb work and cost-of-transport with ankle impairment than without. This is especially interesting since the manner of walking (e.g., speed and temporal-spatial parameters) did not change across conditions, so individuals were able to compensate for reduced ankle work and still produce the same temporal-spatial gait characteristics. Relative constituent work analyses revealed that the compensatory strategy resulting from bilateral ankle impairment was not simply the addition of two unilateral ankle impairment compensatory strategies. There were additional compensations at the hip in stance phase during bilateral ankle impairment compared to unilateral ankle impairment, which only showed a compensation at the knee during stance phase. Results from the Work-Energy Profiles approach on this data set revealed that partial ankle impairment unilaterally and bilaterally induced compensatory strategies resulting in changes in net work done by the constituents during double support phase of gait, but did not change the effectiveness of the strategies to propel the body compared to walking without ankle impairment (Chapter 8). With a unilateral ankle impairment, net work increased in initial double support due to decreased negative work and net work decreased in terminal double support due to decreased positive work. Despite this change in net work, the energy forms did not significantly change across conditions. With bilateral ankle impairment, more mechanical work was done to change the gravitational potential energy during single support rise such that the strategy was less effective in raising the COM compared to without ankle impairment. Aim 3 showed the applicability of the CLEW and Work-Energy Profiles approaches and found the compensatory adaptations when walking with unilateral and bilateral ankle impairment were not additive, but were similarly effective at propelling the body into its next step compared to unimpaired walking.

9.2 Future Work

The GEAR framework consisting of the CLEW and Work-Energy Profiles approaches is general and broadly applicable to understanding the principles guiding gait strategy adaptations across a spectrum of conditions and factors. Aim 3 provides evidence that these approaches can be used to identify the interaction governing compensatory strategy formation. Future work could explore gait strategy adaptations across the spectrum of any cyclic movement task beyond walking speed, like walking on a gradient, running at a range of speeds, walking on increasingly variable terrain, etc. Furthermore, these approaches could be used to explore the governing interactions for compensatory strategies when changing (1) level of impairment (e.g., as measured by the percentage of constituent work decreased from typical due to the impairment) or (2) number of constituents impaired. While the goal for Aim 3 of this dissertation was to keep level of impairment constant and modulate number of constituents impaired, it is possible the interaction between these levels and numbers of constituents is highly complex and has yet to be quantified. Exploring the interaction between impairment level and constituents impaired could revolutionize design of rehabilitation and assistive devices.

The CLEW approach is powerful in its ability to analyze the mechanical constituent and limb work across any cyclic task. Future studies should use relative constituent work calculations to quantify how constituent contributions vary for atypical gait patterns. For example, determining how relative work may change bilaterally with use of a prosthetic device would improve our understanding of the primary constituents that drive compensatory gait strategies with increasing gait speed. While this dissertation focused on characterizing gait adaptations from slow to typical speeds, further investigations are needed to identify how relative constituent work adapts across faster walking speeds and for other tasks, like running. Furthermore, future clinical studies will be necessary to determine how a clinical treatment affects the work distribution of the limb.

The Work-Energy Profiles can be used to evaluate the relative effectiveness of tasks performed by different patient populations or at various intensities compared to unimpaired gait. Profiles investigating greater than typical speeds may reveal constituent work thresholds. Interestingly, while a few healthy subjects had work-energy patterns (i.e., positive or negative net values) that did not follow the other subjects' patterns while walking at slow and moderate speeds, all subjects had consistent work-energy patterns while walking at typical speeds in Aims 1 and 2. This could provide further support for why healthy, unimpaired individuals tend not to walk at slower than typical speeds. In the future, these profiles can be used to analyze the relative effectiveness of compensatory strategies that develop when more than one constituent is impaired (such as the ankle and the knee).

A power flow analysis and an induced acceleration analysis can be beneficial tools to address some of the limitations in interpretation from the CLEW and Work-Energy Profiles approaches. The power flow analysis can be a useful tool to track how constituent moments transfer mechanical energy across the leg and trunk segments (Siegel et al., 2004). Induced acceleration analysis can provide a direct relationship between the effects of a constituent or muscle moment on the acceleration of the body (Zajac et al., 2002).

9.3 Conclusions

This dissertation developed two novel, generalizable approaches using mechanical work and energy in order to quantify how constituents of the body coordinate to achieve a gait strategy (Constituent Lower Extremity Work – CLEW approach) and how gait strategies are effective in achieving the sub-tasks of the task (Work-Energy Profiles approach). The CLEW approach confirmed the ankle-foot complex primarily adapts to increased walking speed, while the Work-Energy Profiles approach revealed the strategy implemented at a slow speed uses more pendular mechanics to raise the COM, while the strategy at a typical speed is more effective at propelling the body. An application of these two approaches was then conducted by artificially impairing the ankles of typical individuals unilaterally and bilaterally to determine the interaction that governs how compensatory adaptations are formed. The CLEW and Work-Energy Profiles approaches can be used to provide a complete understanding of lower limb adaptations using energetics variables.

REFERENCES

Adamczyk, P. G., & Kuo, A. D. (2009). Redirection of center-of-mass velocity during the step-to-step transition of human walking. *Journal of Experimental Biology, 212*, 2668–2678.

Adamczyk, P. G., & Kuo, A. D. (2015). Mechanisms of gait asymmetry due to push-off deficiency in unilateral amputees. *IEEE Transactions on Neural Systems and Rehabilitation Engineering, 23*(5), 776–785.

Aleshinsky, S. Y. (1986). An energy “sources” and “fractions” approach to the mechanical energy expenditure problem – V. The mechanical energy expenditure reduction during motion of the multi-link system. *Journal of Biomechanics, 19*(4), 287–293.

Alexander, R. M. (1991). Energy-saving mechanisms in walking and running. *Journal of Experimental Biology, 160*, 55–69.

Allen, J. L., Kautz, S. A., & Neptune, R. R. (2011). Step length asymmetry is representative of compensatory mechanisms used in post-stroke hemiparetic walking. *Gait & Posture*, *33*(4), 538–543.

Allen, N. E., Sherrington, C., Canning, C. G., & Fung, V. S. C. (2010). Reduced muscle power is associated with slower walking velocity and falls in people with Parkinson’s disease. *Parkinsonism & Related Disorders, 16*(4), 261–264.

Andrews, A. W., Chinworth, S. A., Bourassa, M., Garvin, M., Benton, D., & Tanner, S. (2010). Update on distance and velocity requirements for community ambulation. *Journal of Geriatric Physical Therapy*, *33*(3), 128–134.

Arch, E. S., & Fylstra, B. L. (2016). Combined ankle-foot energetics are conserved when distal foot energy absorption is minimized. *Journal of Applied Biomechanics, 32*(6), 571–577.

Au, S. K., Weber, J., & Herr, H. (2009). Powered ankle–foot prosthesis improves walking metabolic economy. *IEEE Transactions on Robotics, 25*(1), 51–66.

Baker, R. (2007). The history of gait analysis before the advent of modern computers. *Gait & Posture, 26*(3), 331–342.

Bejek, Z., Paróczai, R., Illyés, A., & Kiss, R. M. (2006). The influence of walking speed on gait parameters in healthy people and in patients with osteoarthritis. *Knee Surgery, Sports Traumatology, Arthroscopy, 14*(7), 612–622.

Bertram, J. E. A., & Hasaneini, S. J. (2013). Neglected losses and key costs: tracking the energetics of walking and running. *Journal of Experimental Biology, 216*(6), 933–938.

Bregman, D. J. J., Harlaar, J., Meskers, C. G. M., & de Groot, V. (2012). Spring-like ankle foot orthoses reduce the energy cost of walking by taking over ankle work. *Gait & Posture, 35*(1), 148–153.

Buczek, F. L., Kepple, T. M., Siegel, K. L., & Stanhope, S. J. (1994). Translational and rotational joint power terms in a six degree-of-freedom model of the normal ankle complex. *Journal of Biomechanics, 27*(12), 1447–1457.

Buczek, F. L., Sanders, J. O., Concha, M. C., & Cooney, K. M. (2000). Posture versus power: How does this patient move? *Pediatric Gait: A New Millennium in Clinical Care and Motion Analysis Technology*, 92–98.

Buddhadev, H. H., & Martin, P. E. (2016). Effects of age and physical activity status on redistribution of joint work during walking. *Gait & Posture, 50,* 131–136.

Caldwell, G. E., & Forrester, L. W. (1992). Estimates of mechanical work and energy transfers: demonstration of a rigid body power model of the recovery leg in gait. *Medicine & Science in Sports & Exercise, 24*(12), 1396–1412.

Cappozzo, A., Figura, F., Marchetti, M., & Pedotti, A. (1976). The interplay of muscular and external forces in human ambulation. *Journal of Biomechanics, 9*(1), 35–43.

Cavagna, G. A. (1974). Force platforms as ergometers. *Journal of Applied Physiology, 39*(1), 174–179.

Cavagna, G. A., Thys, H., & Zamboni, A. (1976). The sources of external work in level walking and running. *The Journal of Physiology, 262*(3), 639–657.

Cavagna, G. A., & Kaneko, M. (1977). Mechanical work and efficiency in level walking and running. *The Journal of Physiology, 268*(2), 467–481.

Cavagna, G. A., Willems, P. A., & Heglund, N. C. (2000). The role of gravity in human walking: pendular energy exchange, external work and optimal speed. *The Journal of Physiology, 528*(3), 657–668.

Chen, C. L., Chen, H. C., Tang, S. F. T., Wu, C. Y., Cheng, P. T., & Hong, W. H. (2003). Gait performance with compensatory adaptations in stroke patients with different degrees of motor recovery. *American Journal of Physical Medicine & Rehabilitation*, *82*(12), 925–935.

Chen, I. H., Kuo, K. N., & Andriacchi, T. P. (1997). The influence of walking speed on mechanical joint power during gait. *Gait & Posture, 6*(3), 171–176.

Cofré, L. E., Lythgo, N., Morgan, D., & Galea, M. P. (2011). Aging modifies joint power and work when gait speeds are matched. *Gait & Posture, 33*(3), 484–489.

Convery, P., Greig, R. J., Ross, R. S., & Sockalingam, S. (2004). A three centre study of the variability of ankle foot orthoses due to fabrication and grade of polypropylene. *Prosthetics and Orthotics International, 28*(2), 175–182.

Crétual, A., & Fusco, N. (2011). Additional energetic cost due to belt speed variations when walking on a treadmill. *Journal of Electromyography and Kinesiology, 21*(3), 551–556.

Crompton, R. H., Yu, L., Weijie, W., Günther, M., & Savage, R. (1998). The mechanical effectiveness of erect and "bent-hip, bent-knee" bipedal walking in *Australopithecus afarensis*. *Journal of Human Evolution, 35*(1), 55–74.

Cruz, T. H., Lewek, M. D., & Dhaher, Y. Y. (2009). Biomechanical impairments and gait adaptations post-stroke: Multi-factorial associations. *Journal of Biomechanics, 42*(11), 1673–1677.

Czerniecki, J. M., & Gitter, A. (1992). Insights into amputee running: A muscle work analysis. *American Journal of Physical Medicine & Rehabilitation, 71*(4), 209–218.

De Asha, A. R., Munjal, R., Kulkarni, J., & Buckley, J. G. (2013). Walking speed related joint kinetic alterations in trans-tibial amputees: impact of hydraulic "ankle" damping. *Journal of NeuroEngineering and Rehabilitation, 10*(107), 1–15.

de Looze, M. P., Bussman, J. B. J., Kingma, I., & Toussaint, H. M. (1992). Different methods to estimate total power and its components during lifting. *Journal of Biomechanics, 25*(9), 1089–1095.

Detrembleur, C., Dierick, F., Stoquart, G., Chantraine, F., & Lejeune, T. (2003). Energy cost, mechanical work, and efficiency of hemiparetic walking. *Gait & Posture, 18*(2), 47–55.

DeVita, P., Helseth, J., & Hortobagyi, T. (2007). Muscles do more positive than negative work in human locomotion. *Journal of Experimental Biology, 210*(19), 3361–3373.

Donelan, J. M., & Kram, R. (1997). The effect of reduced gravity on the kinematics of human walking: a test of the dynamic similarity hypothesis for locomotion. *Journal of Experimental Biology*, *200*(24), 3193–3201.

Donelan, J. M., Kram, R., & Kuo, A. D. (2001). Simultaneous positive and negative external mechanical work in human walking. *Journal of Biomechanics, 35*(1), 117–124.

Donelan, J. M., Kram, R., & Kuo, A. D. (2002). Mechanical work for step-to-step transitions is a major determinant of the metabolic cost of human walking. *Journal of Experimental Biology*, *205*(23), 3717–3727.

Ebrahimi, A., Goldberg, S. R., & Stanhope, S. J. (2017a). Changes in relative work of the lower extremity joints and distal foot with walking speed. *Journal of Biomechanics*, *58*, 212–216.

Ebrahimi, A., Goldberg, S. R., Wilken, J. M., & Stanhope, S. J. (2017b). Constituent Lower Extremity Work (CLEW) approach: A novel tool to visualize joint and segment work. *Gait & Posture, 56*, 49–53.

Ebrahimi, A., Collins, J. D., Kepple, T. M., Takahashi, K. Z., Higginson, J. S., & Stanhope, S. J. (2018). A mathematical analysis to address the 6 degree-of-freedom segmental power imbalance. *Journal of Biomechanics*, *66*, 186–193.

Farris, D. J., & Sawicki, G. S. (2012). The mechanics and energetics of human walking and running: a joint level perspective. *Journal of The Royal Society Interface, 9*, 110–118.

Farris, D. J., Hampton, A., Lewek, M. D., & Sawicki, G. S. (2015). Revisiting the mechanics and energetics of walking in individuals with chronic hemiparesis following stroke: from individual limbs to lower limb joints. *Journal of NeuroEngineering and Rehabilitation, 12*(24), 1–12.

Flanagan, S. P., & Salem, G. J. (2005). The validity of summing lower extremity individual joint kinetic measures. *Journal of Applied Biomechanics, 21*(2), 181–188.

Franz, J. R., Lyddon, N. E., & Kram, R. (2012). Mechanical work performed by the individual legs during uphill and downhill walking. *Journal of Biomechanics, 45*(2), 257–262.

Frost, G., Dowling, J., Bar-Or, O., & Dyson, K. (1997). Ability of mechanical power estimations to explain differences in metabolic cost of walking and running among children. *Gait & Posture, 5*(2), 120–127.

Geboers, J. F., Drost, M. R., Spaans, F., Kuipers, H., & Seelen, H. A. (2002). Immediate and long-term effects of ankle-foot orthosis on muscle activity during walking: A randomized study of patients with unilateral foot drop. *Archives of Physical Medicine and Rehabilitation, 83*(2), 240–245.

Geil, M. D., Parnianpour, M., Quesada, P., Berme, N., & Simon, S. (2000). Comparison of methods for the calculation of energy storage and return in a dynamic elastic response prosthesis. *Journal of Biomechanics, 33*(12), 1745–1750.

Goldberg, S. R., & Stanhope, S. J. (2013). Sensitivity of joint moments to changes in walking speed and body-weight-support are interdependent and vary across joints. *Journal of Biomechanics, 46*(6), 1176–1183.

Griffin, T. M., Tolani, N. A., & Kram, R. (1999). Walking in simulated reduced gravity: mechanical energy fluctuations and exchange. *Journal of Applied Physiology, 86*(1), 383–390.

Guo, L. Y., Su, F. C., Wu, H. W., & An, K. N. (2003). Mechanical energy and power flow of the upper extremity in manual wheelchair propulsion. *Clinical Biomechanics, 18*(2), 106–114.

Harper, N. G., Esposito, E. R., Wilken, J. M., & Neptune, R. R. (2014). The influence of ankle-foot orthosis stiffness on walking performance in individuals with lower-limb impairments. *Clinical Biomechanics, 29*(8), 877–884.

Herr, H. M., & Grabowski, A. M. (2012). Bionic ankle-foot prosthesis normalizes walking gait for persons with leg amputation. *Proceedings of the Royal Society B: Biological Sciences, 279*(1728), 457–464.

Hicks, J. L., Uchida, T. K., Seth, A., Rajagopal, A., & Delp, S. (2015). Is my model good enough? Best practices for verification and validation of musculoskeletal models and simulations of human movement. *Journal of Biomechanical Engineering, 137*(2), 20905.

Hof, A. L., Van Zandwijk, J. P., & Bobbert, M. F. (2002). Mechanics of human triceps surae muscle in walking, running and jumping. *Acta Physiologica, 174*(1), 17–30.

Hof, A. L., van Bockel, R. M., Schoppen, T., & Postema, K. (2007). Control of lateral balance in walking. Experimental findings in normal subjects and above-knee amputees. *Gait & Posture, 25*(2), 250–258.

Holden, J. P., Chou, G., & Stanhope, S. J. (1997). Changes in knee joint function over a wide range of walking speeds. *Clinical Biomechanics, 12*(6), 375–382.

Honert, E. C., & Zelik, K. E. (2016). Inferring muscle-tendon unit power from ankle joint power during the push-off phase of human walking: Insights from a multiarticular EMG-driven model. *Plos One, 11*(10), e0163169.

Huang, T. W. P., & Kuo, A. D. (2014). Mechanics and energetics of load carriage during human walking. *Journal of Experimental Biology, 217*(4), 605–613.

Huang, T. W. P., Shorter, K. A., Adamczyk, P. G., & Kuo, A. D. (2015). Mechanical and energetic consequences of reduced ankle plantar-flexion in human walking. *Journal of Experimental Biology, 218*(22), 3541–3550.

Inman, V., Ralston, H., & Todd, F. (1981). *Human Walking*. Baltimore, MD: Williams & Wilkins.

Jonkers, I., Delp, S., & Patten, C. (2009). Capacity to increase walking speed is limited by impaired hip and ankle power generation in lower functioning persons post-stroke. *Gait & Posture*, *29*(1), 129–137.

Kautz, S. A., Hull, M. L., & Neptune, R. R. (1994). A comparison of muscular mechanical energy expenditure and internal work in cycling. *Journal of Biomechanics, 27*(12), 1459–1467.

Kautz, S. A., & Neptune, R. R. (2002). Biomechanical determinants of pedaling energetics: internal and external work are not independent. *Exercise and Sport Sciences Reviews*, *30*(4), 159–165.

Kelly-Hayes, M., Robertson, J. T., Broderick, J. P., Duncan, P. W., Hershey, L. A., Roth, E. J., … Trombly, C. A. (1998). The American Heart Association Stroke Outcome Classification. *Stroke, 29*(6), 1274–1280.

Kepple, T. M., Siegel, K. L., & Stanhope, S. J. (1997). Relative contributions of the lower extremity joint moments to forward progression and support during gait. *Gait & Posture, 6*(1), 1–8.

Kirtley, C., Whittle, M. W., & Jefferson, R. J. (1985). Influence of walking speed on gait parameters. *Journal of Biomedical Engineering, 7*(4), 282–288.

Kuo, A. D. (2002). Energetics of actively powered locomotion using the simplest walking model. *Journal of Biomechanical Engineering, 124*(1), 113–120.

Kuo, A. D. (2007). The six determinants of gait and the inverted pendulum analogy: A dynamic walking perspective. *Human Movement Science*, *26*(4), 617–656.

Kuo, A. D., & Donelan, J. M. (2010). Dynamic principles of gait and their clinical implications. *Physical Therapy*, *90*(2), 157–174.

Kuo, A. D., Donelan, J. M., & Ruina, A. (2005). Energetic consequences of walking like an inverted pendulum: Step-to-step transitions. *Exercise and Sport Sciences Reviews, 33*(2), 88–97.

Lee, C. R., & Farley, C. T. (1998). Determinants of the center of mass trajectory in human walking and running. *Journal of Experimental Biology*, *201*(21), 2935–2944.

Lejeune, T. M., Willems, P. A., & Heglund, N. C. (1998). Mechanics and energetics of human locomotion on sand. *Journal of Experimental Biology, 201*(13), 2071–2080.

Lelas, J. L., Merriman, G. J., Riley, P. O., & Kerrigan, D. C. (2003). Predicting peak kinematic and kinetic parameters from gait speed. *Gait & Posture, 17*(2), 106–112.

Lewis, C. L., & Ferris, D. P. (2008). Walking with increased ankle pushoff decreases hip muscle moments. *Journal of Biomechanics, 41*(10), 2082–2089.

Lobet, S., Hermans, C., Bastien, G. J., Massaad, F., & Detrembleur, C. (2012). Impact of ankle osteoarthritis on the energetics and mechanics of gait: The case of hemophilic arthropathy. *Clinical Biomechanics, 27*(6), 625–631.

Mahon, C. E., Farris, D. J., Sawicki, G. S., & Lewek, M. D. (2015). Individual limb mechanical analysis of gait following stroke. *Journal of Biomechanics, 48*(6), 984–989.

Malatesta, D., Vismara, L., Menegoni, F., Galli, M., Romei, M., & Capodaglio, P. (2009). Mechanical external work and recovery at preferred walking speed in obese subjects. *Medicine & Science in Sports & Exercise, 41*(2), 426–434.

Malcolm, P., Quesada, R. E., Caputo, J. M., & Collins, S. H. (2015). The influence of push-off timing in a robotic ankle-foot prosthesis on the energetics and mechanics of walking. *Journal of NeuroEngineering and Rehabilitation, 12*(21), 1–14.

Martin, A. E., & Schmiedeler, J. P. (2014). Predicting human walking gaits with a simple planar model. *Journal of Biomechanics*, *47*(6), 1416–1421.

Massaad, F., Lejeune, T. M., & Detrembleur, C. (2007). The up and down bobbing of human walking: a compromise between muscle work and efficiency. *The Journal of Physiology, 582*(2), 789–799.

McDowell, B., Cosgrove, A., & Baker, R. (2002). Estimating mechanical cost in subjects with myelomeningocele. *Gait & Posture, 15*(1), 25–31.

McGeer, T. (1993). Dynamics and control of bipedal locomotion. *Journal of Theoretical Biology, 163*(3), 277–314.

McGibbon, C. A., & Krebs, D. E. (1998). The influence of segment endpoint kinematics on segmental power calculations. *Gait & Posture, 7*(3), 237–242.

Mian, O. S., Thom, J. M., Ardigò, L. P., Narici, M. V, & Minetti, A. E. (2006). Metabolic cost, mechanical work, and efficiency during walking in young and older men. *Acta Physiologica, 186*(2), 127–139.

Miller, C. A., & Verstraete, M. C. (1996). Determination of the step duration of gait initiation using a mechanical energy analysis. *Journal of Biomechanics, 29*(9), 1195–1199.

Miller, W. C., Speechley, M., & Deathe, B. (2001). The prevalence and risk factors of falling and fear of falling among lower extremity amputees. *Archives of Physical Medicine and Rehabilitation*, *82*(8), 1031–1037.

Murray, M. P., Mollinger, L. A., Gardner, G. M., & Sepic, S. B. (1984). Kinematic and EMG patterns during slow, free, and fast walking. *Journal of Orthopaedic Research*, *2*(3), 272–280.

Neptune, R. R., & Van Den Bogert, A. J. (1998). Standard mechanical energy analyses do not correlate with muscle work in cycling. *Journal of Biomechanics*, *31*(3), 239–245.

Neptune, R. R., Kautz, S. A., & Zajac, F. E. (2001). Contributions of the individual ankle plantar flexors to support, forward progression and swing initiation during walking. *Journal of Biomechanics*, *34*(11), 1387–1398.

Neptune, R. R., Zajac, F. E., & Kautz, S. A. (2004). Muscle mechanical work requirements during normal walking: the energetic cost of raising the body's center-of-mass is significant. *Journal of Biomechanics*, *37*(6), 817–825.

Neptune, R. R., Sasaki, K., & Kautz, S. A. (2008). The effect of walking speed on muscle function and mechanical energetics. *Gait & Posture, 28*(1), 135–143.

Olney, S. J., Costigan, P. A., & Hedden, D. M. (1987). Mechanical energy patterns in gait of cerebral palsied children with hemiplegia. *Physical Therapy, 67*(9), 1348–1354.

Olney, S. J., Monga, T. N., & Costigan, P. A. (1986). Mechanical energy of walking of stroke patients. *Archives of Physical Medicine and Rehabilitation, 67*(2), 92–98.

Orendurff, M. S., Segal, A. D., Klute, G. K., Berge, J. S., Rohr, E. S., & Kadel, N. J. (2004). The effect of walking speed on center of mass displacement. *Journal of Rehabilitation Research & Development, 41*(6A), 829–834.

Ortega, J. D., & Farley, C. T. (2005). Minimizing center of mass vertical movement increases metabolic cost in walking. *Journal of Applied Physiology, 99*(6), 2099–2107.

Pai, Y. C., Yang, F., Wening, J. D., & Pavol, M. J. (2006). Mechanisms of limb collapse following a slip among young and older adults. *Journal of Biomechanics, 39*(12), 2194–2204.

Perry, J. (1992). *Gait analysis: Normal and pathological function (2nd ed.).* Thorofare, NJ: Slack, Inc.

Peterson, C. L., Cheng, J., Kautz, S. A., & Neptune, R. R. (2010). Leg extension is an important predictor of paretic leg propulsion in hemiparetic walking. *Gait & Posture, 32*(4), 451–456.

Prilutsky, B. I., & Zatsiorsky, V. M. (1994). Tendon action of two-joint muscles: transfer of mechanical energy between joints during jumping, landing, and running. *Journal of Biomechanics, 27*(1), 25–34.

Purkiss, S. B. A., & Robertson, D. G. E. (2003). Methods for calculating internal mechanical work: comparison using elite runners. *Gait & Posture, 18*(3), 143–149.

Qiao, M., & Jindrich, D. L. (2016). Leg joint function during walking acceleration and deceleration. *Journal of Biomechanics, 49*(1), 66–72.

Queen, R. M., Sparling, T. L., & Schmitt, D. (2016). Hip, knee, and ankle osteoarthritis negatively affects mechanical energy exchange. *Clinical Orthopaedics and Related Research, 474*(9), 2055–2063.

Research Plan for the National Center for Medical Rehabilitation Research. (1993).

Riddick, R. C., & Kuo, A. D. (2016). Soft tissues store and return mechanical energy in human running. *Journal of Biomechanics, 49*(3), 436–441.

Robertson, D. G. E., & Winter, D. A. (1980). Mechanical energy generation, absorption and transfer amongst segments during walking. *Journal of Biomechanics, 13*(10), 845–854.

Robertson, D. G. E., Caldwell, G. E., Hamill, J., Kamen, G., & Whittlesey, S. N. (2013). *Research methods in biomechanics (2nd ed.)*. Champaign, IL: Human Kinetics.

Sadeghi, H., Allard, P., & Duhaime, M. (2000). Contributions of lower-limb muscle power in gait of people without impairments. *Physical Therapy, 80*(12), 1188–1196.

Safaeepour, Z., Esteki, A., Ghomshe, F. T., & Abu Osman, N. A. A. (2014). Quantitative analysis of human ankle characteristics at different gait phases and speeds for utilizing in ankle-foot prosthetic design. *Biomedical Engineering Online, 13*(19), 1–8.

Sawicki, G. S., Lewis, C. L., & Ferris, D. P. (2009). It pays to have a spring in your step. *Exercise and Sport Sciences Reviews, 37*(3), 130–138.

Schache, A. G., Brown, N. A. T., & Pandy, M. G. (2015). Modulation of work and power by the human lower-limb joints with increasing steady-state locomotion speed. *Journal of Experimental Biology, 218*(15), 2472–2481.

Schmid, S., Schweizer, K., Romkes, J., Lorenzetti, S., & Brunner, R. (2013). Secondary gait deviations in patients with and without neurological involvement: A systematic review. *Gait & Posture, 37*(4), 480–493.

Schmider, E., Ziegler, M., Danay, E., Beyer, L., & Bühner, M. (2010). Is it really robust?: Reinvestigating the robustness of ANOVA against violations of the normal distribution assumption. *Methodology, 6*(4), 147–151.

Seeley, M. K., Umberger, B. R., & Shapiro, R. (2008). A test of the functional asymmetry hypothesis in walking. *Gait & Posture, 28*(1), 24–28.

Siegel, K. L., Kepple, T. M., & Caldwell, G. E. (1996). Improved agreement of foot segmental power and rate of energy change during gait: inclusion of distal power terms and use of three-dimensional models. *Journal of Biomechanics, 29*(6), 823–827.

Siegel, K. L., Kepple, T. M., & Stanhope, S. J. (2004). Joint moment control of mechanical energy flow during normal gait. *Gait & Posture, 19*(1), 69–75.

Siegel, K. L., Kepple, T. M., & Stanhope, S. J. (2006). Using induced accelerations to understand knee stability during gait of individuals with muscle weakness. *Gait & Posture, 23*(4), 435–440.

Siegel, K. L., Kepple, T. M., & Stanhope, S. J. (2007). A case study of gait compensations for hip muscle weakness in idiopathic inflammatory myopathy. *Clinical Biomechanics, 22*(3), 319–326.

Siegler, S., & Liu, W. (1997). Inverse Dynamics in Human Locomotion. In P. Allard, A. Cappozzo, A. Lundberg, & C. L. Vaughan (Eds.), *Three-Dimensional Analysis of Human Locomotion* (191–209). New York, NY: Wiley.

Silverman, A. K., Fey, N. P., Portillo, A., Walden, J. G., Bosker, G., & Neptune, R. R. (2008). Compensatory mechanisms in below-knee amputee gait in response to increasing steady-state walking speeds. *Gait & Posture, 28*(4), 602–609.

Soo, C. H., & Donelan, J. M. (2010). Mechanics and energetics of step-to-step transitions isolated from human walking. *Journal of Experimental Biology, 213*(24), 4265–4271.

Sparling, T. L., Schmitt, D., Miller, C. E., Guilak, F., Somers, T. J., Keefe, F. J., & Queen, R. M. (2014). Energy recovery in individuals with knee osteoarthritis. *Osteoarthritis and Cartilage, 22*(6), 747–755.

Sutherland, D. H., Cooper, L., & Daniel, D. (1980). The role of the ankle plantar flexors in normal walking. *The Journal of Bone & Joint Surgery, 62*(3), 354–363.

Takahashi, K. Z., Kepple, T. M., & Stanhope, S. J. (2012). A unified deformable (UD) segment model for quantifying total power of anatomical and prosthetic below-knee structures during stance in gait. *Journal of Biomechanics, 45*(15), 2662–2667.

Takahashi, K. Z., & Stanhope, S. J. (2013). Mechanical energy profiles of the combined ankle-foot system in normal gait: insights for prosthetic designs. *Gait & Posture, 38*(4), 818–823.

Takahashi, K. Z., Horne, J. R., & Stanhope, S. J. (2015). Comparison of mechanical energy profiles of passive and active below-knee prostheses: A case study. *Prosthetics and Orthotics International, 39*(2), 150–156.

Teixeira-Salmela, L. F., Nadeau, S., Milot, M. H., Gravel, D., & Requião, L. F. (2008). Effects of cadence on energy generation and absorption at lower extremity joints during gait. *Clinical Biomechanics*, *23*(6), 769–778.

Umberger, B. R., & Martin, P. E. (2007). Mechanical power and efficiency of level walking with different stride rates. *Journal of Experimental Biology, 210*(18), 3255–3265.

Van de Walle, P., Hallemans, A., Schwartz, M., Truijen, S., Gosselink, R., & Desloovere, K. (2012). Mechanical energy estimation during walking: Validity and sensitivity in typical gait and in children with cerebral palsy. *Gait & Posture, 35*(2), 231–237.

van Ingen Schenau, G. J., & Cavanagh, P. R. (1990). Power equations in endurance sports. *Journal of Biomechanics, 23*(9), 865–881.

Vanderpool, M. T., Collins, S. H., & Kuo, A. D. (2008). Ankle fixation need not increase the energetic cost of human walking. *Gait & Posture, 28*(3), 427–433.

Voloshina, A. S., Kuo, A. D., Daley, M. A., & Ferris, D. P. (2013). Biomechanics and energetics of running on uneven terrain. *Journal of Experimental Biology, 216*(5), 3963–3970.

Willems, P. A., Cavagna, G. A., & Heglund, N. C. (1995). External, internal and total work in human locomotion. *Journal of Experimental Biology, 198*(2), 379–393.

Williams, G., & Schache, A. G. (2016). The distribution of positive work and power generation amongst the lower-limb joints during walking normalises following recovery from traumatic brain injury. *Gait & Posture*, *43*, 265–269.

Winter, D. A., & Robertson, D. G. E. (1978). Joint torque and energy patterns in normal gait. *Biological Cybernetics, 29*(3), 137–142.

Winter, D. A. (1979). A new definition of mechanical work done in human movement. *Journal of Applied Physiology: Respiratory, Environmental and Exercise Physiology, 46*(1), 79–83.

Winter, D. A. (1983). Energy generation and absorption at the ankle and knee during fast, natural, and slow cadences. *Clinical Orthopaedics and Related Research,* (175), 147–154.

Winter, D. A. (1984). Kinematic and kinetic patterns in human gait: Variability and compensating effects. *Human Movement Science, 3*(1–2), 51–76.

Winter, D. A. (1991). *The biomechanics and motor control of human gait: Normal, elderly and pathological. (2nd ed.)*. Ontario, Canada: Waterloo Biomechanics.

Winter, D. A. (2009). *Biomechanics and motor control of human movement (4th ed.).* Hoboken, NJ: John Wiley & Sons, Inc.

Wu, Q., & Chan, C. Y. A. (2001). Design of energy efficient joint profiles for a planar five-link biped robot. In *Proceedings of 2001 IEEE International Symposium on Computational Intelligence in Robotics and Automation*, 35–40.

Wutzke, C. J., Sawicki, G. S., & Lewek, M. D. (2012). The influence of a unilateral fixed ankle on metabolic and mechanical demands during walking in unimpaired young adults. *Journal of Biomechanics, 45*(14), 2405–2410.

Zajac, F. E., Neptune, R. R., & Kautz, S. A. (2002). Biomechanics and muscle coordination of human walking. Part I: Introduction to concepts, power transfer, dynamics and simulations. *Gait & Posture, 16*(3), 215–232.

Zelik, K. E., & Kuo, A. D. (2010). Human walking isn't all hard work: evidence of soft tissue contributions to energy dissipation and return. *Journal of Experimental Biology, 213*(24), 4257–4264.

Zelik, K. E., & Kuo, A. D. (2012). Mechanical work as an indirect measure of subjective costs influencing human movement. *PloS One*, *7*(2), e31143.

Zelik, K. E., La Scaleia, V., Ivanenko, Y. P., & Lacquaniti, F. (2014). Coordination of intrinsic and extrinsic foot muscles during walking. *European Journal of Applied Physiology, 115*(4), 691–701.

Zelik, K. E., Takahashi, K. Z., & Sawicki, G. S. (2015). Six degree-of-freedom analysis of hip, knee, ankle and foot provides updated understanding of biomechanical work during human walking. *Journal of Experimental Biology, 218*(6), 876–886.

Ziegler-Graham, K., MacKenzie, E. J., Ephraim, P. L., Travison, T. G., & Brookmeyer, R. (2008). Estimating the prevalence of limb loss in the United States: 2005 to 2050. *Archives of Physical Medicine and Rehabilitation, 89*(3), 422–429.

Appendix A

PERMISSIONS

AUTHOR AND USER RIGHTS

INTRODUCTION

Elsevier requests transfers of copyright, or in some cases exclusive rights, from its journal authors in order to ensure that we have the rights necessary for the proper administration of electronic rights and online dissemination of journal articles, authors and their employers retain (or are granted/transferred back) significant scholarly rights in their work. We take seriously our responsibility as the steward of the online record to ensure the integrity of scholarly works and the sustainability of journal business models, and we actively monitor and pursue unauthorized and unsubscribed uses and re-distribution (for subscription models).

In addition to authors' scholarly rights, anyone who is affiliated with an institution with a journal subscription can use articles from subscribed content under the terms of their institution's license, while there are a number of other ways in which anyone (whether or not an author or subscriber) can make use of content published by Elsevier, which is free at the point of use or accessed under license.

Author Rights

As a journal author, you have rights for a large range of uses of your article, including use by your employing institute or company. These rights can be exercised without the need to obtain specific permission.

How authors can use their own journal articles

Authors publishing in Elsevier journals have wide rights to use their works for teaching and scholarly purposes without needing to seek permission.

Table of Author's Rights

	Preprint version (with a few exceptions- see below *)	**Accepted Author Manuscript**	**Published Journal Articles**
Use for classroom teaching by author or author's institution and presentation at a meeting or conference and distributing copies to attendees	Yes	Yes	Yes
Use for internal training by author's company	Yes	Yes	Yes
Distribution to colleagues for their research use	Yes	Yes	Yes
Use in a subsequent compilation of the author's works	Yes	Yes	Yes
Inclusion in a thesis or dissertation	Yes	Yes	Yes
Reuse of portions or extracts from the article in other works	Yes	Yes with full acknowledgement of final article	Yes with full acknowledgement of final article
Preparation of derivative works (other than for commercial purposes)	Yes	Yes with full acknowledgement of final article	Yes with full acknowledgement of final article
Preprint servers	Yes	Yes with the specific written permission of Elsevier	No
Voluntary posting on open web sites operated by author or author's institution for scholarly purposes	Yes (author may later add an appropriate bibliographic citation, indicating subsequent publication by Elsevier and journal title)	Yes, with appropriate bibliographic citation and a link to the article once published	Only with the specific written permission of Elsevier
Mandated deposit or deposit in or posting to subject-oriented or centralized repositories	Yes under specific agreement between Elsevier and the repository	Yes under specific agreement between Elsevier and the repository**	Yes under specific agreement between Elsevier and the repository
Use or posting for commercial gain or to substitute for services provided directly by journal	Only with the specific written permission of Elsevier	Only with the specific written permission of Elsevier	Only with the specific written permission of Elsevier

** Voluntary posting of Accepted Author Manuscripts in the arXiv subject repository is permitted.

Appendix B

A BRIEF HISTORY OF WORK AND ENERGY CALCULATIONS

Typical bipedal walking has been well-examined to utilize the most energetically economic coordination of limbs (Kuo and Donelan, 2010). During walking, the body center of mass (COM) experiences changes primarily in two forms of energy: gravitational potential energy and translational kinetic energy, similar to a conserved pendulum (Buczek et al., 2000; Cavagna and Kaneko, 1977; Inman et al., 1981; Kuo, 2007; Perry, 1992). Under the assumption of a relatively straight stance limb (Massaad et al., 2007), the inverted pendulum model was developed and has been widely accepted in the literature (Buczek et al., 2000; Cavagna et al., 2000; Kuo, 2007; Kuo and Donelan, 2010; Lee and Farley, 1998). This characteristic energy pattern in gait has been demonstrated in subsequent gait models from a simple two-link system (McGeer, 1993) to a more complex five-link (Wu and Chan, 2001) or six-link (Martin and Schmiedeler, 2014) system. Furthermore, the atypical exchange of kinetic and potential energy patterns of individuals with impairments has been used to characterize gait deviations of individuals post-stroke (Olney et al., 1986) and of children with cerebral palsy (Olney et al., 1987).

The transfer of energy occurs due to forces (e.g., from muscles) doing mechanical work; thus, several approaches have been used to quantify the mechanical work on the COM. The work done by the COM was first coined by Cavagna and Kaneko as “external work” (Cavagna and Kaneko, 1977), or later referred to as the “combined limbs method” (Donelan et al., 2001). While there is some inconsistency in the calculation of this measure (Zelik et al., 2015), it is typically presented in some form as the integrated dot product of the total ground reaction force and the COM velocity as a measure of work done to maintain the motion of the COM (Willems et al., 1995). Cavagna and colleagues also defined a measure of "recovery" representing the magnitude of energy reused through the transfer between potential and kinetic energy from work done by the limbs where 100% would represent perfect exchange of kinetic and potential energy (Cavagna et al., 1976). While Cavagna and colleagues found ~65% recovery at intermediate speeds (Cavagna et al., 1976), other researchers have found recovery changes with different populations when analyzing the gait of individuals with knee osteoarthritis (Lobet et al., 2012; Queen et al., 2016; Sparling et al., 2014), with obesity (Malatesta et al., 2009), and with hemiparesis (Detrembleur et al., 2003), as well as individuals walking in sand (Lejeune et al., 1998) and with varied COM movement (Massaad et al., 2007; Ortega and Farley, 2005). An individual limb method (Donelan et al., 2001) has been used to evaluate power by the leading and trailing limb separately (Donelan et al., 2001; Kuo, 2002), during uphill and downhill walking (Franz et al., 2012), while walking with a load (Huang and Kuo, 2014), while walking with restricted ankles (Vanderpool et al., 2008) or with a prosthesis (Adamczyk and Kuo, 2015), and while walking post-stroke (Farris et al., 2015; Mahon et al., 2015).

Segmental power analyses and the inclusion of work done at the segmental level can further elucidate the total mechanical work done by the body during a movement task. The internal work (Cavagna and Kaneko, 1977; Lejeune et al., 1998), or sometimes called peripheral work (Zelik et al., 2015; Zelik and Kuo, 2012), is the integrated rate of energy change of the segmental rotational and translational energies for segments of the lower limb relative to the COM. The sum of the external and internal work is deemed a measure of whole body mechanical work. Another approach to quantify whole body mechanical work was proposed by Winter (Winter, 1979) in a summed segmental energies approach, where integrated time derivatives of segmental kinetic and potential energies of all body segments are summed. Although the external and internal work and the summed segmental energies approaches are theoretically equivalent, the latter can elucidate the transfer of energy across segments (Frost et al., 1997; Willems et al., 1995).

While whole body or individual limb work is a useful metric for work done on the COM, work done by the individual constituents can reveal more about the function of the limb itself during a given task. Researchers have used principles of inverse dynamics to calculate rotational joint power defined as the net joint moment multiplied by the angular velocity in various gait speeds and populations (Czerniecki and Gitter, 1992; DeVita et al., 2007; Farris et al., 2015; Flanagan and Salem, 2005; Huang and Kuo, 2014; Lewis and Ferris, 2008; Qiao and Jindrich, 2016; Sadeghi et al., 2000; Schache et al., 2015; Vanderpool et al., 2008; Voloshina et al., 2013; Williams and Schache, 2016; Winter, 1991). Expanding on the rotational joint power approach is the 6 degree-of-freedom (DOF) approach (Buczek et al., 1994), which includes translational joint powers in addition to rotational joint powers. While the contribution of the translational powers may be small (Farris et al., 2015), a 6 DOF approach is more comprehensive and a closer match to the whole body mechanical work (Zelik et al., 2015). This 6 DOF power analysis has been successful in analyzing energetics of prosthetic limbs (De Asha et al., 2013; Geil et al., 2000; Takahashi et al., 2015). A distal foot segmental power component has also been presented (Siegel et al.,

1996) which better estimates the true work done by the ankle-foot system (Takahashi and Stanhope, 2013) and has recently been included in several 6 DOF constituent power analyses (Ebrahimi et al., 2017a, 2017b; Takahashi et al., 2012; Takahashi and Stanhope, 2013; Zelik et al., 2015).

Overall, the metrics for calculating mechanical work provide insight into work done to move the COM, although analyzing the individual constituent work provides more information on the mechanism for how a task is performed compared to a combined limb or an individual limb approach. The mathematical relationship between work and energy can be capitalized on in motion analyses to relate work done by the constituents to changes in the energy state of the body for any given movement.

Appendix C

SUPPLEMENTAL TABLES

Table C.1: Positive, negative, and absolute relative constituent work ($^{+}RW_{constituent}$, $^{-}RW_{constituent}$, and $^{abs}RW_{constituent}$, respectively) as a percentage of absolute limb work (mean ± standard deviation). Note, distal foot calculations are not applicable in swing phase as the foot is not in contact with the ground. A phase-by-speed interaction is denoted with an asterisk by the constituent name ($p < 0.05$) which indicates that the effect of speed is dependent on the phase (stance or swing). A † denotes that the value is significantly different from the value at the slow speed in that phase, and a ‡ denotes that the value is significantly different from the value at the moderate speed in that phase.

		Slow		*Moderate*		*Typical*	
		Stance	Swing	Stance	Swing	Stance	Swing
Hip	$^{+}RW_{hip}$ (%)*	14.6 ± 2.7	3.9 ± 0.9	13.7 ± 2.1	4.6 ± 1.6	12.1 ± 1.8	4.8 ± 2.0
	$^{-}RW_{hip}$ (%)	11.4 ± 3.2	0.2 ± 0.2	11.7 ± 3.1	0.1 ± 0.1	11.3 ± 3.3	0.2 ± 0.2
	$^{abs}RW_{hip}$ (%)	25.9 ± 4.9	4.1 ± 0.8	25.4 ± 4.3	4.7 ± 1.6	23.5 ± 4.7	5.0 ± 1.9
Knee	$^{+}RW_{knee}$ (%)*	16.8 ± 2.5	1.1 ± 0.2	14.7 ± 2.3†	0.8 ± 0.3	13.9 ± 2.0	1.0 ± 0.2
	$^{-}RW_{knee}$ (%)	6.8 ± 1.8	7.8 ± 1.4	7.2 ± 1.4	9.1 ± 1.9	8.0 ± 1.6	9.3 ± 2.1
	$^{abs}RW_{knee}$ (%)*	23.6 ± 1.7	8.8 ± 1.4	21.9 ± 2.0	9.9 ± 1.7†	21.9 ± 2.5	10.3 ± 2.1
Ankle	$^{+}RW_{ankle}$ (%)*	12.8 ± 2.5	0.2 ± 0.1	15.1 ± 1.8†	0.2 ± 0.1	17.1 ± 2.4†‡	0.3 ± 0.1†
	$^{-}RW_{ankle}$ (%)*	13.6 ± 3.0	0.4 ± 0.1	11.1 ± 2.7†	0.4 ± 0.1	8.7 ± 2.4†‡	0.3 ± 0.1‡
	$^{abs}RW_{ankle}$ (%)	26.4 ± 4.1	0.6 ± 0.1	26.1 ± 3.7	0.6 ± 0.2	25.7 ± 3.5	0.6 ± 0.1
Distal Foot	$^{+}RW_{distal\ foot}$ (%)	1.7 ± 0.4	N/A	1.5 ± 0.1	N/A	2.0 ± 0.2	N/A
	$^{-}RW_{distal\ foot}$ (%)	8.9 ± 1.5	N/A	9.8 ± 0.5†	N/A	11.1 ± 0.5†‡	N/A
	$^{abs}RW_{distal\ foot}$ (%)	10.6 ± 1.5	N/A	11.3 ± 1.4	N/A	13.2 ± 1.8†‡	N/A

Table C.2: Positive and negative relative constituent work ($^{+}RW_{constituent}$ and $^{-}RW_{constituent}$, respectively) as a percentage of absolute limb work for an average of a sample (n = 8) of unimpaired individuals (mean ± standard deviation), as well as an individual subject (n = 1) with a unilateral amputation wearing an above-knee prosthetic. Note, no distal foot work could be calculated during swing phase. $RW_{ankle\text{-}foot}$ represents the work produced by the combined ankle-foot, calculated for the prosthetic limb using the unified deformable power method and for the intact limb and unimpaired limbs by summing the ankle and distal foot relative work.

	Stance phase				*Swing phase*			
	Unimpaired (n = 8)		**Subject (n = 1)**		**Unimpaired (n = 8)**		**Subject (n = 1)**	
Limb	Left	Right	Pros-thetic	Intact	Left	Right	Pros-thetic	Intact
$^{+}RW_{hip}$ (%)	12 ± 2	14 ± 3	24	7	5 ± 2	5 ± 2	18	5
$^{-}RW_{hip}$ (%)	11 ± 3	10 ± 3	5	11	0 ± 0	0 ± 0	14	0
$^{+}RW_{knee}$ (%)	14 ± 2	15 ± 4	1	6	1 ± 0	1 ± 0	0	2
$^{-}RW_{knee}$ (%)	8 ± 2	7 ± 2	2	13	9 ± 2	9 ± 2	19	10
$^{+}RW_{ankle}$ (%)	17 ± 2	17 ± 3	N/A	26	0 ± 0	0 ± 0	0	1
$^{-}RW_{ankle}$ (%)	9 ± 2	8 ± 2	N/A	3	0 ± 0	0 ± 0	0	0
$^{+}RW_{distal\ foot}$ (%)	2 ± 0	2 ± 0	N/A	2	N/A	N/A	N/A	N/A
$^{-}RW_{distal\ foot}$ (%)	11 ± 1	12 ± 0	N/A	14	N/A	N/A	N/A	N/A
$^{+}RW_{ankle\text{-}foot}$ (%)	19 ± 2	19 ± 3	7	28				
$^{-}RW_{ankle\text{-}foot}$ (%)	20 ± 3	20 ± 2	9	17				

Table C.3: Mean absolute relative displacement power ($|P_{m/m-1}|_{mean}$) for the left and right hips (m = 4 for the pelvis, m = 3 for the thigh) averaged across a minimum of 10 gait cycles for each subject. Note, these summed absolute values are slightly larger in magnitude than the mean absolute power imbalance between the segmental rate of energy change and the anatomically relevant kinetic method for the pelvis (see Fig. 5.4 in text). This is because the left and right hip relative displacement powers may negate each other in some parts of the gait cycle.

Subjects	*1*	*2*	*3*	*4*	*5*	*6*	*7*	*8*	*9*
$\|P_{4/3,\,right}\|_{mean}$ (W/kg)	0.010	0.015	0.014	0.057	0.008	0.008	0.017	0.009	0.010
$\|P_{4/3,\,left}\|_{mean}$ (W/kg)	0.021	0.010	0.011	0.025	0.016	0.007	0.020	0.009	0.012
$\|P_{4/3,\,sum}\|_{mean}$ (W/kg)	**0.031**	**0.026**	**0.024**	**0.081**	**0.024**	**0.015**	**0.037**	**0.018**	**0.022**

Table C.4: Absolute percent difference between whole body power and rate of energy change at distinct intervals of the gait cycle for all 10 subjects, including the average and standard deviation (SD) across subjects, never exceeds an average of 1.0%. Intervals represent: (1) initial double support, (2) single support rise, (3) single support fall, (4) terminal double support, and swing phase in reference to the ipsilateral limb gait cycle.

Absolute % Difference	**Interval**					**Gait Cycle (%)**
Subjects	**1 (%)**	**2 (%)**	**3 (%)**	**4 (%)**	**Swing (%)**	
1	0.2	0.1	0.1	0.2	0.2	0.8
2	0.2	0.2	0.2	0.1	0.3	0.9
3	0.1	0.1	0.2	0.1	0.5	1.1
4	0.3	0.2	0.2	0.1	0.5	1.3
5	0.2	0.1	0.1	0.1	0.3	0.8
6	0.2	0.1	0.2	0.2	0.3	0.9
7	0.1	0.1	0.2	0.1	0.2	0.7
8	0.1	0.2	0.2	0.2	0.4	1.1
9	0.1	0.2	0.2	0.2	0.3	1.0
10	0.2	0.2	0.2	0.2	0.4	1.1
Average	**0.2**	**0.1**	**0.2**	**0.2**	**0.3**	**1.0**
SD	**0.1**	**0.0**	**0.0**	**0.0**	**0.1**	**0.2**

Table C.5: There were significant interval-by-speed interactions based on a two-way ANOVA for all constituents and energy forms except for the contralateral hip. Violations in normality are denoted with an "*," and Greenhouse-Geisser corrections for sphericity are noted with superscripted "G-G" (all $p < 0.05$). Intervals correspond to single support rise (SS Rise), single support fall (SS Fall), and terminal double support (Term DS) in reference to the ipsilateral limb gait cycle. "I" and "C" prior to a constituent denotes ipsilateral or contralateral limb, respectively, and ${}^{+}W_{wb}$ and ${}^{-}W_{wb}$ correspond to the summed positive and negative work by all the constituents (mean ± standard deviation). The ΔE_{wb}, ΔGPE_{wb}, ΔTKE_{wb}, and ΔRKE_{wb} correspond to the net, gravitational potential, translational kinetic, and rotational kinetic energies of the whole body, respectively.

Work or Energy	Interval	Speed			*p*-values				
		Slow (J/kg)	Moderate (J/kg)	Typical (J/kg)	Inter-action	Main effect	Slow-Mod	Slow-Typ	Mod-Typ
I. Foot	SS Rise	-0.01 ± 0.01	-0.01 ± 0.01	-0.00 ± 0.01	<0.001	0.705			
	SS Fall	-0.01 ± 0.01	-0.03 ± 0.01	-0.04 ± 0.02		<0.001^{G-G}	0.002	0.001	0.008
	Term DS	-0.02 ± 0.01	-0.03 ± 0.02	-0.04 ± 0.03		0.006^{G-G}	0.012	0.025	0.182
I. Ankle	SS Rise	-0.02 ± 0.02	-0.02 ± 0.02	-0.01 ± 0.02	<0.001^{G-G}	0.146			
	SS Fall	-0.04 ± 0.03	-0.06 ± 0.03	-0.05 ± 0.05		0.270^{G-G}			
	Term DS	0.10 ± 0.03	0.18 ± 0.03	0.24 ± 0.04		<0.001^{G-G}	<0.001	<0.001	<0.001
I. Knee	SS Rise	0.03 ± 0.02	0.06 ± 0.02	0.08 ± 0.03	<0.001	<0.001	0.003	0.001	0.013
	SS Fall	0.04 ± 0.01	0.05 ± 0.03	0.05 ± 0.04*		0.128			
	Term DS	-0.03 ± 0.05	-0.07 ± 0.06	-0.07 ± 0.06		<0.001	0.007	0.012	0.961
I. Hip	SS Rise	-0.00 ± 0.02	-0.02 ± 0.02	-0.01 ± 0.03	<0.001^{G-G}	0.310^{G-G}			
	SS Fall	-0.05 ± 0.02	-0.08 ± 0.04	-0.10 ± 0.05		<0.001	0.052	0.004	0.018
	Term DS	0.09 ± 0.04	0.12 ± 0.03	0.12 ± 0.03		0.001^{G-G}	0.007	0.002	0.008
HAT	SS Rise	0.01 ± 0.02	0.04 ± 0.02	0.08 ± 0.03	<0.001^{G-G}	<0.001^{G-G}	0.004	<0.001	<0.001
	SS Fall	-0.03 ± 0.01	-0.04 ± 0.02	-0.08 ± 0.03		<0.001^{G-G}	0.049	0.001	<0.001
	Term DS	-0.01 ± 0.01	-0.03 ± 0.03	-0.05 ± 0.04		0.003^{G-G}	0.109	0.011	0.001
C. Hip	SS Rise	0.02 ± 0.01	0.03 ± 0.01	0.05 ± 0.02	0.178^{G-G}	0.005^{G-G}	0.001	0.020	0.481
	SS Fall	0.01 ± 0.01	0.02 ± 0.01	0.02 ± 0.02					
	Term DS	0.02 ± 0.03	0.04 ± 0.04	0.04 ± 0.05*					

Table C.5: continued.

Work or Energy	Interval	Speed: Slow (J/kg)	Moderate (J/kg)	Typical (J/kg)	*p*-values: Inter-action	Main effect	Slow-Mod	Slow-Typ	Mod-Typ
C. Knee	SS Rise	-0.01 ± 0.01*	-0.02 ± 0.01	-0.03 ± 0.01	<0.001$^{G\text{-}G}$	0.003$^{G\text{-}G}$	0.134	0.013	0.003
	SS Fall	-0.05 ± 0.02	-0.09 ± 0.02	-0.11 ± 0.02		<0.001$^{G\text{-}G}$	<0.001	<0.001	0.001
	Term DS	0.03 ± 0.01	0.02 ± 0.02	0.03 ± 0.04		0.417$^{G\text{-}G}$			
C. Ankle	SS Rise	0.00 ± 0.00*	0.00 ± 0.00	0.00 ± 0.00	<0.001$^{G\text{-}G}$	<0.001	0.009	<0.001	0.003
	SS Fall	-0.00 ± 0.00	-0.00 ± 0.00*	-0.00 ± 0.00*		<0.001	0.011	<0.001	0.096
	Term DS	-0.03 ± 0.01	-0.03 ± 0.01	-0.05 ± 0.01		<0.001	0.059	<0.001	<0.001
C. Foot	SS Rise	0.00 ± 0.00	0.00 ± 0.00	0.00 ± 0.00	N/A				
	SS Fall	-0.00 ± 0.00	-0.00 ± 0.00	-0.00 ± 0.00					
	Term DS	-0.04 ± 0.01*	0.04 ± 0.01	-0.06 ± 0.01		<0.001	0.037	<0.001	<0.001
$^{+}W_{wb}$	SS Rise	0.07 ± 0.02	0.13 ± 0.04	0.22 ± 0.05	N/A	<0.001	<0.001	<0.001	<0.001
	SS Fall	0.05 ± 0.02	0.07 ± 0.03	0.08 ± 0.03		<0.001	0.001	<0.001	0.114
	Term DS	0.25 ± 0.05	0.36 ± 0.05	0.44 ± 0.06		<0.001	<0.001	<0.001	<0.001
$^{-}W_{wb}$	SS Rise	-0.05 ± 0.03	-0.06 ± 0.03	-0.07 ± 0.03	N/A	0.089			
	SS Fall	-0.19 ± 0.04	-0.30 ± 0.04	-0.40 ± 0.07		<0.001$^{G\text{-}G}$	<0.001	<0.001	<0.001
	Term DS	-0.13 ± 0.04	-0.20 ± 0.04	-0.27 ± 0.05		< 0.001	<0.001	<0.001	<0.001
ΔE_{wb}	SS Rise	0.02 ± 0.02	0.07 ± 0.04	0.16 ± 0.05	<0.001$^{G\text{-}G}$	<0.001$^{G\text{-}G}$	0.001	<0.001	<0.001
	SS Fall	-0.14 ± 0.04	-0.23 ± 0.04	-0.32 ± 0.07		<0.001$^{G\text{-}G}$	<0.001	<0.001	<0.001
	Term DS	0.11 ± 0.03	0.16 ± 0.04	0.17 ± 0.05		<0.001	<0.001	0.002	0.761
ΔGPE_{wb}	SS Rise	0.09 ± 0.02	0.17 ± 0.05	0.28 ± 0.09	<0.001$^{G\text{-}G}$	<0.001$^{G\text{-}G}$	<0.001	<0.001	<0.001
	SS Fall	-0.13 ± 0.03	-0.20 ± 0.04	-0.29 ± 0.06		<0.001$^{G\text{-}G}$	<0.001	<0.001	<0.001
	Term DS	0.04 ± 0.03	0.03 ± 0.03	0.01 ± 0.03		<0.001$^{G\text{-}G}$	0.180	0.001	<0.001
ΔTKE_{wb}	SS Rise	-0.06 ± 0.03	-0.10 ± 0.05	-0.13 ± 0.06	<0.001$^{G\text{-}G}$	<0.001$^{G\text{-}G}$	0.001	0.001	0.006
	SS Fall	-0.00 ± 0.01	-0.02 ± 0.03	-0.01 ± 0.03		0.109$^{G\text{-}G}$			
	Term DS	0.06 ± 0.03	0.12 ± 0.03	0.15 ± 0.04		<0.001$^{G\text{-}G}$	<0.001	< 0.001	0.001
ΔRKE_{wb}	SS Rise	-0.00 ± 0.00	0.00 ± 0.00	0.00 ± 0.00	<0.001	<0.001	0.009	0.001	0.03
	SS Fall	-0.01 ± 0.00*	-0.01 ± 0.00*	-0.01 ± 0.00		<0.001$^{G\text{-}G}$	<0.001	<0.001	<0.001
	Term DS	0.01 ± 0.00	0.01 ± 0.00	0.01 ± 0.00		<0.001$^{G\text{-}G}$	0.009	0.002	0.004

Table C.6: Data corresponding to the proportions of the resulting net work and changes in energy forms over three intervals of the gait cycle in Figs. 6.2 – 6.4 in text are presented as averages with range [max to min]. Over all intervals, ${}^{net}W_{\%}$ is the net work relative to the summed positive and absolute negative work over the interval. During single support rise, $\Delta E_{\%,\Delta GPE}$, $\Delta TKE_{\%,\Delta GPE}$, and $\Delta RKE_{\%,\Delta GPE}$ are the percentages of change in net energy, translational kinetic energy, and rotational kinetic energy relative to change in gravitational potential energy, respectively. During single support fall and terminal double support, $\Delta GPE_{\%,\Delta E}$, $\Delta TKE_{\%,\Delta E}$, and $\Delta RKE_{\%,\Delta E}$ are the percentages of change in gravitational potential energy, translational kinetic energy, and rotational kinetic energy relative to change in net energy, respectively. Violations in normality are denoted with an "*," outliers with an "^," and Greenhouse-Geisser corrections for sphericity are noted with superscripted "G-G" (all p < 0.05).

Interval	**Work or Energy**	**Speed**			***p*-values**			
		Slow	**Moderate**	**Typical**	**Main effect**	**Slow-Mod**	**Slow-Typ**	**Mod-Typ**
Single Support Rise	${}^{net}W_{\%}$	27% [65% to -11%]	39% [62% to -4%]	55%* [68% to 28%]	0.003	0.357	0.036	0.014
	$\Delta E_{\%,\Delta GPE}$	28% [62% to -23%]	43% [76% to -6%]	56% [78% to 34%]	<0.001	0.006	0.003	0.021
	$\Delta TKE_{\%,\Delta GPE}$	72% [120% to 37%]	58% [108% to 32%]	45% [68% to 25%]	<0.001	0.018	0.005	0.017
	$\Delta RKE_{\%,\Delta GPE}$	0% [5% to -4%]	-1%*^ [2% to -8%]	-1% [0% to -3%]	0.024	0.054	0.153	1.000
Single Support Fall	${}^{net}W_{\%}$	-60%* [-29% to -78%]	-62% [-40% to -76%]	-66% [-47% to -83%]	$0.044^{G\text{-}G}$	1.000	0.126	0.010
	$\Delta GPE_{\%,\Delta E}$	-96%* [-82% to -132%]	-89% [-70% to -109%]	-92% [-75% to -106%]	0.078			
	$\Delta TKE_{\%,\Delta E}$	0% [37% to -14%]	-6% [16% to -25%]	-3% [14% to -21%]	$0.061^{G\text{-}G}$			
	$\Delta RKE_{\%,\Delta E}$	-4% [-3% to -6%]	-5% [-3% to -8%]	-5%* [-3% to -8%]	$0.479^{G\text{-}G}$			

Table C.6: continued.

Interval	Work or Energy	Speed			p-values			
		Slow	Moderate	Typical	Main effect	Slow-Mod	Slow-Typ	Mod-Typ
Terminal Double Support	$^{net}W_{\%}$	30% [41% to 18%]	28% [39% to 15%]	24% [38% to 11%]	$0.005^{G\text{-}G}$	0.616	0.013	0.001
	$\Delta GPE_{\%,\Delta E}$	38% [74% to 7%]	18% [37% to -2%]	1% [27% to -22%]	$<0.001^{G\text{-}G}$	0.009	< 0.001	< 0.001
	$\Delta TKE_{\%,\Delta E}$	57% [88% to 21%]	76% [97% to 57%]	92% [117% to 68%]	$<0.001^{G\text{-}G}$	0.009	< 0.001	< 0.001
	$\Delta RKE_{\%,\Delta E}$	5% [8% to 2%]	6% [8% to 4%]	7%* [14% to 5%]	$0.151^{G\text{-}G}$			

Table C.7: Temporal-spatial parameter data for Shoes, RiAFO, and BiAFO conditions (mean ± standard deviation).

Condition	Stance Time (s)		Swing Time (s)		Step Length (m)		Step Width (m)
	Left	Right	Left	Right	Left	Right	
Shoes	0.65 ± 0.02	0.64 ± 0.03	0.39 ± 0.02	0.39 ± 0.02	0.71 ± 0.07	0.71 ± 0.07	0.17 ± 0.03
RiAFO	0.65 ± 0.03	0.64 ± 0.03	0.39 ± 0.02	0.40 ± 0.02	0.71 ± 0.07	0.71 ± 0.06	0.17 ± 0.02
BiAFO	0.65 ± 0.02	0.64 ± 0.02	0.39 ± 0.02	0.40 ± 0.02	0.71 ± 0.07	0.72 ± 0.07	0.18 ± 0.03

Table C.8: Positive and negative relative constituent work as a percentage of absolute limb work ($^{+}RW_{constituent}$ and $^{-}RW_{constituent}$, respectively) (mean ± standard deviation). Except for positive and negative relative hip and foot work in stance, there were significant limb-by-condition interactions based on several two-way repeated measures ANOVAs. Violations in normality are denoted with an "*," outliers are noted with a "^," and Greenhouse-Geisser corrections for sphericity are noted with superscripted "G-G" (all $p < 0.05$).

Metric	Phase	Limb	Shoes	RiAFO	BiAFO	*p*-values				
						Inter-action	Main effect	Sh-Ri	Sh-Bi	Ri-Bi
$^{+}RW_{hip}$ (%)	Stance	Left	12.5 ± 2.9*^	13.3 ± 3.4	14.1 ± 3.6*	0.803	0.001	0.073	0.005	0.068
		Right	12.9 ± 2.1	13.6 ± 1.6	14.2 ± 2.3					
	Swing	Left	7.7 ± 1.9	8.2 ± 2.2	9.7 ± 2.2	<0.001	$<0.001^{G\text{-}G}$	0.016	<0.001	<0.001
		Right	7.4 ± 1.5	9.3 ± 1.7	9.3 ± 2.0		<0.001	<0.001	<0.001	1.000
$^{-}RW_{hip}$ (%)	Stance	Left	13.3 ± 2.6*	13.2 ± 2.4	14.0 ± 3.1	0.116	0.011	0.790	0.013	0.209
		Right	12.2 ± 2.7	12.9 ± 2.6	13.1 ± 2.7					
	Swing	Left	0.1 ± 0.1*	0.1 ± 0.1*	0.1 ± 0.1*	$0.737^{G\text{-}G}$	0.327			
		Right	0.1 ± 0.1*	0.1 ± 0.2*	0.1 ± 0.1*					
$^{+}RW_{knee}$ (%)	Stance	Left	11.9 ± 2.6	12.1 ± 2.6	13.9 ± 3.2	<0.001	<0.001	1.000	<0.001	<0.001
		Right	11.6 ± 2.0	13.6 ± 2.1	13.7 ± 2.6		<0.001	<0.001	<0.001	1.000
	Swing	Left	0.4 ± 0.3	0.4 ± 0.3*	0.6 ± 0.4	<0.001	<0.001	0.043	0.001	<0.001
		Right	0.5 ± 0.5*	0.8 ± 0.6	0.8 ± 0.6*		<0.001	0.001	0.001	0.462

Table C.8: continued.

Metric	Phase	Limb	Shoes	RiAFO	BiAFO	*p*-values				
						Inter-action	Main effect	Sh-Ri	Sh-Bi	Ri-Bi
$^{-}RW_{knee}$ (%)	Stance	Left	8.2 ± 2.1	8.2 ± 1.9	9.9 ± 2.4	0.022	<0.001	1.000	0.001	0.005
		Right	7.8 ± 2.2	8.8 ± 2.2	8.8 ± 2.3		0.017	0.025	0.103	1.000
	Swing	Left	10.2 ± 1.2	10.6 ± 1.6	12.1 ± 1.8	<0.001	<0.001	0.080	<0.001	<0.001
		Right	9.8 ± 1.1	11.8 ± 1.0	11.9 ± 1.4		<0.001	<0.001	<0.001	1.000
$^{+}RW_{ankle}$ (%)	Stance	Left	16.1 ± 1.9	15.0 ± 1.6	10.0 ± 1.9	<0.001	<0.001	0.004	<0.001	<0.001
		Right	15.9 ± 1.5	10.8 ± 2.1	10.3 ± 2.3		$<0.001^{G\text{-}G}$	<0.001	<0.001	0.291
	Swing	Left	0.3 ± 0.1	0.3 ± 0.1	0.1 ± 0.0*	<0.001	$<0.001^{G\text{-}G}$	0.251	<0.001	<0.001
		Right	0.3 ± 0.1*	0.1 ± 0.0	0.1 ± 0.0		$<0.001^{G\text{-}G}$	<0.001	<0.001	1.000
$^{-}RW_{ankle}$ (%)	Stance	Left	8.3 ± 1.8	8.4 ± 1.9	5.2 ± 1.4	<0.00	<0.001	1.000	<0.001	<0.001
		Right	9.3 ± 2.0	6.4 ± 1.5	6.2 ± 1.1		$<0.001^{G\text{-}G}$	<0.001	<0.001	1.000
	Swing	Left	0.5 ± 0.1	0.6 ± 0.1	0.1 ± 0.0	<0.001	<0.001	0.296	<0.001	<0.001
		Right	0.5 ± 0.1	0.1 ± 0.0	0.1 ± 0.0		$<0.001^{G\text{-}G}$	<0.001	<0.001	0.027
$^{+}RW_{foot}$ (%)	Stance	Left	2.0 ± 0.7	2.2 ± 0.7	2.9 ± 0.8	0.130	0.001	0.118	0.008	0.116
		Right	2.2 ± 1.0	2.5 ± 0.7	2.6 ± 0.9					
$^{-}RW_{foot}$ (%)	Stance	Left	8.4 ± 1.8	7.5 ± 1.0	7.2 ± 1.5	0.394	0.008	0.181	0.019	0.553
		Right	9.5 ± 1.7	9.2 ± 1.0	8.7 ± 1.4					

Table C.9: Data corresponding to the proportions of the resulting net work and changes in energy forms over four intervals of the gait cycle in Figs. 8.1 – 8.4 in text are presented as averages with range [max to min]. Over all intervals, ${}^{net}W_{\%}$ is the net work relative to the summed positive and absolute negative work over the interval. During single support rise, $\Delta E_{\%,\Delta GPE}$, $\Delta TKE_{\%,\Delta GPE}$, and $\Delta RKE_{\%,\Delta GPE}$ are the percentages of change in net energy, translational kinetic energy, and rotational kinetic energy relative to change in gravitational potential energy, respectively. During single support fall and double support (both initial and terminal), $\Delta GPE_{\%,\Delta E}$, $\Delta TKE_{\%,\Delta E}$, and $\Delta RKE_{\%,\Delta E}$ are the percentages of change in gravitational potential energy, translational kinetic energy, and rotational kinetic energy relative to change in net energy, respectively. Violations in normality are denoted with an "*," if outliers were present, the data are marked with a "^," and Greenhouse-Geisser corrections for sphericity are noted with superscripted "G-G" (all p < 0.05).

Interval	Work or Energy	Conditions			*p*-values			
		Shoes	RiAFO	BiAFO	Main effect	Sh-Ri	Sh-Bi	Ri-Bi
Initial Double Support	${}^{net}W_{\%}$	20% [27% to 14%]	27% [41% to 16%]	25% [40% to 12%]	<0.001	<0.001	0.023	0.434
	$\Delta GPE_{\%,\Delta E}$	9% [42% to -40%]	15%*^ [46% to -32%]	9% [48% to -63%]	$0.124^{G\text{-}G}$			
	$\Delta TKE_{\%,\Delta E}$	82% [129% to 49%]	77%*^ [120% to 48%]	79% [146% to 43%]	$0.302^{G\text{-}G}$			
	$\Delta RKE_{\%,\Delta E}$	9% [15% to 6%]	8%* [12% to 5%]	12% [18% to 7%]	$< 0.001^{G\text{-}G}$	0.002	0.001	<0.001
Single Support Rise	${}^{net}W_{\%}$	71% [89% to 47%]	67% [84% to 47%]	70% [88% to 56%]	0.295			
	$\Delta E_{\%,\Delta GPE}$	75% [94% to 59%]	78% [97% to 63%]	86%*^ [126% to 66%]	<0.001	0.742	0.002	0.005
	$\Delta TKE_{\%,\Delta GPE}$	25% [42% to 7%]	23% [37% to 5%]	14% [34% to -22%]	<0.001	0.814	0.003	0.004
	$\Delta RKE_{\%,\Delta GPE}$	0%^ [2% to -3%]	-1% [1% to -3%]	0% [2% to -4%]	0.905			

Table C.9: continued.

Interval	Work or Energy	Conditions			*p*-values			
		Shoes	RiAFO	BiAFO	Main effect	Sh-Ri	Sh-Bi	Ri-Bi
Single Support Fall	$^{net}W_{\%}$	-63% [-48% to -76%]	-62% [-44% to -84%]	-63% [-45% to -78%]	$0.627^{G\text{-}G}$			
	$\Delta GPE_{\%,\Delta E}$	-87% [-69% to -106%]	-83%^ [-66% to -93%]	-86% [-62% to -97%]	0.006	0.006	1.000	0.028
	$\Delta TKE_{\%,\Delta E}$	-9% [10% to -27%]	-13%^ [-4% to -30%]	-10% [1% to -34%]	0.005	0.005	1.000	0.014
	$\Delta RKE_{\%,\Delta E}$	-4% [-3% to -5%]	-4% [-3% to -4%]	-4% [-3% to -5%]	0.403			
Terminal Double Support	$^{net}W_{\%}$	20% [28% to 7%]	19%^ [32% to 5%]	24% [43% to 12%]	0.015	1.000	0.152	0.033
	$\Delta GPE_{\%,\Delta E}$	0%*^ [36% to -164%]	-8%* [43% to -105%]	-2% [42% to -76%]	0.579			
	$\Delta TKE_{\%,\Delta E}$	91%*^ [245% to 57%]	94% [162% to 49%]	90% [162% to 42%]	0.391			
	$\Delta RKE_{\%,\Delta E}$	9%*^ [19% to 6%]	14%*^ [52% to 8%]	12% [19% to 8%]	$0.041^{G\text{-}G}$	0.063	0.018	1.000

Table C.10: Constituent work values over the specified interval corresponding to Figs. 8.5 – 8.6 in text. Intervals correspond to initial double support (Init DS), single support rise (SS Rise), single support fall (SS Fall), and terminal double support (Term DS) in reference to the right limb gait cycle. "L" and "R" prior to a constituent denotes left or right limb, respectively.

Variable	Region	Shoes (J/kg)	RiAFO (J/kg)	BiAFO (J/kg)
L. foot	Init DS	-0.04 ± 0.03	-0.03 ± 0.02	-0.01 ± 0.02
	SS Rise	N/A		
	SS Fall			
	Term DS	-0.03 ± 0.02	-0.03 ± 0.01	-0.03 ± 0.01
L. ankle	Init DS	0.21 ± 0.04	0.20 ± 0.03	0.12 ± 0.03
	SS Rise	N/A		
	SS Fall			
	Term DS	-0.06 ± 0.02	-0.06 ± 0.02	0.00 ± 0.01
L. knee	Init DS	-0.09 ± 0.05	-0.09 ± 0.05	-0.06 ± 0.05
	SS Rise	-0.03 ± 0.01	-0.03 ± 0.01	-0.03 ± 0.01
	SS Fall	-0.13 ± 0.02	-0.14 ± 0.02	-0.14 ± 0.02
	Term DS	0.03 ± 0.02	0.03 ± 0.02	-0.02 ± 0.02
L. hip	Init DS	0.12 ± 0.03	0.13 ± 0.04	0.12 ± 0.03
	SS Rise	0.08 ± 0.02	0.08 ± 0.02	0.10 ± 0.03
	SS Fall	0.04 ± 0.02	0.05 ± 0.02	0.04 ± 0.02
	Term DS	0.01 ± 0.05	0.02 ± 0.05	0.03 ± 0.05
HAT	Init DS	-0.02 ± 0.03	-0.01 ± 0.02	-0.02 ± 0.02
	SS Rise	0.10 ± 0.02	0.10 ± 0.02	0.11 ± 0.03
	SS Fall	-0.10 ± 0.03	-0.11 ± 0.02	-0.12 ± 0.03
	Term DS	-0.02 ± 0.04	-0.03 ± 0.03	-0.03 ± 0.03
R. foot	Init DS	-0.04 ± 0.02	-0.05 ± 0.01	-0.04 ± 0.02
	SS Rise	0.01 ± 0.01	0.00 ± 0.01	0.00 ± 0.01
	SS Fall	-0.04 ± 0.02	-0.04 ± 0.01	-0.03 ± 0.01
	Term DS	-0.05 ± 0.02	-0.02 ± 0.02	-0.02 ± 0.02
R. ankle	Init DS	-0.06 ± 0.02	-0.00 ± 0.01	0.00 ± 0.01
	SS Rise	-0.00 ± 0.03	-0.02 ± 0.02	-0.02 ± 0.02
	SS Fall	-0.05 ± 0.05	-0.05 ± 0.03	-0.05 ± 0.03
	Term DS	0.22 ± 0.03	0.13 ± 0.04	0.13 ± 0.04
R. knee	Init DS	0.03 ± 0.03	-0.01 ± 0.03	-0.01 ± 0.02
	SS Rise	0.06 ± 0.03	0.08 ± 0.02	0.08 ± 0.03
	SS Fall	0.06 ± 0.03	0.07 ± 0.03	0.07 ± 0.03
	Term DS	-0.08 ± 0.03	-0.06 ± 0.03	-0.07 ± 0.03
R. hip	Init DS	0.01 ± 0.06	0.01 ± 0.04	0.02 ± 0.05
	SS Rise	0.01 ± 0.03	0.01 ± 0.04	0.03 ± 0.03
	SS Fall	-0.14 ± 0.03	-0.14 ± 0.03	-0.15 ± 0.03
	Term DS	0.13 ± 0.02	0.13 ± 0.03	0.12 ± 0.03

Appendix D

SUPPLEMENTAL FIGURES

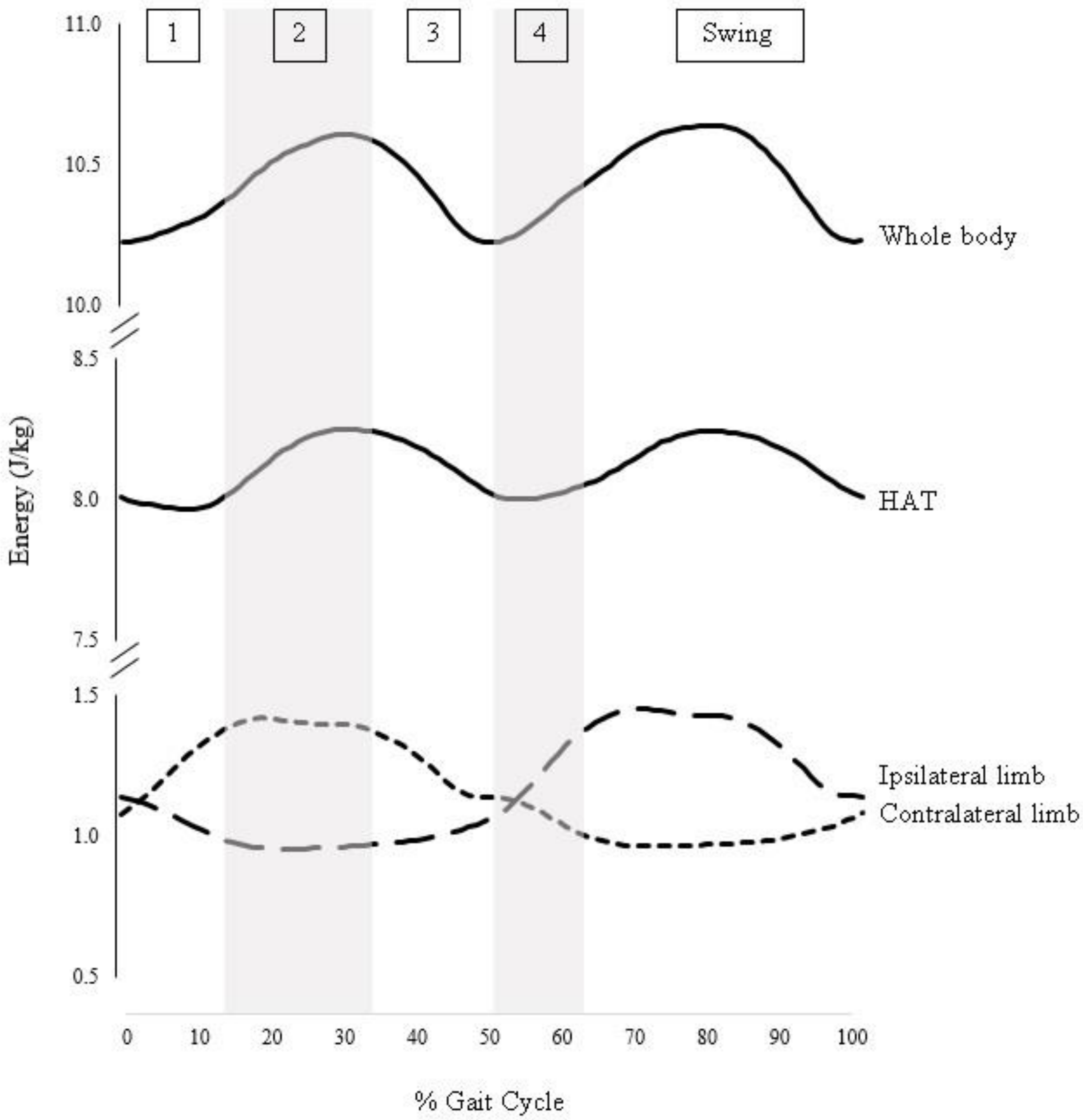

Figure D.1: Energy for the whole body, summed HAT, and ipsilateral and contralateral limbs shown for a representative subject over 100% of an ipsilateral gait cycle. Regions correspond to (1) initial double support, (2) single support rise, (3) single support fall, (4) terminal double support, and swing phase.

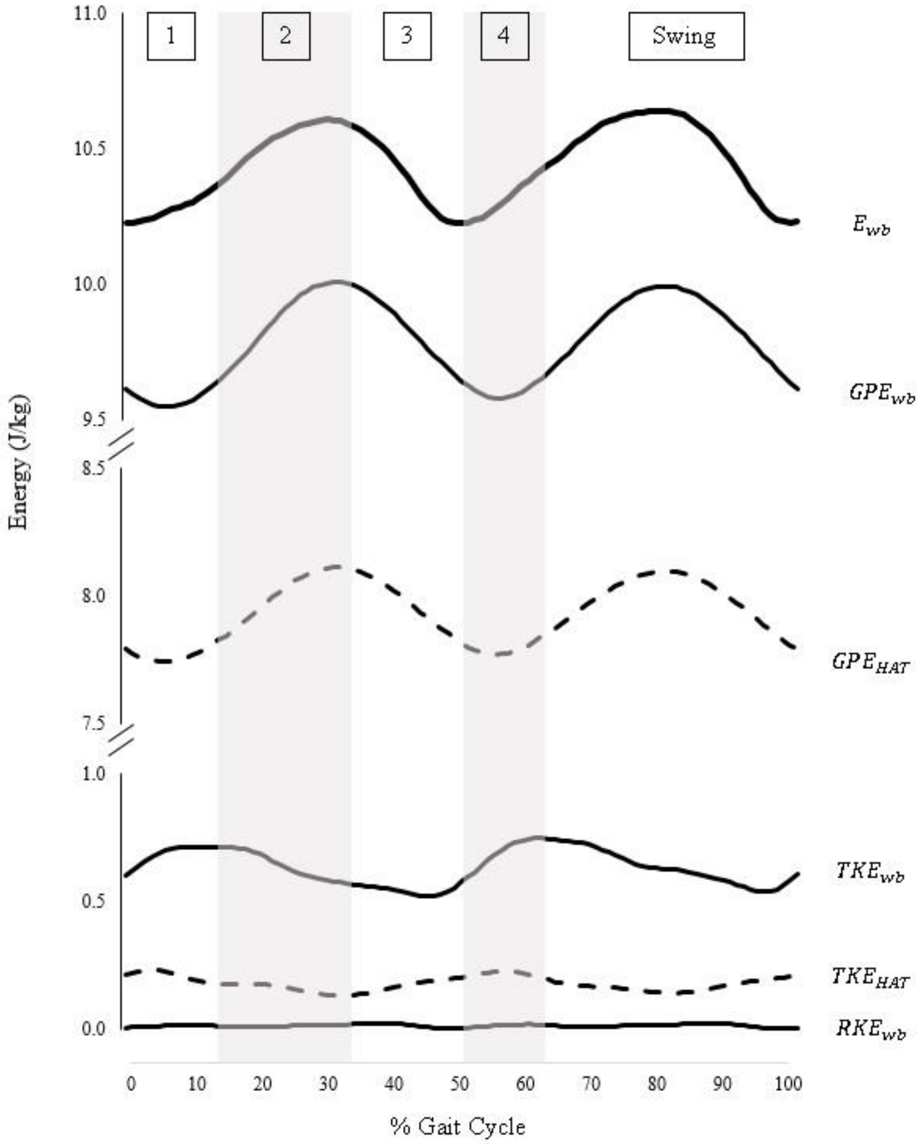

Figure D.2: Gravitational potential energy (GPE), translational kinetic energy (TKE), rotational kinetic energy (RKE), and summed energy (E) for the whole body (wb) and summed head-arms-trunk (HAT). Data over 100% of an ipsilateral gait cycle are from a representative subject. Regions correspond to (1) initial double support, (2) single support rise, (3) single support fall, (4) terminal double support, and swing phase.

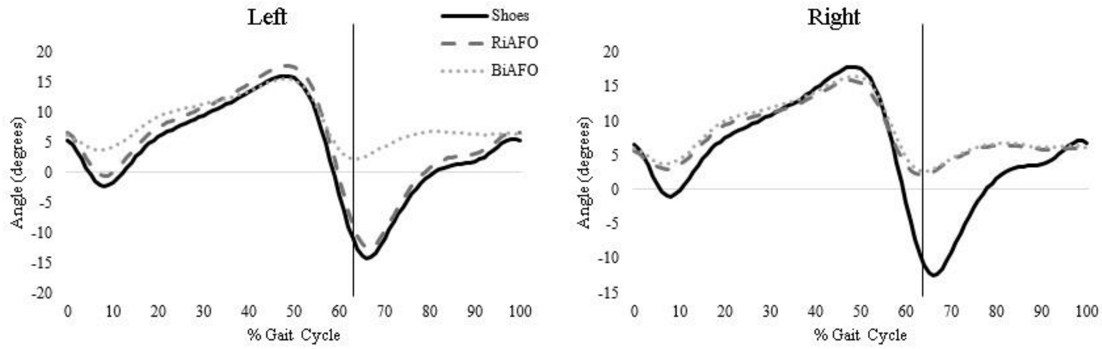

Figure D.3: Ankle angle curves averaged across all subjects appear to maintain their shape over 100% of the gait cycle across Shoes, RiAFO, and BiAFO conditions. Vertical line indicates end of stance phase (62% of gait cycle).

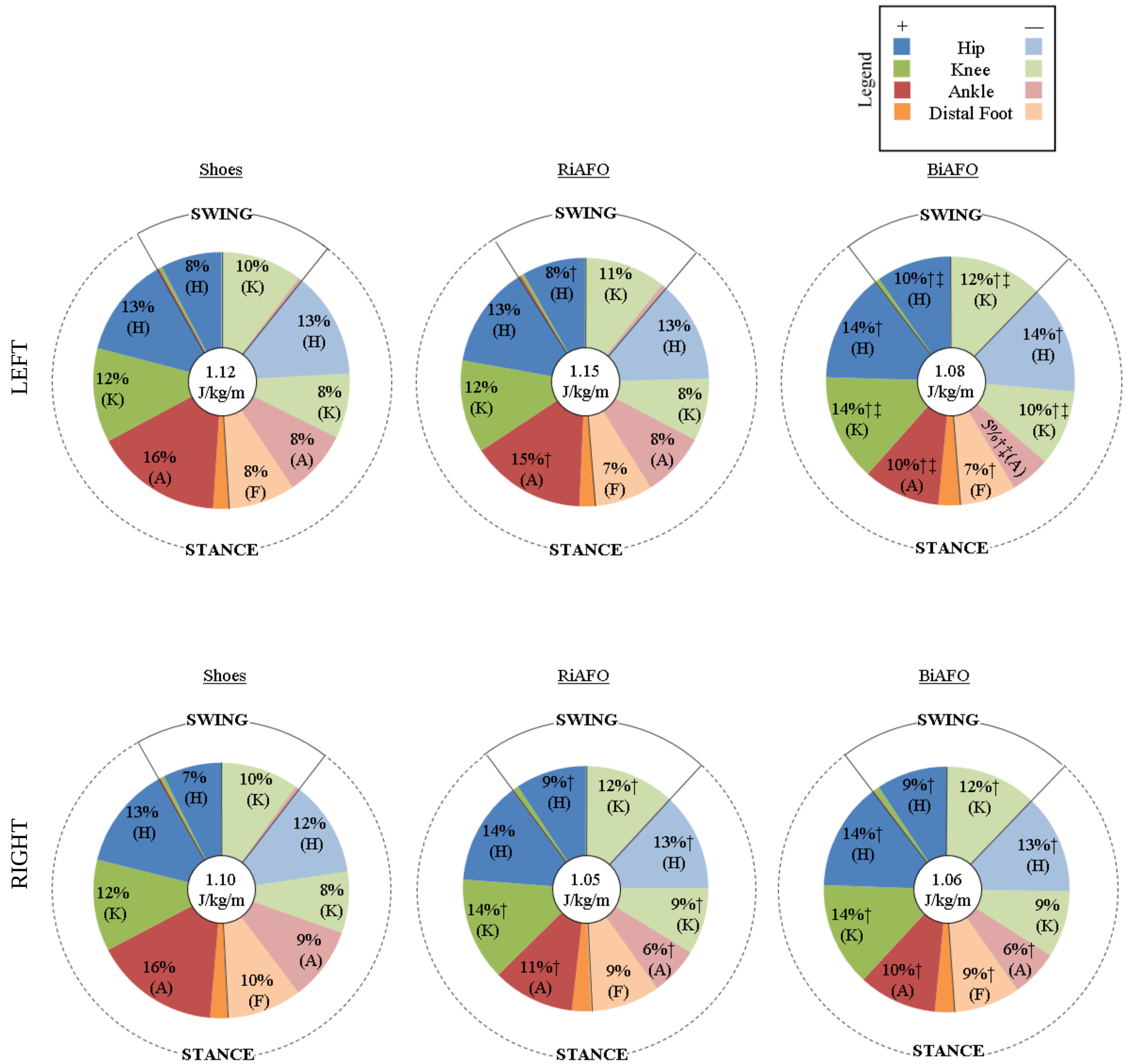

Figure D.4: Relative work data from Fig. 7.3 presented as Constituent Lower Extremity Work (CLEW) pie charts (see Chapter 4).

Appendix E

IRB APPROVAL LETTERS

UNIVERSITY OF DELAWARE

RESEARCH OFFICE

210 Hullihen Hall
University of Delaware
Newark, Delaware 19716-1551
Ph: 302/831-2136
Fax: 302/831-2828

DATE:	June 20, 2016
TO:	Anahid Ebrahimi, B.S.
FROM:	University of Delaware IRB
STUDY TITLE:	[906688-1] Evaluation of Ankle-Foot Orthoses with Healthy Persons
SUBMISSION TYPE:	New Project
ACTION:	APPROVED
APPROVAL DATE:	June 20, 2016
EXPIRATION DATE:	June 19, 2017
REVIEW TYPE:	Expedited Review
REVIEW CATEGORY:	Expedited review category # *(4,7)*

Thank you for your submission of New Project materials for this research study. The University of Delaware IRB has APPROVED your submission. This approval is based on an appropriate risk/benefit ratio and a study design wherein the risks have been minimized. All research must be conducted in accordance with this approved submission.

This submission has received Expedited Review based on the applicable federal regulation.

Please remember that informed consent is a process beginning with a description of the study and insurance of participant understanding followed by a signed consent form. Informed consent must continue throughout the study via a dialogue between the researcher and research participant. Federal regulations require each participant receive a copy of the signed consent document.

Please note that any revision to previously approved materials must be approved by this office prior to initiation. Please use the appropriate revision forms for this procedure.

All SERIOUS and UNEXPECTED adverse events must be reported to this office. Please use the appropriate adverse event forms for this procedure. All sponsor reporting requirements should also be followed.

Please report all NON-COMPLIANCE issues or COMPLAINTS regarding this study to this office.

Please note that all research records must be retained for a minimum of three years.

Based on the risks, this project requires Continuing Review by this office on an annual basis. Please use the appropriate renewal forms for this procedure.

UNIVERSITY OF DELAWARE

RESEARCH OFFICE

210 Hullihen Hall
University of Delaware
Newark, Delaware 19716-1551
Ph: 302/831-2136
Fax: 302/831-2828

DATE:	June 9, 2017
TO:	Anahid Ebrahimi, B.S.
FROM:	University of Delaware IRB
STUDY TITLE:	[906688-2] Evaluation of Ankle-Foot Orthoses with Healthy Persons
SUBMISSION TYPE:	Continuing Review/Progress Report
ACTION:	APPROVED
APPROVAL DATE:	June 9, 2017
EXPIRATION DATE:	June 19, 2018
REVIEW TYPE:	Expedited Review
REVIEW CATEGORY:	Expedited review categories 4 and 7

Thank you for your submission of Continuing Review/Progress Report materials for this research study. The University of Delaware IRB has APPROVED your submission. This approval is based on an appropriate risk/benefit ratio and a study design wherein the risks have been minimized. All research must be conducted in accordance with this approved submission.

This submission has received Expedited Review based on the applicable federal regulation.

Please remember that informed consent is a process beginning with a description of the study and insurance of participant understanding followed by a signed consent form. Informed consent must continue throughout the study via a dialogue between the researcher and research participant. Federal regulations require each participant receive a copy of the signed consent document.

Please note that any revision to previously approved materials must be approved by this office prior to initiation. Please use the appropriate revision forms for this procedure.

All SERIOUS and UNEXPECTED adverse events must be reported to this office. Please use the appropriate adverse event forms for this procedure. All sponsor reporting requirements should also be followed.

Please report all NON-COMPLIANCE issues or COMPLAINTS regarding this study to this office.

Please note that all research records must be retained for a minimum of three years.

Based on the risks, this project requires Continuing Review by this office on an annual basis. Please use the appropriate renewal forms for this procedure.

UNIVERSITY OF DELAWARE

RESEARCH OFFICE

210 Hullihen Hall
University of Delaware
Newark, Delaware 19716-1551
Ph: 302/831-2136
Fax: 302/831-2828

DATE: August 31, 2017

TO: Anahid Ebrahimi, B.S.
FROM: University of Delaware IRB

STUDY TITLE: [906688-3] Evaluation of Ankle-Foot Orthoses with Healthy Persons

SUBMISSION TYPE: Amendment/Modification

ACTION: APPROVED
APPROVAL DATE: August 31, 2017
EXPIRATION DATE: June 19, 2018
REVIEW TYPE: Expedited Review

REVIEW CATEGORY: Expedited review category # *(4,7)*

Thank you for your submission of Amendment/Modification materials for this research study. The University of Delaware IRB (HUMANS) has APPROVED your submission. This approval is based on an appropriate risk/benefit ratio and a study design wherein the risks have been minimized. All research must be conducted in accordance with this approved submission.

This submission has received Expedited Review based on the applicable federal regulation.

Please remember that informed consent is a process beginning with a description of the study and insurance of participant understanding followed by a signed consent form. Informed consent must continue throughout the study via a dialogue between the researcher and research participant. Federal regulations require each participant receive a copy of the signed consent document.

Please note that any revision to previously approved materials must be approved by this office prior to initiation. Please use the appropriate revision forms for this procedure.

All SERIOUS and UNEXPECTED adverse events must be reported to this office. Please use the appropriate adverse event forms for this procedure. All sponsor reporting requirements should also be followed.

Please report all NON-COMPLIANCE issues or COMPLAINTS regarding this study to this office.

Please note that all research records must be retained for a minimum of three years.

Based on the risks, this project requires Continuing Review by this office on an annual basis. Please use the appropriate renewal forms for this procedure.